

DESIGN AND ANALYSIS OF OPPORTUNISTIC MAC PROTOCOLS FOR
COGNITIVE RADIO WIRELESS NETWORKS

A Dissertation

by

HANG SU

Submitted to the Office of Graduate Studies of
Texas A&M University
in partial fulfillment of the requirements for the degree of

DOCTOR OF PHILOSOPHY

December 2010

Major Subject: Computer Engineering

DESIGN AND ANALYSIS OF OPPORTUNISTIC MAC PROTOCOLS FOR
COGNITIVE RADIO WIRELESS NETWORKS

A Dissertation

by

HANG SU

Submitted to the Office of Graduate Studies of
Texas A&M University
in partial fulfillment of the requirements for the degree of
DOCTOR OF PHILOSOPHY

Approved by:

Chair of Committee,	Xi Zhang
Committee Members,	A. L. Narasimha Reddy
	Jennifer Lundelius Welch
	Dmitri Loguinov
Head of Department,	Costas N. Georghiades

December 2010

Major Subject: Computer Engineering

ABSTRACT

Design and Analysis of Opportunistic MAC Protocols for Cognitive Radio Wireless

Networks. (December 2010)

Hang Su, B.S., Zhejiang University;

M.S., Zhejiang University

Chair of Advisory Committee: Dr. Xi Zhang

As more and more wireless applications/services emerge in the market, the already heavily crowded radio spectrum becomes much scarcer. Meanwhile, however, as it is reported in the recent literature, there is a large amount of radio spectrum that is under-utilized. This motivates the concept of cognitive radio wireless networks that allow the unlicensed secondary-users (SUs) to dynamically use the vacant radio spectrum which is not being used by the licensed primary-users (PUs).

In this dissertation, we investigate protocol design for both the synchronous and asynchronous cognitive radio networks with emphasis on the medium access control (MAC) layer. We propose various spectrum sharing schemes, opportunistic packet scheduling schemes, and spectrum sensing schemes in the MAC and physical (PHY) layers for different types of cognitive radio networks, allowing the SUs to opportunistically utilize the licensed spectrum while confining the level of interference to the range the PUs can tolerate. First, we propose the cross-layer based multi-channel MAC protocol, which integrates the cooperative spectrum sensing at PHY layer and the interweave-based spectrum access at MAC layer, for the synchronous cognitive radio networks. Second, we propose the channel-hopping based single-transceiver MAC protocol for the hardware-constrained synchronous cognitive radio networks, under which the SUs can identify and exploit the vacant channels by dynamically switching

across the licensed channels with their distinct channel-hopping sequences. Third, we propose the opportunistic multi-channel MAC protocol with the two-threshold sequential spectrum sensing algorithm for asynchronous cognitive radio networks. Fourth, by combining the interweave and underlay spectrum sharing modes, we propose the adaptive spectrum sharing scheme for code division multiple access (CDMA) based cognitive MAC in the uplink communications over the asynchronous cognitive radio networks, where the PUs may have different types of channel usage patterns. Finally, we develop a packet scheduling scheme for the PU MAC protocol in the context of time division multiple access (TDMA)-based cognitive radio wireless networks, which is designed to operate friendly towards the SUs in terms of the vacant-channel probability.

We also develop various analytical models, including the Markov chain models, $M/G^Y/1$ queuing models, cross-layer optimization models, etc., to rigorously analyze the performance of our proposed MAC protocols in terms of aggregate throughput, access delay, and packet drop rate for both the saturation network case and non-saturation network case. In addition, we conducted extensive simulations to validate our analytical models and evaluate our proposed MAC protocols/schemes. Both the numerical and simulation results show that our proposed MAC protocols/schemes can significantly improve the spectrum utilization efficiency of wireless networks.

To my family

ACKNOWLEDGMENTS

First of all, I would like to devote my greatest appreciation to my Ph.D. advisor, Professor Xi Zhang, for his guidance and contribution to this research. Without his insightful advice, constant encouragement, excellent judgement, and the offer of funding support, this dissertation would not be possible. His persistent commitment to research, great passion for solving problems, and strong demand for excellence impress me most and will have great impact on the rest of my research career. He gives me freedom to conduct research while providing all kinds of help that he can. Furthermore, he is always willing to share his knowledge and career experience with me, and encourage me whenever needed. Not only is he an adviser, but he is also a friend.

I would like to express my gratitude to the dissertation committee members, Professor A. L. Narasimha Reddy, Professor Jennifer Lundelius Welch, and Professor Dmitri Loguinov. I greatly appreciate their precious time and efforts. Their valuable comments and suggestions help me improve the quality of this dissertation.

Furthermore, I would also like to take this opportunity to sincerely thank all my friends and fellow students at Texas A&M University for making my life in College Station enjoyable and memorable. My appreciation also goes deeply to current and former Networking and Information Systems Laboratory (NISL) colleagues for making my stay at the NISL a wonderful memory. Especially, I would like to express my sincere appreciation to Qinghe Du for his friendship, insightful discussion, and kind help on my research. I am also grateful to my professors and the administration staff in the Department of Electrical and Computer Engineering at Texas A&M University who have contributed in the academic program and outstanding research environment.

Last, but not least, this dissertation is dedicated to all of my family members, my father, Su Xinsheng, my mother, Liang Lizhen, my wife, Teng Yun, my daughter, Chloe, and my mother-in-law, Luo Niansi, for their continuous love, support, and encouragement.

The funding for this research was supported in part by the National Science Foundation CAREER Award under Grant ECS-0348694.

TABLE OF CONTENTS

CHAPTER		Page
I	INTRODUCTION	1
	A. Background of the Research	1
	1. The Overview of Cognitive Radio Networks	1
	2. Spectrum Sharing Methodologies in Cognitive Ra- dio Networks	3
	3. Research Challenges and Motivations	5
	B. Related Work	6
	1. Underlay Spectrum Sharing Mode Based MAC	6
	2. Interweave Spectrum Sharing Mode Based MAC	7
	a. MAC Protocols for Synchronous Cognitive Ra- dio Networks	7
	b. MAC Protocols for Asynchronous Cognitive Radio Networks	8
	3. Spectrum Sensing in Cognitive Radio Networks	9
	C. Research Contributions	10
	D. Outline of the Dissertation	13
II	CROSS-LAYER BASED OPPORTUNISTIC MAC PROTO- COLS FOR SYNCHRONOUS COGNITIVE RADIO NET- WORKS	16
	A. Introduction	16
	B. The PUs' Channel-Usage Model	18
	C. Our Proposed Cross-Layer Based Multi-Channel Op- portunistic MAC Protocols	20
	1. Overview	20
	2. Channel Negotiation and Data Exchange	23
	3. Channel Sensing Policies	24
	D. Throughput Analyses for the Saturation Network Case	28
	1. The p -Persistent CSMA Scheme for Negotiating Phase	28
	2. The Aggregate Throughput for the Saturation Net- work Case	30
	a. Employing the Random Sensing Policy	30

CHAPTER	Page
b. Employing the Negotiation-Based Sensing Policy	32
E. Throughput and Packet Transmission Delay Analyses for the Non-Saturation Network Case	32
F. Performance Evaluations	39
G. Summary	46
 III CHANNEL-HOPPING BASED SINGLE TRANSCEIVER MAC FOR SYNCHRONOUS COGNITIVE RADIO NET- WORKS	48
A. Introduction	48
B. Our Proposed Channel-Hopping Cognitive MAC Protocol	49
1. The PUs' Channel-Usage Model	49
2. The Protocol Description	50
C. Throughput Analysis	53
D. Performance Evaluations	61
E. Summary	64
 IV CREAM-MAC: COGNITIVE RADIO-ENABLED MULTI- CHANNEL MAC PROTOCOL FOR ASYNCHRONOUS COG- NITIVE RADIO NETWORKS	66
A. Introduction	66
B. The System Models	68
1. Primary Users' Behaviors	68
2. The Spectrum Sensing Model	70
3. Channel Aggregating Technique	71
C. The Proposed CREAM-MAC Protocol	71
1. Protocol Overview	71
2. The Maximum Allowable Transmission Duration for SUs	75
3. The Selection of Licensed Channels	76
4. Channel Contention	77
5. Channel Negotiation	78
6. Data Transmissions	79
7. The Distributed Spectrum Sensing Scheme	80
D. Throughput Analysis for the Saturation Network Case .	84
1. The Analysis for the Licensed Data Channels	84
2. The Analysis for the Control Channels	85

CHAPTER	Page
3. The Aggregate Throughput	88
E. Performance Analysis for the Special Non-Saturation Network Case	92
F. Performance Evaluations	98
G. Summary	103
 V	
ADAPTIVE CDMA-BASED UPLINK MAC FOR ASYN- CHRONOUS COGNITIVE RADIO NETWORKS	104
A. Introduction	104
B. The System Models	105
1. The Network Model	105
2. The Primary Channel Model	108
3. Channel Sensing and Data Transmission Models	108
C. Our Proposed Opportunistic Spectrum Sharing Schemes for Uplink Cognitive MAC	109
1. The Overview of Our Proposed Opportunistic Spec- trum Sharing Schemes	109
2. Power and Rate Allocations	110
3. The Interference Probability of Intrusive Spectrum Sharing Operations	116
4. The Optimal Transmission Duration of the Intru- sive Spectrum Sharing Mode	118
5. The Selection Between the Intrusive Spectrum Shar- ing Mode and the Non-Intrusive Spectrum Sharing Mode	121
6. Mandatory Channel Sensing	123
7. The Fairness	126
8. The Details of Our Proposed Scheme	127
D. Performance Evaluations	129
E. Summary	142
 VI	
SECONDARY-USER-FRIENDLY TDMA-BASED MAC FOR PRIMARY USERS NETWORKS	144
A. Introduction	144
B. Related Work	146
C. The System Models	147
D. Our Proposed Secondary-User-Friendly Scheme	150

CHAPTER	Page
E. The Analytical Model	152
F. Performance Evaluations	161
1. Numerical Results	161
2. Case Study	166
G. Summary	169
VII CONCLUSIONS	170
A. Summary of the Dissertation	170
B. Future Work	173
1. Development of the More-Sophisticated Primary Users' Channel Usage Models	173
2. Impact of the SUs' Behaviors on Primary Users' Channel Usage Patterns	174
3. Secondary-User-Friendly MAC for Different Pri- mary User Networks	175
REFERENCES	176
APPENDIX A	192
APPENDIX B	193
VITA	197

LIST OF TABLES

TABLE		Page
I	The parameters for our proposed opportunistic multi-channel cognitive MAC protocol.	39
II	The parameters for channel-hopping cognitive MAC protocol modeling	56
III	The parameters for design and analysis of the CREAM-MAC protocol.	89
IV	The parameters for design and analysis of our proposed adaptive uplink CDMA-based cognitive MAC scheme.	130
V	Case study of our proposed secondary-user-friendly scheme when $\bar{\gamma} = 15$ dB.	169

LIST OF FIGURES

FIGURE	Page
1	Dissertation organization. 13
2	The channel state for the i -th channel. 19
3	The ON-OFF channel usage model for PUs. 19
4	The principle of our proposed MAC protocols. 21
5	Pseudo code of the MAC protocol for the SUs, where NAC is the number of identified vacant channels, LAC is the list of identified vacant channels. 22
6	The $(n + 1)$ -state Markov chain $\{S_u\}$ for the number of sensed channels, where the variable in each circle represents the number of distinct channels sensed by the SUs. 24
7	The time spent to attain the desired state by the negotiation-based sensing policy against the number of SUs with different γ 's. (a) The case with $n = 10$. (b) The case with $n = 6$ 40
8	The saturation throughput achieved by two different channel-sensing policies against the number (u) of SUs with different γ 's when the number (n) of licensed channels is 10. 41
9	The average packet transmission delay (W_s) against the system utilization (ρ) of SUs with different number of SUs (u) when the channel utilization (γ) of PUs is 0.6. The number (n) of licensed channels is 5. The solid lines represent the average packet transmission delay under negotiation-based sensing policy, and the dashed lines represent the average packet transmission delay under the random sensing policy. 42

FIGURE	Page	
10	<p>The aggregate throughput (η) of SUs against different system utilization (ρ) of SUs when the number (u) of SUs is equal to 20 and 8. The channel utilization (γ) of PUs is 0.6, and the number (n) of licensed channels is 5. The solid line represents the negotiation-based sensing policy for both $u = 8$ and $u = 20$, the dashed line represents the random sensing policy with $u = 20$, the dashdotted line represents the random sensing policy with $u = 8$.</p>	43
11	<p>The average packet transmission delay (W_s) against the channel utilization (γ) of PUs with different number of SUs (u) when the system utilization (ρ) of SUs is 0.1. The number (n) of licensed channels is 5. The solid lines represent the negotiation-based sensing policy, and the dashed lines represent the random sensing policy.</p>	45
12	<p>The aggregate throughput (η) of SUs varies with different channel utilization (γ) of PUs when the number (u) of SUs is equal to 20 and 8. The system utilization (ρ) of SUs is 0.1 and the number (n) of licensed channels is 5. The solid line represents the negotiation-based sensing policy for both $u = 8$ and $u = 20$, the dashed line represents the random sensing policy with $u = 20$, the dashdotted line represents the random sensing policy with $u = 8$.</p>	46
13	<p>The average packet transmission delay (W_s) varies with different γ's and λ's under negotiation-based sensing policy. The number (n) of licensed channels is 5 and the number (u) of SUs is 20.</p>	47
14	<p>Illustrations of our proposed opportunistic MAC protocol. The shadowed rectangles represent the time slots during which the PUs are active. The empty rectangles represent the unused time slots. Let A, B, and C be three SUs. If A wants to send packets to B, A follows the B's hopping sequence to meet with it and exchange the negotiation packets if the channel is unused by the PUs.</p>	51
15	<p>The diagram of node states transition from $(t - 1)$-th time slot to t-th time slot. \mathcal{I}, \mathcal{C}, \mathcal{R}, and \mathcal{N} imply the sets of idle nodes, communicating nodes, nodes that are ready to transmit/receive, buffered nodes, respectively.</p>	54

FIGURE	Page
16	The two-dimensional Markov chain for the number of exclusive channels in a given time slot. 57
17	The aggregate throughput of SUs against the packet generation rate. The average packet size is set to 170 bytes. The number of SUs $N = 20$. γ is set to 0.05, 0.2, 0.4 and 0.7, respectively. 61
18	The aggregate throughput of SUs against the channel utilization of PUs. The packet generation rate $\lambda = 0.5$. The number of SUs $N = 20$. The average packet size is set to 2388, 398 and 170 bytes, respectively. 62
19	The aggregate throughput of SUs against the average packet size. The packet generation rate $\lambda = 0.5$. The number of SUs $N = 20$. γ is set to 0, 0.1, 0.3 and 0.7, respectively. 63
20	The aggregate throughput against the packet generation rate with $\gamma = 0.1$ when $N = 20$ and 30, respectively. 64
21	Illustration of PUs' channel utilization in cognitive-radio based DSA networks. There are M licensed channels. The ON and OFF states of PUs operating at different licensed channels are unsynchronized. 68
22	The ON/OFF channel model for the i -th licensed data channel. 69
23	Illustrations of the CREAM-MAC protocol for an example case with 1 control channel and 3 data channels (CH 1, CH 2, CH 3) which form a Channel Group. 74
24	The illustration of the relationship between the P_{FA} and P_{MD} in the two-threshold sequential sensing. The two thresholds β_1 and β_2 control P_{MD} and P_{FA} , respectively. 83

FIGURE

Page

25	Illustrations of the CREAM-MAC protocol for the saturation network case. (a) The case where the number of channel group is 4 and the <i>control channel gets saturated</i> . (b) The case where the number of channel group is 2 and the <i>control channel does not get saturated</i> , implying that the data channels get saturated. Here CG i represents Channel Group i . The channel occupation blocks drawn with the <i>same</i> filling pattern and color in either Fig. 25(a) or Fig. 25(b) represent that the control-channel and data-channel resources are occupied by the <i>same</i> pair of SU sender and SU receiver. The average duration of the channel negotiation is equal to $\mathbb{E}[T_c]$ and the duration for the exchange data block is equal to T_d^{\max}	90
26	The aggregate throughput against the size of contention window (CW_{min}). The number (n) of sensors is set to be 4. The channel utilization (γ) of PUs is set to be 0.5. R_c and R_d are set to be 1 Mbps.	97
27	The aggregate throughput against the channel utilization of PUs, when the number (M) of licensed channels is set to be 30, the number (u) of contending SUs is set to be 30, and $CW_{min} = 256$	99
28	The aggregate throughput against the number of sensors in each SU, when the channel utilization (γ) of the PUs is set to be 0.5, the number (M) of licensed channels is set to be 30, the number (u) of contending secondary is set to be 30, and $CW_{min} = 256$	100
29	The packet transmission delay against the channel utilization of PUs with the combinations of the number (u) of contending SUs being set to be 5 or 10 and the number (n) of licensed channels being set to be 4 or 5.	101
30	Analytical and simulation results for the non-saturation network case when the packet arrival rate varies. The number (u) of contending SUs is set to be 10, the number (n) of licensed channels is set to be 4, the channel utilization (γ) of PUs is set to be 0.5.	102

FIGURE	Page	
31	Illustration of the CDMA-based secondary (users) network. The sub-figure on the bottom right corner shows the detailed topology of the secondary (users) network. The secondary (users) network consists of a set of SUs and a secondary base station (SBS). The SUs transmit data to the SBS by opportunistically accessing the licensed spectrum of the PUs in the primary (users) network.	106
32	Illustration of our proposed spectrum access schemes. The transmission duration τ_t depends on τ_f and the interference constraints. The SUs may interfere with the PUs when both the SUs and PUs access the spectrum.	119
33	The pseudo code of our proposed schemes for the selection between the intrusive spectrum sharing mode and the non-intrusive spectrum sharing mode.	128
34	The impact of distance between the secondary network and primary network on the normalized aggregate throughput of our proposed scheme when the PUs' traffic follows lognormal distribution.	131
35	The Jain fairness index vs. the distance between the secondary network and primary network. The channel utilization of PUs is 0.17 and the PUs' traffic follows lognormal distribution.	133
36	The normalized aggregate throughput vs. the average duration of OFF state when the PUs' activity follows the lognormal distribution.	136
37	The interference index vs. average duration of OFF state when the PUs' activity follows the lognormal distribution.	137
38	The normalized aggregate throughput vs. channel utilization of PUs when the PUs' activity follows the pareto distribution.	138
39	The interference index vs. channel utilization of PUs when the PUs' activity follows the pareto distribution.	139
40	The normalized aggregate throughput vs. channel utilization of PUs when the PUs' activity follows the gamma distribution.	140

FIGURE	Page	
41	The interference index vs. channel utilization of PUs when the PUs' activity follows the gamma distribution.	141
42	Given the same interference index, the normalized aggregate throughput comparison between our proposed scheme and the fixed transmission scheme when the PUs' activity follows the gamma distribution. Note that in the above figure, the plots with the same line style represent that the corresponding schemes have the same interference index.	142
43	The network model. PU and SU denotes PUs and SUs, respectively. The PUs communicate with the base station in a TDMA way. The SUs equipped with the cognitive radio, which are synchronized with the primary users, sense and utilize the vacant channels.	148
44	Queue-driven secondary-user-friendly TDMA scheduling model. . .	149
45	Diagram of the evolution of the queue states.	152
46	The performance metrics of the proposed scheme against average SNR with different combinations of θ_A , θ_B , and θ_C . The packet arrival rate (λ) is set to be 53 packets per second and the Nakagami fading parameter (m) is 1. (a) The idle probability of time slots. (b) The average queuing delay. (c) The packet drop rate. (d) The probability that the HOL delay is larger than 6 frame periods. In each sub-figure, the plots with thin solid line, thickly solid line, thickly dashed line, thickly dotted line, and thickly dashed-dotted line denote our scheme with triplets (1, 1, 2), (2, 2, 5), (2, 3, 5), (3, 4, 25), and (6, 10, 20), respectively.	162
47	The idle probability of time slots against the packet arrival rate. The average SNR ($\bar{\gamma}$) is 10 dB.	164
48	The probability that the HOL delay is larger than 3 frame periods when the packet arrival rate varies and the average SNR ($\bar{\gamma}$) is 10 dB.	165

FIGURE	Page
49 The probability that the HOL delay is larger than 6 frame periods when the packet arrival rate varies and the average SNR ($\bar{\gamma}$) is 10 dB.	166
50 The average packet delay against the packet arrival rate. The average SNR ($\bar{\gamma}$) is 10 dB.	167
51 The packet drop rate against the packet arrival rate. The average SNR ($\bar{\gamma}$) is 10 dB.	168

CHAPTER I

INTRODUCTION

A. Background of the Research

1. The Overview of Cognitive Radio Networks

The rapid growth in the ubiquitous wireless services has imposed increasing stress on the fixed and limited radio spectrum. Allocating a fixed frequency band to each wireless service, which is the current frequency allocation policies, is an easy and natural approach to eliminate interference between different wireless services. However, extensive measurements reported indicate that the static frequency allocation results in a low utilization of the licensed radio spectrum in most of the time [1, 2]. Even when a channel is actively used, the bursty nature of most data traffics still implies that a great amount of opportunities exist in using the spare spectrum.

In order to better utilize the licensed spectrum, the Federal Communication Committee (FCC) has recently suggested a new concept/policy for *dynamically* allocating the spectrum [3, 4]. Consequently, a promising implementation technique of this concept, called the *cognitive radio* [5], is proposed to take advantage of this more open spectrum policy for alleviating the severe scarcity of spectrum bandwidth. Cognitive radio is typically built on top of the software-defined radio (SDR) technology, in which the transmitter's operating parameters, such as the frequency range, modulation type, and maximum transmission power can be dynamically adjusted by software [6–10]. In the cognitive radio networks, the *secondary* (unlicensed) users (SUs) can periodically scan and identify the vacant channels in the spectrum. Based

This dissertation follows the style of *IEEE Journal on Selected Areas in Communications*.

on the scanned results, the SUs dynamically tune their transceivers to the identified spare channel spectrum to communicate among themselves while limiting their interference imposed onto the *primary* (licensed) users (PUs) to an acceptable low and harmless level.

The cognitive radio technology has received intensive attention since it was first coined by Dr. J. Mitola III in 1999 [11]. The cognitive radio wireless networks can be broadly categorized into the following two types: synchronous cognitive radio wireless networks [12–17] and asynchronous cognitive radio wireless networks [18–24]. In the synchronous cognitive radio networks, the time axis is divided into slots. The SU networks are synchronized with the PU networks. In other words, the SUs have the same knowledge on the boundary of time slots as the PUs. In the synchronous cognitive radio networks, a given PU starts utilizing the licensed spectrum only at the beginning of a time slot. If the PU uses the licensed spectrum at the beginning of the time slot, it continues to utilize the spectrum for the rest of this time slot. Since the SUs are synchronized with the PUs, the SUs only need to sense the licensed spectrum at the beginning of a time slot to determine whether this time slot is available to be used. In the asynchronous cognitive radio networks, the SUs repeat the sensing-transmission cycle for every time slot. If the spectrum sensing returns perfect sensing results, there is no interference caused to the PUs.

On the other hand, unlike the counterpart in synchronous cognitive radio networks, the SUs in asynchronous cognitive radio networks cannot be synchronized with the PUs. For example, the PU networks are based on the carrier sensing multiple access (CSMA)-like random access. Due to the half-duplex characteristic of the wireless radio, SUs cannot sense the channel while concurrently transmitting their own signals, which implies that the SUs cannot accurately know whether the PUs become active again when the SUs are utilizing the PUs' licensed spectrum. Therefore, if the

PUs become active when the SUs are occupying the spectrum, the SUs may cause the PUs to incorrectly transmit/receive signals for a while, significantly impairing the performance of PUs. Since the interference caused by the SUs is unavoidable in the asynchronous cognitive radio networks, it is critical to limit the SUs' interference to an acceptable low level.

2. Spectrum Sharing Methodologies in Cognitive Radio Networks

According to the relationship between the PUs' and SUs' signals, the approaches to implementing the opportunistic spectrum sharing can be categorized into three types, namely *overlay*, *underlay*, and *interweave* [25,26]. For the overlay spectrum sharing mode (e.g., [9,27–29]), the PUs' and SUs' signals can co-exist at the same frequency band simultaneously. The key idea of the overlay spectrum sharing mode is that SUs may use a part of their energy to assist the communications of PUs through cooperative communications techniques [30,31] and the rest of the energy to transmit their own signals. As a result, the interference from the SUs' signals can be compensated with the gain for the PUs' signal quality through the cooperation of the SUs. However, the implementation of the overlay spectrum sharing mode requires the SUs to know the PUs' packets before the PUs begin their transmissions, which is not practical in the realistic cognitive radio networks.

Second, in the underlay spectrum sharing mode the PUs' and SUs' signals can also co-exist at the same frequency band simultaneously. In particular, the SUs can “share” the licensed spectrum with the PUs simultaneously by using spread spectrum techniques, such as ultrawide band (UWB) and code division multiple access (CDMA). Thus, the SUs transmit signals in such a low power level that the interference caused by the SUs is below the noise floor of the spectrum. In other words, in the view point of PUs, the transmissions by SUs are nothing but noise with the low-

level power. To maintain the low-level interference, in the underlay spectrum sharing mode the SUs need to have many aspects of information about the PUs, such as the channel between SUs and PUs, PUs' transmit power, PUs' locations, etc. Since the PU cannot perceive the existence of SUs, we also call the underlay spectrum sharing mode as the *non-intrusive spectrum sharing* mode.

Third, in the interweave spectrum sharing mode the SUs opportunistically exploit the *spectral holes* to communicate. Specifically, the SUs frequently sense the channel. When the SUs discover that the PUs are absent from the licensed spectrum, the SUs do not need to worry about the interference temperature constraint¹ of PUs and can significantly relax the power constraints imposed onto SUs as compared with the underlay spectrum sharing mode. In other words, the SUs can fully take over the licensed spectrum, and thus use any transmit power level which is not limited by the PUs. For the case where the SUs can be synchronized with the PUs (i.e., the synchronous cognitive radio networks) and the perfect sensing can be achieved, SUs will not impose any interference to PUs. However, due to half-duplex of the wireless radio, SUs cannot sense the channel while concurrently transmitting their own signals simultaneously, which implies that the SUs cannot accurately know when the PUs become active again, especially when the SUs are not synchronized with PUs (i.e., the asynchronous cognitive radio networks). Therefore, the SUs may cause the PUs to be unable to correctly transmit/receive signals for a certain period, which significantly impairs the performance of PUs. In this sense, we also call the interweave spectrum sharing mode as the *intrusive spectrum sharing* mode in the asynchronous cognitive radio networks.

¹The interference temperature constraint is defined as the maximum acceptable level of RF interference at the receiver antenna in the frequency band of interest. In other words, any transmission is considered to be harmful if it increases the noise floor above the interference-temperature constraint.

In practice, as compared with the underlay spectrum sharing mode, the interweave spectrum sharing mode requires less information about the PUs and it can utilize the spectrum more efficiently because of no transmit power constraint. As a result, the interweave spectrum sharing mode has more application targets than the underlay spectrum sharing mode.

3. Research Challenges and Motivations

Simple as the basic idea of cognitive radio is, the efficient design of cognitive radio networks imposes the new challenges that are not present in the conventional wireless networks [6–8, 32–34]. The variation of spectrum availability over the time and space due to coexistence with PUs, as well as the time-varying wireless channel characteristics, imposes critical design challenges in different aspects for cognitive radio wireless networks. Specifically, identifying the time-varying channel availability imposes a number of nontrivial design problems to the medium access control (MAC) layer. One of the most difficult, but important, design problems is how the SUs decide when and which channel they should tune to in order to transmit/receive the SUs' packets without causing harmful interference to the PUs [35–37]. This problem becomes even more challenging in wireless ad hoc networks where there are no centralized controllers, such as basestations or accessing points. Furthermore, designing MAC protocols for cognitive radio networks significantly depends on if the SUs are able to globally synchronized with the PUs.

In particular, we summarize the major challenges in developing opportunistic MAC protocols for cognitive radio networks as follows.

- Control channel configuration
- Spectrum sensing policies

- Opportunistic spectrum access and sharing
- Multi-channel hidden terminal problem
- Paradox between spectrum utilization and interference
- Hardware limitations

In this dissertation, we propose various spectrum sensing schemes, spectrum sharing schemes, and opportunistic packet scheduling schemes in the MAC layer to tackle the aforementioned challenges for different types of synchronous and asynchronous cognitive radio networks.

B. Related Work

1. Underlay Spectrum Sharing Mode Based MAC

There exist literatures on the underlay spectrum sharing mode based MAC for cognitive radio networks [38–43]. The authors of [38] proposed a code assignment scheme for the SUs in the asynchronous CDMA underlay cognitive radio networks over multipath fading channels, which aims at minimizing interference caused to the PUs. The authors of [39] focused on the CDMA-based underlay cognitive radio systems where the PUs can increase transmit power to counterbalance the harmful interference caused by the SUs. In particular, they studied the relationship among the interference threshold of SUs, the transmit rate of SUs, and the transmit power of PUs. In [40], the authors proposed a two-phase channel and power allocation scheme for the underlay-based multi-cell cognitive radio networks to improve the system throughput which is defined as the total number of simultaneously served subscribers. The authors of [41] proposed single input multiple output (SIMO) MAC with joint beam forming and power allocation, which takes into account the peak power constraints

for SUs and interference power constraints for PUs. In [42], the authors proposed a MAC framework for multi-carrier DS CDMA modulation based cognitive radio ad hoc networks using multi-carrier DS CDMA modulation, which targets at avoiding interference to the existing PUs' communications while minimizing total power consumption of the SUs. The authors of [43] developed the joint admission control and rate/power adaptation scheme to maximize the number of admitted SUs for the given fairness constraints.

2. Interweave Spectrum Sharing Mode Based MAC

a. MAC Protocols for Synchronous Cognitive Radio Networks

The research community has proposed several interweave spectrum sharing mode based MAC protocols for the synchronous cognitive radio networks [12, 13, 15, 44–50]. In particular, the authors of [12, 13] developed a cognitive-radio MAC protocol based on the partially observable Markov decision processes (POMDPs) framework. The author of [44] proposed a multi-channel opportunistic MAC protocol when the PU network is the Global System for Mobile Communications (GSM) cellular network. The authors of [45] developed a multi-channel cognitive MAC protocol, called C-MAC, which is closely based on the IEEE 802.22 standard. In [15], we developed a simple, but efficient, random sensing policy based opportunistic MAC protocol without taking into account the channel bonding/aggregation techniques. The authors of [46] developed the game-theory based synchronous MAC framework to analyze the behavior of cognitive radios for distributed adaptive channel allocation. In the work [47, 48], the sensing slot duration and transmission slot duration for cognitive MAC are studied, whose goal is to maximize the achievable throughput for the SUs in the synchronous cognitive radio networks. The authors of [49] proposed a decentralized game-theoretic

MAC protocol for synchronous cognitive radio networks, which applies an adaptive regret based learning procedure to identify and share temporarily vacant radio spectrum between multiple SUs by tracking the set of correlated equilibria of the game. The authors of [50] analyzed the structure, optimality, and performance of the myopic sensing policy in multi-channel MAC for synchronous cognitive radio networks under the independent and stochastically identical Gilbert-Elliot channel model with imperfect spectrum sensing.

b. MAC Protocols for Asynchronous Cognitive Radio Networks

For the asynchronous cognitive radio networks, the authors of [18] proposed a cognitive MAC protocol aiming to opportunistically utilize the TV broadcast bands. In [24], we developed an interference-constrained cognitive MAC protocol for the single-channel asynchronous cognitive radio networks, which can dynamically adjust the transmit duration of SUs based on the sensing results to balance the interference caused to PUs and the overall spectrum utilization efficiency. The authors of [51] proposed the dynamic open spectrum sharing (DOSS) MAC protocol providing an innovative solution to the hidden terminal problem by using three sets of radios. The authors of [52] proposed an opportunistic spectrum accessing scheme, which limits the power of secondary signal to satisfy the Quality-of-Service (QoS) constraints of the PUs. The authors of [53] studied the asynchronous MAC protocol by formulating a dynamic game where the strategy of an SU is selected solely based on the pricing information. The authors of [54] proposed the cognitive MAC with statistical channel allocation, in which the SUs select the channel that has the highest successful transmission probability to send packets based on the channel statistics. In [55], the authors proposed the spectral-agile MAC for multi-channel asynchronous cognitive radio network, which integrates jointly the spectral opportunity discovery, spectral

opportunity management, and spectral use coordination, to improve both spectrum utilization efficiency and secondary networks performance. The authors of [56] studied the data capacity of SUs in opportunistic spectrum access and proposed three random access schemes in MAC layer to exploit the spectral opportunities in licensed bands. In [57], the authors proposed a threshold-based sensing-transmission structure for asynchronous cognitive radio networks. The authors of [19] developed a MAC framework and studied performance limit on the throughput of asynchronous cognitive radio networks given the constraint on the number of PUs' packet collisions. The optimum spectrum access strategy for MAC under the developed framework for the perfect sensing case was also presented in [19]. In [58], the authors evaluated a cognitive MAC protocol in the wireless local area networks (WLANs) environment and studied the coexistence of the cognitive MAC protocol with multiple parallel WLAN channels by using the experimental testbed.

3. Spectrum Sensing in Cognitive Radio Networks

Spectrum sensing and channel probing, which provide the real-time spectrum/channel information required by the cognitive MAC layer, are a critical part for the cognitive radio networks. The review of spectrum sensing in cognitive radio networks can be found in [59, 60]. In terms of the signal detection pattern, the spectrum sensing can be categorized as the following three types: matched filter detection [61, 62], energy detection [62–64], and feature detection [65–68]. Both the matched filter detection-based spectrum sensing and feature detection-based spectrum sensing require the SUs to know the signal features of PUs, which significantly limit the application areas of these two types of spectrum sensing because the knowledge of PUs' signal features are typically not known by the SUs. In this dissertation, we mainly focus on the energy detection approach because its hardware implementation is simple, but efficient, and

more importantly, the energy detection approach does not require the knowledge of signal features of PUs.

The sensing scheduling plays an important role in the spectrum sensing because the sensing duration should be optimized to obtain an accurate sensing result while minimizing the sensing overhead. There are a number of literatures on the spectrum sensing scheduling schemes [15, 41, 69–75]. In [69], we proposed the power-efficient periodic spectrum sensing schemes. In [15], we developed the efficient collaborative sensing scheme for the multi-channel networks. The authors of [70] developed a game-theoretic sensing algorithm for multi-channel networks. The authors of [71] proposed to use the spectrum sensor cluster to enhance the accuracy of the sensing outcome. In [48], the authors studied the optimal sensing duration to maximize the SUs' achievable throughput. The authors of [72] presented an adaptive sensing scheduling scheme based on the channel conditions, which aims at maximizing the spectrum efficiency of the cognitive radio operations. The authors of [76] designed the myopic sensing policy for channel selection to maximize the average reward in the formulated multi-arm restless bandit process for the multi-channel network where the channels' states evolve as Markov chains. The authors of [73] developed the relay sensing scheme that exploits the spatial diversity in different SUs to improve the spectrum sensing capabilities. Since the SUs at different locations may have different knowledge about the PUs, the cooperative sensing strategies are proposed to improve the accuracy of the spectrum sensing results [74, 75, 77–80].

C. Research Contributions

The main contributions of this dissertation are listed as follows:

1. We propose various packet scheduling schemes and spectrum sharing schemes

in the MAC layer for different types of synchronous and asynchronous cognitive radio networks. Our proposed MAC protocols enable the SUs to opportunistically utilize the licensed spectrum while imposing zero or limited interference onto the PUs.

- (a) For the synchronous cognitive radio networks, we propose a cross-layer based multi-channel MAC protocol, which integrates the spectrum sensing at PHY layer and opportunistic spectrum access at MAC layer. Applying the interweave spectrum sharing mode, the proposed MAC protocol enables the SUs to identify and utilize the maximum number of vacant-channels that are not used by the PUs without causing any interference to the PUs.
- (b) For the hardware-constrained synchronous cognitive radio networks, we propose a channel-hopping single transceiver based MAC protocol. In our proposed channel-hopping MAC protocol, the SUs dynamically utilize the vacant channels by switching across the licensed channels with their distinct channel-hopping sequences. The main advantages of our proposed channel-hopping MAC are summarized as follows: 1) no extra control channel is needed; 2) it overcomes the single-control-channel bottleneck problem; and 3) only one transceiver is needed.
- (c) For the asynchronous cognitive radio networks, we propose an efficient Cognitive Radio-Enabled Multi-channel MAC (CREAM-MAC) protocol, which allows the SUs to best utilize the vacant licensed channels while avoiding the collisions among SUs and collisions between SUs and PUs. Employing the four-way handshakes of control packets, the CREAM-MAC protocol with a single transceiver can efficiently handle the traditional

hidden terminals and the multi-channel hidden terminals.

- (d) We propose an adaptive spectrum sharing scheme for CDMA based cognitive MAC in the uplink communications over the asynchronous cognitive radio networks, where the PUs may have different types of channel usage patterns. The proposed adaptive spectrum sharing scheme for cognitive MAC can adaptively choose between the interweave and underlay spectrum sharing modes to maximize the overall spectrum utilization in a way that constrains the level of interference to the range the PUs can tolerate.
2. We propose the novel spectrum sensing schemes and algorithms in the MAC and PHY layers. First, we propose two cooperative channel sensing policies, 1) the simple, but efficient random sensing policy; 2) the performance-enhanced negotiation-based sensing policy. Second, we propose the two-threshold based sequential sensing policy to reduce the false alarm probability while limiting the missed detection probability when there exist sensing errors.
 3. We utilize various analytical models, including the Markov chain models, $M/G^Y/1$ queuing models, cross-layer optimization models, etc., to rigorously analyze the performance of our proposed MAC protocols, in terms of throughput, delay, and packet drop rate, for the saturation network and non-saturation network cases, respectively.
 4. Besides developing MAC protocols for SU networks, we develop a packet scheduling scheme for the PU MAC protocol in the context of time division multiplex access (TDMA)-based cognitive radio wireless networks. The proposed SU-friendly TDMA MAC protocol is designed to operate friendly towards the SUs in terms of vacant-channel probability. The analytical results show that our

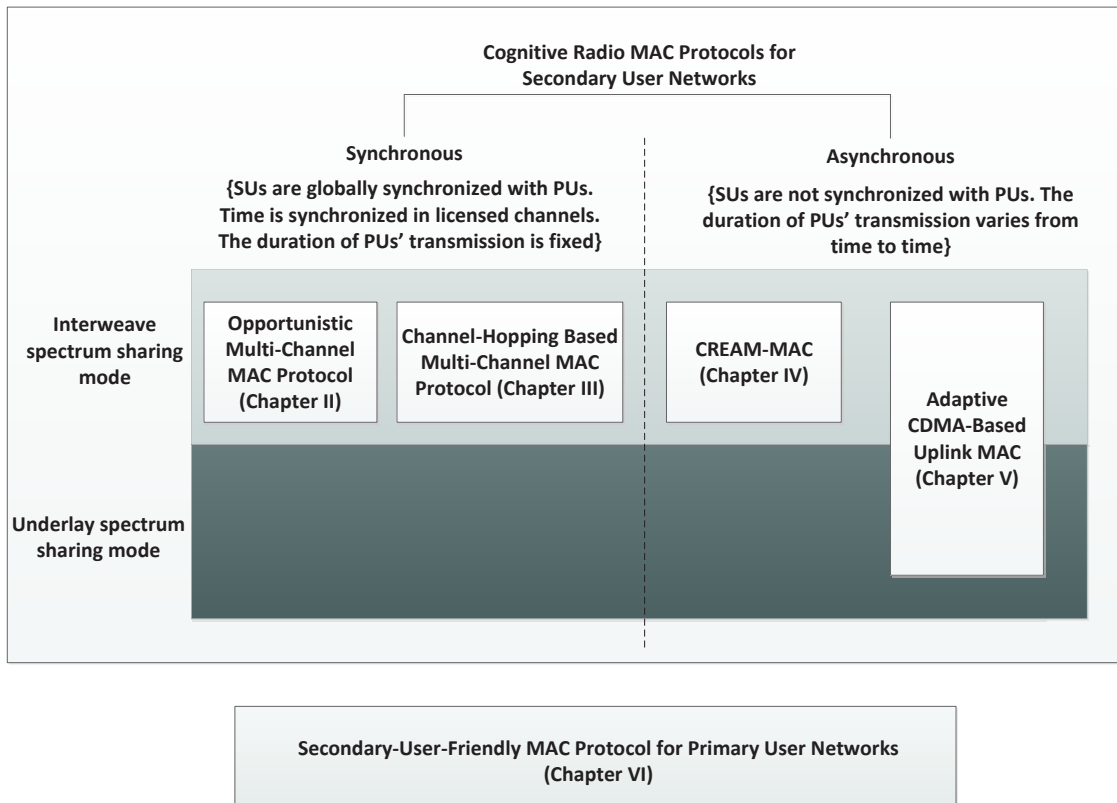


Fig. 1. Dissertation organization.

proposed scheme can generate more vacant-channel opportunities for SUs, at the expense of little increasing packet delay for PUs, as compared with the traditional wireless TDMA scheduling algorithm.

D. Outline of the Dissertation

The remainder of this dissertation is organized as follows. Fig. 1 illustrates the connections among Chapters II through VI.

In Chapter II, we propose and analyze the opportunistic multi-channel MAC protocol for the synchronous cognitive radio networks where the SUs are synchronized with the PUs. To detect the availabilities of the vacant licensed channels, we propose

two different channel sensing policies: the random sensing policy and the negotiation-based sensing policy. Applying the Markov chain model and the $M/G^Y/1$ queueing model, we develop analytical models to evaluate the performance of our proposed protocol with two channel sensing policies for both the saturation network case and non-saturation network case. Chapter II is in part a reprint of the material in the papers [14, 16].

In Chapter III, we propose and analyze the channel-hopping based cognitive MAC protocol for the synchronous cognitive radio networks, where each SU follows its own channel-hopping pattern when it doesn't have packets to send, while it follows its intended receiver's channel-hopping pattern if it wants to send packets to the intended receiver. We develop a Markov chain based analytical model to analyze the performance of our proposed cognitive MAC protocol in terms of aggregate throughput. We also identify the tradeoff between the channel utilization and the packet transmission delay. Chapter III is in part a reprint of the material in the paper [17].

In Chapter IV, we propose an efficient Cognitive Radio-Enabled Multi-channel MAC (CREAM-MAC) protocol, which integrates the cooperative sequential spectrum sensing at physical layer and the packet scheduling at MAC layer, over the asynchronous cognitive radio networks where the SUs are not synchronized with the PUs. We develop the Markov chain model and $M/G^Y/1$ queueing model to rigorously study our proposed CREAM-MAC protocol for both the saturation networks and the non-saturation networks. We also conduct extensive simulations to validate and evaluate our developed CREAM-MAC protocol. Chapter IV is in part a reprint of the material in the papers [20, 21].

In Chapter V, to achieve the optimal tradeoff between the spectrum utilization and the interference caused by SUs, we propose the adaptive spectrum sharing scheme for CDMA based cognitive MAC in the uplink communications over the asyn-

chronous cognitive radio networks. Our proposed scheme addresses the joint problems of channel sensing, data transmission, and power and rate allocations. We develop the adaptive selection principle for the SUs to choose between the interweave spectrum sharing mode and the underlay spectrum sharing mode to transmit data to secondary base station based on the channel utilization, traffic load, and interference constraints. We also conduct extensive simulations to validate and evaluate our proposed scheme, which shows the superiority of our proposed scheme as compared with the other existing schemes. Chapter V is in part a reprint of the material in the papers [22, 23].

Unlike the previous works focusing on the SU networks, in Chapter VI we propose and analyze the secondary-friendly MAC for PU networks. In particular, by exploiting the unique property of the wireless fading channel and cross-layer design technique, we develop a packet scheduling scheme for the PUs in the context of wireless TDMA networks, which is set up to operate friendly towards the SUs in terms of the vacant-channel probability. We develop a rigorous queuing model, and then quantitatively analyze the tradeoff among multiple performance metrics to identify when and where the cost for favoring the SUs is worthy. We also present the numerical and simulation results showing the performance of our proposed secondary-friendly MAC. Chapter VI is in part a reprint of the material in the paper [81].

In Chapter VII, we summarize the dissertation and point out future research directions.

CHAPTER II

CROSS-LAYER BASED OPPORTUNISTIC MAC PROTOCOLS FOR
SYNCHRONOUS COGNITIVE RADIO NETWORKS

A. Introduction

In this chapter, we focus on the synchronous cognitive radio networks where the secondary users (SUs) are globally time-synchronized with the primary users (PUs). In the synchronous cognitive radio networks, time is divided into time slots with equal length. The SUs have the same knowledge on the boundary of times slots as the PUs. The PUs are assumed to occupy the channel for the entire time slot if they access the channel at the beginning of the time slot. Since the SUs are synchronized with the PUs, the SUs have the full knowledge about the boundaries of the time slots.

The research community has proposed several opportunistic MAC protocols for cognitive radio networks. In particular, the authors of [12, 13] developed a cognitive-radio MAC protocol based on the partially observable Markov decision processes (POMDPs) framework. Although this policy can well exploit the available frequency spectrum, its implementation is complicated and hardware constraint because each SU needs to be equipped with multiple sensors to detect the channel activity in their scheme. The authors of [54] proposed the cognitive MAC with statistical channel allocation, in which the SUs select the channel that has the highest successful transmission probability to send packets based on the channel statistics. However, the computational complexity for determining the successful transmission probabilities

©2008 IEEE. Part of the material presented in this chapter is reprinted with permission from “Cross-layer based opportunistic MAC protocols for QoS provisionings over cognitive radio wireless networks” by H. Su and X. Zhang, published in *IEEE Journal on Selected Areas in Communications*, vol. 26, no. 1, pp. 118-129, Jan. 2008.

increases quickly with the number of licensed channels. The author of [44] proposed a multi-channel opportunistic MAC protocol, which however targets only at the Global System for Mobile Communications (GSM) cellular networks. The authors of [45] developed a multi-channel cognitive MAC protocol, called C-MAC, which, however, does not differentiate the PUs and the SUs. In [15], we developed a simple, but efficient, random sensing policy based opportunistic MAC protocol without taking into account the channel bonding/aggregation techniques. In addition, all these previous works do not address the delay analyses, which play an important role in designing the Quality-of-Service (QoS)-provisionings over cognitive radio wireless networks.

To amend the aforementioned problems of the existing schemes, in this chapter we propose the cross-layer based opportunistic multi-channel MAC protocols for synchronous cognitive-radio based ad hoc networks. Our proposed schemes integrate the spectrum sensing policy at the physical (PHY) layer with packet scheduling at the MAC layer. Under our proposed schemes, each SU consists of a control transceiver working on the dedicated control channel and a SDR-based transceiver that can be dynamically tuned to any one of the licensed channels to sense for the spare spectrum, and then to receive/transmit the SUs' packets. To detect the availability of the vacant channels, we propose the following two channel sensing policies, 1) the simple, but efficient, random sensing policy; 2) the performance-enhanced negotiation-based sensing policy. Our schemes smoothly coordinate the two transceivers of the SUs, enabling them to collaboratively sense and dynamically utilize the available frequency spectrum. In addition, our proposed cognitive-radio MAC protocols do not need any centralized controllers.

We also rigorously analyze the throughput and the delay-QoS performances of our proposed schemes for the saturation network and the non-saturation network cases, respectively. First, in the saturation network case, where the SUs always

have *non-empty* queues, we develop the Markov chain model to analyze the saturation throughput for our proposed schemes. Second, based on the $M/G^Y/1$ queueing theory, we also develop an analytical model to investigate the more generalized non-saturation network case, in which the packet arrivals are characterized by a Poisson process. The average aggregate throughput and the average delay analyses derived for non-saturation network case can help devise the important parameters, such as the packet arrival rate, to support the QoS requirements for wireless networks.

The rest of this chapter is organized as follows. Section B introduces the PUs' channel-usage model. Section C develops our proposed opportunistic multi-channel MAC protocols. Section D develops the analytical model to analyze our proposed MAC protocols in the saturation network case. Applying the $M/G^Y/1$ queueing model, Section E analyzes the packet transmission delay and throughput of our proposed cognitive-radio MAC protocols in the non-saturation network case. Section F evaluates our multi-channel MAC protocols based on our developed analytical models. The chapter concludes with Section G.

B. The PUs' Channel-Usage Model

As shown in Fig. 2, we consider a licensed spectrum band consisting of n channels. Each licensed channel is synchronous such that the PUs communicate with each other in a synchronous manner. Meanwhile, a number of SUs, which are synchronized with the PUs, opportunistically access the licensed spectrum without imposing interference to the PUs. In this chapter, we mainly focus on the scenarios where all SUs utilize the licensed channels used by the same set of PUs. This implies that the licensed channel availability information sensed by each SUs is consistent among all SUs. We model each channel as an ON-OFF source alternating between state ON (active)

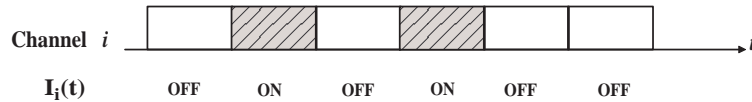


Fig. 2. The channel state for the i -th channel.

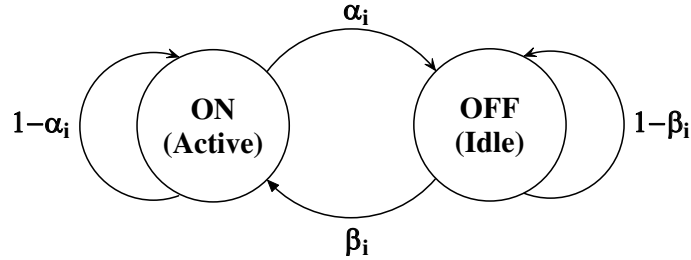


Fig. 3. The ON-OFF channel usage model for PUs.

and state OFF (inactive). An ON/OFF channel usage model specifies a time slot in which the PU signals is or isn't occupying a channel. The SUs can utilize the OFF time slot to transmit their own packets. Suppose that each channel changes its state independently. Let α_i be the probability that the i -th channel transits from state ON to state OFF and β_i be the probability that the i -th channel transits from state OFF to state ON, where $1 \leq i \leq n$. Then, the channel state can be characterized by a two-state Markov chain as shown in Fig. 3.

For the i -th channel in time slot indexed by t with $t = 1, 2, \dots, T, (T + 1), (T + 2), \dots$, the state of the i -th channel, denoted by $I_i(t)$, corresponds to a binary random variable, with 0 and 1 representing the *idle* and the *active* states, respectively. Hence, sensing a given channel produces a binary random sequence. The network state in the t -th time slot can be characterized as $[I_1(t), I_2(t), \dots, I_n(t)]$. Then, the i -th channel utilization, denoted by γ_i , with respect to the PUs, can be written as:

$$\gamma_i = \lim_{T \rightarrow \infty} \frac{\sum_{t=1}^T I_i(t)}{T} = \frac{\beta_i}{\alpha_i + \beta_i}, \quad (2.1)$$

where $1 \leq i \leq n$.

C. Our Proposed Cross-Layer Based Multi-Channel Opportunistic MAC Protocols

1. Overview

In our proposed cognitive radio-based multi-channel MAC protocols, each SU is equipped with two transceivers. The first transceiver (called the control transceiver) is devoted to operating over the dedicated control channel. The SUs use their control transceivers to obtain the information of the vacant licensed channels, and to negotiate with the other SUs through the contention-based algorithms, such as IEEE 802.11 distributed coordination function (DCF) [82] and p -persistent carrier sense multiple access (CSMA) [83] protocols. The second transceiver consists of a SDR module such that it can tune to any one of the n licensed channels to sense for spare spectrum, receive/transmit the SUs' packets. For convenience, we call the first transceiver the control transceiver and the second transceiver the SDR transceiver, respectively, in the rest of this chapter. Our protocols do not need any centralized controllers, which is an attractive feature for all distributed wireless ad hoc cognitive radio networks.

Fig. 4 shows the principle of our proposed schemes. In the control channel, the time axis is divided into a number of periodical time slots. All the time slots of the control channel have the same length as those of licensed channels and the slots of both control channel and licensed channels are synchronized. In the control channel, each slot is divided into two phases, namely, the *reporting phase* and the *negotiating phase*. The reporting phase can be further divided into n mini-slots, each of them corresponding to one of the n licensed channels.

Fig. 5 describes the pseudo code for our proposed scheme. At the beginning of each time slot, SUs sense the licensed channels, and then report the channel state by

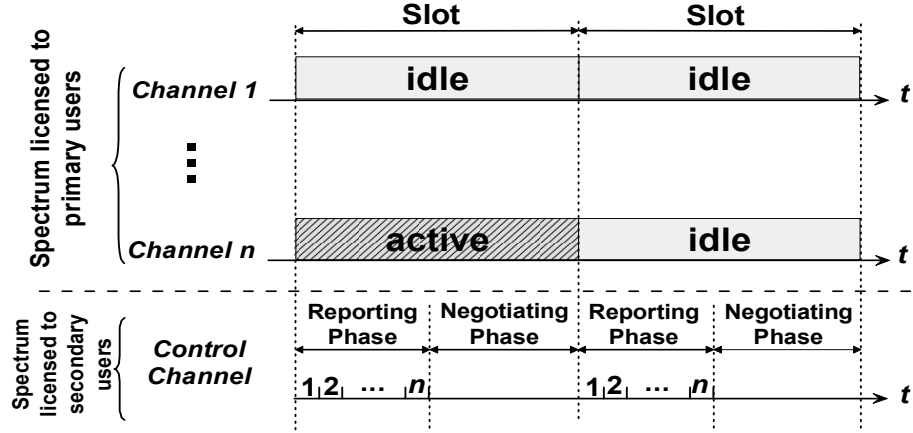


Fig. 4. The principle of our proposed MAC protocols.

sending the beacons in the mini-slots. Since each SU is equipped with only one SDR transceiver, which can operate on one channel at a time, it cannot accurately know the states of all the channels by itself. The goal of the channel-state-report process is to enable the SUs to have a large picture of all the channels' states through their cooperations. In particular, the SUs use SDR transceivers to sense one of n licensed channels, say i -th channel, ($1 \leq i \leq n$). If the SU perceives that the i -th channel is idle, then it uses the control transceiver to send a beacon during the i -th mini-slot over the control channel. Otherwise, it does not send any beacons. Each mini-slot lasts for T_{ms} time units, which is set to be long enough to determine whether channel is busy or not. Following the settings in IEEE 802.11a [82], we set T_{ms} to be equal to $9 \mu s$ in the rest of this chapter. Clearly, if each of the n licensed channels is sensed by at least one SU, all the SUs get the information about the activity of the entire licensed spectrum. We will develop the channel sensing policies which aim at gaining as much channel information as possible in Section C-3. If we denote T_S , T_{RP} , and T_{NP} as the time duration of the time slot, the reporting phase, and the negotiating

Opportunistic MAC protocol: code for every SU

01. Initially: $NAC := 0, LAC := \emptyset, send_flag := 0$

Reporting phase:

For Control transceiver:

02. Listens on the control channel
 03. **Upon** receiving a beacon at k -th mini-slot
 04. $NAC := NAC + 1$ //Update number of vacant channels
 05. $LAC(NAC) := k$ //Update list of vacant channels
 06. **Upon** Informed by SDR that j -th channel is idle
 07. Send a beacon at j -th mini-slot
 08. $NAC := NAC + 1$ //Update number of vacant channels
 09. $LAC(NAC) := k$ //Update list of vacant channels

For SDR transceiver:

10. Senses channel j which is decided by the sensing policy.
 11. **If** channel j is idle
 12. Inform Control transceiver that j -th channel is idle

Negotiating phase:

For Control transceiver:

13. **Upon** receiving RTS
 14. Update the channel it will sense according to sensing policy
 15. send CTS to source node
 16. **Upon** receiving CTS
 17. Update the channel it will sense according to sensing policy
 18. **If** destination address is myself //negotiation is succeeded
 19. Set $send_flag := 1$ at the end of this phase
 20. **If** the outgoing queue is not empty
 21. Contend to send RTS to the destination node

For SDR transceiver:

22. **If** $send_flag = 1$
 23. $send_flag := 0$
 23. Transmit the data packets over all the channels in LAC

Fig. 5. Pseudo code of the MAC protocol for the SUs, where NAC is the number of identified vacant channels, LAC is the list of identified vacant channels.

phase, respectively, then we obtain:

$$T_S = T_{RP} + T_{NP} = nT_{ms} + T_{NP}. \quad (2.2)$$

During the negotiating phase, the SUs use the control transceivers to negotiate about the data channels among the SUs by exchanging request-to-send (RTS) and clear-to-send (CTS) packets over the control channel. Meanwhile, the only SU which is the winner in contending for the data channels during the *last* time slot uses the SDR transceiver to transmit data packets over *all* the vacant licensed channels in the *current* time slot.

2. Channel Negotiation and Data Exchange

When an SU wants to initiate a transmission, it follows the p -persistent CSMA protocol to access the control channel to negotiate with the receiver. Particularly, the sender listens to the control channel and waits until it becomes idle. Then, it transmits the RTS packet with probability p . After the SU successfully receives CTS packet since sending the last RTS, it gets the permission to transmit data packets in the coming next time slot. By using the channel bonding/aggregation techniques [84], this SU utilizes *all* vacant channels collectively to transmit the data packets.

Note that in our proposed scheme, the SUs do not send the data packets over the licensed channels immediately after they successfully reserve the data channels at the same time slot. Instead, the SUs transmit data packets in the next following time slot after they successfully exchange RTS/CTS packets with their destination SUs in the current time slot.

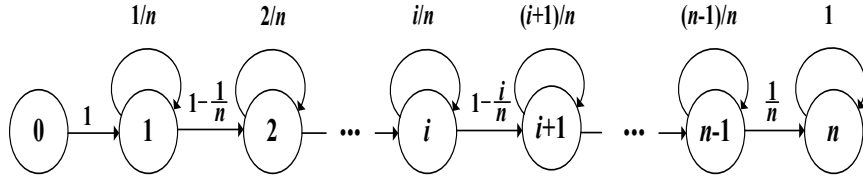


Fig. 6. The $(n + 1)$ -state Markov chain $\{S_u\}$ for the number of sensed channels, where the variable in each circle represents the number of distinct channels sensed by the SUs.

3. Channel Sensing Policies

To identify which channels are idle (i.e., not used by the PUs), the SUs need a channel sensing policy to dynamically detect the states of channels. We develop two simple, but efficient, sensing mechanisms, namely the *random sensing policy* (RSP) and the *negotiation-based sensing policy* (NSP) in this chapter. Our following analyses show that our proposed schemes can also fully utilize the vacant frequency spectrum. We start with the simple random sensing policy, and then describe the enhanced negotiation-based sensing policy.

In the random sensing policy, the SUs cooperate to sense the licensed channels. Each SU randomly chooses one of the n licensed channels for sensing. The chosen channels among all the SUs are independent and identically distributed (i.i.d.). Let u , where $u = 1, 2, \dots$, be the number of SUs in the networks. Define a random variable, S_u , which stands for the total number of distinct channels that the SUs have sensed given that there are u SUs. Then, we develop a Markov chain model to calculate the probability mass function (pmf) of S_u , denoted by $\Pr\{S_u = s\}$, that the number of channels sensed by the SUs is s with $s = 0, 1, \dots, n$. Each SU *independently* and *uniformly* selects one of the n channels with probability of $1/n$. We can model the channel sensing process as a Markov chain, $\{S_u\}$, having $(n + 1)$ states, as shown in Fig. 6, where the variable in the circle represents the number of channels sensed

by the SUs. The transition probability, denoted by $q_{i,j}$, of the Markov chain can be written as

$$q_{i,j} \triangleq \Pr\{S_{u+1} = j | S_u = i\} = \begin{cases} \frac{i}{n}, & j = i, \\ 1 - \frac{i}{n}, & j = i + 1, \\ 0, & \text{otherwise,} \end{cases} \quad (2.3)$$

where $i, j = 0, 1, 2, \dots, n$. Thus, we are able to derive the probability transition matrix for the Markov chain $\{S_u\}$, denoted by \mathbf{Q} , as follows:

$$\mathbf{Q} \triangleq \{q_{i,j}\} = \begin{bmatrix} 0 & 1 & \cdots & 0 & 0 & 0 & \cdots & 0 & 0 \\ 0 & \frac{1}{n} & \cdots & 0 & 0 & 0 & \cdots & 0 & 0 \\ \vdots & \vdots & \ddots & \vdots & \vdots & \vdots & \ddots & \vdots & \vdots \\ 0 & 0 & \cdots & \frac{i}{n} & \frac{n-i}{n} & 0 & \cdots & 0 & 0 \\ 0 & 0 & \cdots & 0 & \frac{i+1}{n} & \frac{n-i-1}{n} & \cdots & 0 & 0 \\ \vdots & \vdots & \ddots & \vdots & \vdots & \vdots & \ddots & \vdots & \vdots \\ 0 & 0 & \cdots & 0 & 0 & 0 & \cdots & \frac{n-1}{n} & \frac{1}{n} \\ 0 & 0 & \cdots & 0 & 0 & 0 & \cdots & 0 & 1 \end{bmatrix}_{(n+1) \times (n+1)} \quad (2.4)$$

where $q_{i,j}$ is defined by Eq. (2.3). Note that \mathbf{Q} is an $(n+1) \times (n+1)$ upper bidiagonal matrix. The probability $\Pr\{S_u = s\}$ that the number of sensed channels is s on the condition that the number of SUs is u is equivalent to the u -step transition probability from the state of 0 to the state of s for the Markov chain $\{S_u\}$, which can be expressed as

$$\Pr\{S_u = s\} = \mathbf{Q}^u|_{(0,s)}, \quad (2.5)$$

where $\mathbf{X}|_{(i,j)}$ denotes the element in position row i and column j of matrix \mathbf{X} . Clearly, the probability that all the licensed channels are sensed by the SUs (i.e., $\Pr\{S_u = n\}$)

only depends on the number of SUs (i.e., u), and this probability gets larger when u increases. Using Eq. (2.5) to get the numerical results, we can further obtain the relationship between the number of SUs and the number of sensed channels. For example, in the case where the number of licensed channels is 10, the probability that all licensed channels are sensed is close to 0.95 when $u = 50$, but this probability reduces to only 0.036 when u is equal to the number of licensed channels. Based on these observations, we obtain the following Facts.

Fact 1. *In the random sensing policy, the more the number of SUs is, the more likely the number of sensed channels is large.*

We further study the asymptotical case in terms of the number of SUs. When the number of SUs goes to infinity, Eq. (2.5) can be rewritten as:

$$\lim_{u \rightarrow \infty} \Pr\{S_u = s\} = \begin{cases} 1, & s = n \\ 0, & 0 \leq s \leq (n - 1), \end{cases} \quad (2.6)$$

which leads to the following Fact.

Fact 2. *When the number of SUs is large enough, the SUs can sense all of the licensed channels even using the simple random sensing policy.*

However, the simple channel-sensing policy is not good enough when the number of SUs is smaller than or close to the number of the licensed channels. To amend this weakness of the random sensing policy, we further propose the negotiation-based sensing policy. The basic idea of the negotiation-based sensing policy is to let the SUs know which channels are already sensed by their neighboring SUs, and then select the different channels to sense at the next time slot.

From the view point of the SUs, there are three types of channels in any given t -th time slot, including 1) the set of channels, denoted by $B_0(t)$, that are idle and

sensed by the SUs, 2) the set of channels, denoted by $B_1(t)$, that are busy and sensed by the SUs, and 3) the set of channels, denoted by $B_2(t)$, that are not sensed by the SUs. Note that $B_0(t)$ is also the set of mini-slots during which the beacon are sent, while $(B_1(t) \cup B_2(t))$ is the set of mini-slots during which no beacons appear in t -th time slot. Let $|B_0(t)|$, $|B_1(t)|$, and $|B_2(t)|$ be the cardinalities of $B_0(t)$, $B_1(t)$, and $B_2(t)$, respectively.

At the very beginning, the negotiation-based sensing policy also requires the SUs to randomly select a licensed channel to sense, and then report the channel state by sending beacons in the reporting phase. Under the negotiation-based sensing policy, each RTS/CTS packet has a byte of special field containing the sensed channel information. During the negotiating phase, the SUs include the information of the channel they have sensed into the RTS/CTS packets. When the SUs exchange the RTS/CTS packets, the neighboring SUs overhear these ongoing RTS/CTS packets transmitted, and then know whether they have sensed the same channels. If there are neighboring SUs that sense the same channels as the sender in t -th time slot, each of them will sense another different licensed channel in the $(t + 1)$ -th time slot, which is randomly picked up from the set of $(B_1(t) \cup B_2(t))$.

Intuitively, the negotiation-based sensing policy will eventually attain the desired state, where all the channels are sensed by the SUs if the number of SUs are larger than or equal to the number channels, or otherwise each channel is sensed by no more than one SU. We show that the desired state is attainable by the negotiation-based sensing policy in the following discussions, and we will also evaluate how long it takes to attain the desired state in Section F.

To prove that the desired state is attainable, we first present the following Proposition.

Proposition 1. (*Non-decreasing Property*) For the negotiation-based sensing policy, the number of licensed channels which are sensed by the SUs in the $(t+1)$ -th time slot is always larger than or equal to that in the t -th time slot, for any given $t = 0, 1, 2, \dots$.

Proof. The proof is detailed in Appendix A. \square

Proposition 2. If the number of SUs is larger than or equal to the number of licensed channels, all the licensed channels can be eventually sensed by using the negotiation-based sensing policy.

Proof. Since the number of licensed channels that are sensed is non-decreasing function in terms of time index as shown in Proposition 1, the number of sensed channels continues to increase with some probability before all the channels are sensed. Thus, Proposition 2 follows, which shows that the desired state is attainable. \square

D. Throughput Analyses for the Saturation Network Case

Without loss of generality, we adopt p -persistent CSMA as the data channel accessing scheme for the SUs during the negotiating phase. In this section, we develop an analytical model to analyze the aggregate throughput of our proposed scheme based on the channel sensing policies and p -persistent CSMA scheme under the saturation network case.

1. The p -Persistent CSMA Scheme for Negotiating Phase

Under the p -persistent CSMA protocol, if the channel is detected as busy, the SU with non-empty queue waits until channel becomes idle, and then transmits the packet with probability p . We consider the *saturation networks*, where each SU *always* has non-empty queue. Thus, all the SUs contend for sending the RTS packets during the negotiating phase by using p -persistent CSMA. If we denote T_{succ} and T_{coll} as

the time spent by a successful transmission and the time spent by an unsuccessful transmission, respectively, then we have

$$\begin{cases} T_{\text{succ}} = RTS + SIFS + CTS + DIFS, \\ T_{\text{coll}} = RTS + DIFS, \end{cases} \quad (2.7)$$

where RTS is the time spent by sending a RTS packet, CTS is the time spent by sending a CTS packet, $SIFS$ is the time interval of short inter-frame space (SIFS), and $DIFS$ is the time interval of DCF inter-frame space (DIFS).

In the p -persistent CSMA, if we denote P_{idle} , P_{succ} , and P_{coll} as the probability that the channel is idle, the probability that a node successfully transmits an RTS packet, and the probability that the collision occurs, respectively, then we obtain

$$\begin{cases} P_{\text{idle}} = (1 - p)^u, \\ P_{\text{succ}} = up(1 - p)^{u-1}, \\ P_{\text{coll}} = 1 - (1 - p)^u - up(1 - p)^{u-1}, \end{cases} \quad (2.8)$$

where u is the number of SUs. Further, we can calculate the average time, denoted by $T(p, u)$, used for a successful transmission as follows:

$$T(p, u) = \frac{T_{ms}P_{\text{idle}} + T_{\text{succ}}P_{\text{succ}} + T_{\text{coll}}P_{\text{coll}}}{P_{\text{succ}}}, \quad (2.9)$$

where T_{ms} is the length of a mini-slot. To ensure that the SUs can successfully exchange the RTS/CTS packets, $T(p, u)$ should be shorter than or equal to the length of negotiating phase, that is,

$$T(p, u) \leq T_{NP}, \quad (2.10)$$

where T_{NP} is defined in Eq. (2.2).

2. The Aggregate Throughput for the Saturation Network Case

We study the aggregate saturation network throughput of the SUs, each of which has a non-empty queue and always contends for data channels. We derive the throughput for the random sensing policy and the throughput for the negotiation-based sensing policy, respectively, in the following.

a. Employing the Random Sensing Policy

Let $M(t)$ be the random number of the vacant channels at the t -th time slot. Suppose that there are n licensed channels and all licensed channels have the same channel utilization, denoted by γ , with respect to the PUs, i.e.,

$$\gamma = \gamma_i = \gamma_j, \forall 1 \leq i, j \leq n \text{ and } i \neq j, \quad (2.11)$$

where γ_i is determined by Eq. (2.1). Since the states among the n licensed channels are independent and the probability that the channel is active is γ , $M(t)$ follows the binomial distribution, that is,

$$\Pr\{M(t) = m\} = \binom{n}{m} \gamma^{n-m} (1 - \gamma)^m. \quad (2.12)$$

Suppose that the SUs can always sense the channels correctly. Similar to the analyses described in Section C, we can use a Markov chain to derive the distribution of the number of vacant channels identified by the SUs. Given $M(t) = m$ at t -th time slot, we can get the conditional transition probabilities, denoted by $w_{i,j}$ with $0 \leq i, j \leq m$, as follows:

$$\Pr\{w_{i,j} | M(t) = m\} = \begin{cases} 1 - \binom{m-i}{n}, & i = j, \\ \binom{m-i}{n}, & j = i + 1, \\ 0, & \text{otherwise.} \end{cases} \quad (2.13)$$

where $0 \leq m \leq n$. Given $M(t) = m$, the above transition probabilities generate the probability transition matrix, denoted by \mathbf{W}_m , which is a $(m+1) \times (m+1)$ upper bidiagonal matrix. Let u be the number of SUs. Given $M(t) = m$, we obtain the probability that the random number, denoted by $L_{RSP}(t)$, of vacant channels perceived by the SUs is equal to i at t -th time slot, as follows:

$$\Pr\{L_{RSP}(t) = i | M(t) = m\} = (\mathbf{W}_m)^u|_{(0,i)}, \quad (2.14)$$

where $0 \leq i \leq n$, and $\mathbf{X}|_{(i,j)}$ represents the element in position row i and column j of matrix \mathbf{X} . Using Eqs. (2.14) and (2.12), we can obtain the pmf for the number of identified vacant channels as follows:

$$\begin{aligned} \Pr\{L_{RSP}(t) = i\} &= \sum_{m=0}^n \Pr\{M(t) = m\} \Pr\{L_{RSP}(t) = i | M(t) = m\} \\ &= \begin{cases} \sum_{m=0}^n \binom{n}{m} \gamma^{n-m} (1-\gamma)^m [(\mathbf{W}_m)^u|_{(0,i)}], & 0 \leq i \leq n, \\ 0, & \text{otherwise.} \end{cases} \end{aligned} \quad (2.15)$$

If we let \bar{L}_{RSP} be the average number of vacant channels that the SUs can utilize, then we obtain

$$\bar{L}_{RSP} = \sum_{i=0}^n i \Pr\{L_{RSP}(t) = i\}. \quad (2.16)$$

Let the data rate of i -th licensed channel for the SUs be R_i , where $0 \leq i \leq n$. Without loss of generality, we assume that all the n licensed channels have the same bandwidth, i.e., $R_i = R_j = R, \forall 0 \leq i, j \leq n$ and $i \neq j$. Since the transmission over the data channels are contention-free in our proposed protocols, we obtain the aggregate throughput, denoted by θ_{RSP} , for the SUs as follows: expressed as:

$$\theta_{RSP} = \frac{\bar{L}_{RSP} R T_{NP}}{T_S}, \quad (2.17)$$

where the factor of T_{NP}/T_S is due to the fact that the data transmission starts immediately after the reporting phase and continues for a period of T_{NP} in every time slot.

b. Employing the Negotiation-Based Sensing Policy

We study the saturation network throughput achieved by the negotiation-based sensing policy after it attains the desired state. We obtain the probability that the random number, denoted by $L_{NSP}(t)$, of the vacant channels perceived by the SUs is equal to i at the t -th time slot as follows:

$$\Pr\{L_{NSP}(t) = i\} = \begin{cases} \binom{n}{i}\gamma^{n-i}(1-\gamma)^i, & u \geq n \text{ and } 0 \leq i \leq n, \\ \binom{u}{i}\gamma^{u-i}(1-\gamma)^i, & u < n \text{ and } 0 \leq i \leq u, \\ 0, & \text{otherwise.} \end{cases} \quad (2.18)$$

If we let \bar{L}_{NSP} be the average number of vacant channels that the SUs can utilize for negotiation-based sensing policy, then we obtain

$$\bar{L}_{NSP} = \sum_{i=0}^n i \Pr\{L_{NSP}(t) = i\}. \quad (2.19)$$

Then, we get the aggregate throughput, denoted by θ_{NSP} , for the saturation networks under the negotiation-based sensing policy as follows:

$$\theta_{NSP} = \frac{\bar{L}_{NSP}RT_{NP}}{T_S}. \quad (2.20)$$

E. Throughput and Packet Transmission Delay Analyses for the Non-Saturation Network Case

In this section, we analyze the our proposed protocols' performance, including the aggregate throughput, queueing delay, and service delay for the non-saturation-network

case, where the SUs may have the empty queues. Without loss of generality while making the analysis trackable, we assume that the packets of the SUs arrive according to the Poisson process with a mean arrival rate λ [83] [85] [86]. For convenience of presentation, we call the procedure, during which an SU successfully reserves the data channels and transmits data packets, a *service procedure*, or simply, a *service*, in the following discussions.

Thanks to the channel-bonding technology, the SUs can send multiple data packets during every time slot which they have successfully reserved in the negotiating phases. Note that the number of data packets that an SU can send at a time slot depends on the number of identified vacant channels during that time slot, which is a random variable. This implies that the service capacity for the SUs *varies* during the different time slots.

Therefore, for this non-saturation-network case, we use the single-server bulk-service queueing model, $M/G^Y/1$, to investigate the aggregate throughput, queueing delay, and service delay, where Y stands for the variable service capacity.

To derive the queueing delay and aggregate throughput, we need to obtain the equilibrium-state distribution of the number of buffered packets in the queue for any given SU at any random points. We start with studying the random number, N_τ^+ , $\tau = 0, 1, 2, \dots$, where τ is used to index the services, of the packets in the system for a given SU immediately after the τ -th service. The probability, denoted by P_j^+ , that the system has j packets in the equilibrium state can be expressed as:

$$P_j^+ = \lim_{\tau \rightarrow \infty} \Pr\{N_\tau^+ = j\}. \quad (2.21)$$

Let Y_τ , $\tau = 0, 1, 2, \dots$ be the service capacity during the τ -th service. That is, the given SU can send $\mathbf{min}\{Y_\tau, \text{entire queue length}\}$ packets during the τ -th service. The distribution of Y_τ depends on the number of identified vacant channels, and thus we

obtain Y_τ 's distributions for random sensing and negotiation-based sensing policies, respectively, as follows:

$$\Pr\{Y_\tau = i\} = \begin{cases} \Pr\{L_{RSP}(\tau) = i\} \lfloor \frac{T_{NPR}}{\ell} \rfloor, & \text{for RSP,} \\ \Pr\{L_{NSP}(\tau) = i\} \lfloor \frac{T_{NPR}}{\ell} \rfloor, & \text{for NSP.} \end{cases} \quad (2.22)$$

where ℓ is the length of the data packets, R is the data rate for each channel, T_{NPR} is the length of the negotiating phase, and the distributions of L_{RSP} and L_{NSP} during the τ -th service are characterized by Eqs. (2.15) and (2.18), respectively. Then, the pmf, denoted by y_i , that the given SU sends i data packets during a service at the equilibrium state, can be determined by

$$y_i = \lim_{\tau \rightarrow \infty} \Pr\{Y_\tau = i\}. \quad (2.23)$$

Note that the sequence of $\{y_i\}$ is independent of the arrival process of the packets for a given SU. Then, we get the average number, denoted by \bar{y} , of packets that an SU can send during a service as follows:

$$\bar{y} = \begin{cases} \bar{L}_{RSP} \lfloor \frac{T_{NPR}}{\ell} \rfloor, & \text{for RSP,} \\ \bar{L}_{NSP} \lfloor \frac{T_{NPR}}{\ell} \rfloor, & \text{for NSP,} \end{cases} \quad (2.24)$$

where \bar{L}_{RSP} and \bar{L}_{NSP} are given by Eqs. (2.16) and (2.19), respectively. We define

$$\begin{cases} \phi_j \triangleq \sum_{m=j}^n y_m, \\ \Phi_j(z) \triangleq \sum_{m=j}^n y_m z^m, \end{cases} \quad (2.25)$$

where $j = 0, 1, 2, \dots$ and n is the number of licensed channels. Note that $\Phi_0(z)$ is the probability generating function (PGF) for $\{y_i\}$ and $\Phi_0(1) = \phi_0$.

Let p_s be the probability that a given SU can successfully reserve the data channels and V be the number of time slots spent to successfully reserve the data channels (i.e., service period) respectively. Since the p -persistent CSMA scheme is fair to each

SU, p_s is inversely proportional to the number of SUs (u), i.e.,

$$p_s = \frac{1}{u}. \quad (2.26)$$

Then, the service period, denoted by V , follows the geometric distribution, which has the following pmf:

$$\Pr\{V = v\} = p_s(1 - p_s)^{v-1} = \frac{(u - 1)^{v-1}}{u^v}, \quad (2.27)$$

where $v = 1, 2, \dots$. Thus, we can get the average service period, denoted by $E[V]$ for a given SU as follows:

$$E[V] = \frac{1}{p_s} = u. \quad (2.28)$$

Consequently, we can calculate the system utilization, denoted by ρ , as follows:

$$\rho \triangleq \frac{\lambda E[V]}{\bar{y}} = \frac{\lambda u}{\bar{y}}, \quad (2.29)$$

where \bar{y} is given by Eq. (2.24). For the equilibrium-state probability distribution to exist, ρ should be less than 1.

Let ψ be the random number of arrived packets for a given SU during the τ -th service. Since the packet arrivals comply with the Poisson process, given that the service period has v time slots, we obtain the probability that the number of arrived packets is j as follows:

$$\Pr\{\psi = j|V = v\} = \frac{e^{-\lambda v}(\lambda v)^j}{j!}. \quad (2.30)$$

Removing the conditioning on V in Eq. (2.30), we get the probability that the number

of arrived packets is j as follows:

$$\begin{aligned} \Pr\{\psi = j\} &= \sum_{v=1}^{\infty} \Pr\{\psi = j|V = v\} \Pr\{V = v\} \\ &= \sum_{v=1}^{\infty} \frac{e^{-\lambda v} (\lambda v)^j}{j!} [p_s(1-p_s)^{v-1}]. \end{aligned} \quad (2.31)$$

Then, we get the PGF, denoted by $\Psi(z)$, of $\Pr\{\psi = j\}$ as follows:

$$\begin{aligned} \Psi(z) &= \sum_{j=0}^{\infty} \Pr\{\psi = j\} z^j \\ &= \sum_{j=0}^{\infty} \sum_{v=1}^{\infty} \frac{e^{-\lambda v} (\lambda v)^j}{j!} [p_s(1-p_s)^{v-1}] z^j \\ &= \frac{e^{\lambda(z-1)}}{u - (u-1)e^{\lambda(z-1)}}. \end{aligned} \quad (2.32)$$

Based on [87], the PGF, denoted by $P^+(z)$, of P_j^+ can be derived as

$$P^+(z) = \frac{\sum_{i=0}^n P_i^+ [z^n \phi_i - z^i \Phi_i(z^{-1})]}{z^n \left[\frac{1}{\Psi(z)} - \Phi_0(z^{-1}) \right]}. \quad (2.33)$$

Setting the denominator of Eq. (2.33) to be zero, we have

$$\Psi(z) \Phi_0(z^{-1}) = 1. \quad (2.34)$$

Solving Eq. (2.34), we can obtain $(n-1)$ roots, denoted by z_1, z_2, \dots, z_{n-1} , respectively, which are located inside the unit circle, and one root which is located on the unit circle [88]. Therefore, P_j^+ can be determined by the following equation:

$$P_j^+ = \begin{cases} \frac{\bar{y}(1-\rho) \prod_{i=1}^{n-1} z_i(z_i-1)^{-1}}{y_n}, & j = 0 \\ P_0^+ a_j - \frac{\sum_{i=n-j}^{n-1} P_{j-n+i}^+ y_i}{y_n}, & 1 \leq j < n \\ \frac{P_0^+ \Pr\{\psi=j-n\} a_j y_j + P_{j-n}^+ - y_n \sum_{i=n}^{j-1} P_i^+ \Pr\{\psi=j-i\} - \sum_{i=0}^{n-1} \sum_{k=0}^{j-n} P_{j+i-k-n}^+ y_i \Pr\{\psi=k\}}{y_n \Pr\{\psi=0\}}, & j \geq n \end{cases} \quad (2.35)$$

where a_j is the coefficient of z^j in $[(1-z) \prod_{i=1}^{n-1} (1-zz_i^{-1})]$, $0 \leq j \leq n$.

The average number of packets, denoted by L^+ , buffered in the system after a service at the equilibrium state is the first moment of N_τ^+ , and thus can be obtained by the following equation:

$$L^+ = \left. \frac{d}{dz} P^+(z) \right|_{z=1} = \frac{\lambda^2 \Psi^{(2)}(1) + \Phi_0^{(2)}(1)}{2\bar{y}(1-\rho)} + \frac{1-n+\rho(n-\rho\bar{y})}{1-\rho} + \sum_{i=1}^{n-1} (1-z_i)^{-1} \quad (2.36)$$

where $f^{(i)}(\cdot)$ indicates the i -th derivative of $f(\cdot)$.

After obtaining all the probability properties of the equilibrium-state number, N_τ^+ , of packets buffered in the system, we proceed to study the properties for number of packets in the queue at any random point. Let N_q be the equilibrium-state number of packets in the queue at a random point in time for a given SU and let $P_j = \Pr\{N_q = j\}$ be the probability that the queue for any given SU has j packets at a random point in the equilibrium state. The PGF, denoted by $P_q(z)$, of P_j can be obtained by [88]:

$$\begin{aligned} P_q(z) &= \sum_{j=0}^{\infty} P_j z^j \\ &= \frac{(1-\Psi(z))P^+(z)}{\bar{y}\rho(1-z)\Psi(z)} \\ &= \frac{\left[\sum_{i=0}^n y_i \left(\sum_{j=0}^i P_j^+ + \sum_{j=1}^{\infty} P_{j+1}^+ z^j \right) \right]}{\bar{y}\rho(1-z)}. \end{aligned} \quad (2.37)$$

Also, the equilibrium-state probability P_j can be calculated by:

$$P_j = \begin{cases} \frac{\sum_{i=0}^n y_i \sum_{k=0}^i P_k^+ - P_0^+}{\bar{y}\rho}, & j = 0 \\ \frac{\sum_{i=0}^n y_i P_{j+i}^+ - P_j^+}{\bar{y}\rho} + P_{j-1}, & j \geq 1 \end{cases} \quad (2.38)$$

where P_j^+ is derived by Eq. (2.35). If we denote the average number of packets that

SUs send during a time slot at the equilibrium state by N_s , then we obtain:

$$N_s = \begin{cases} \min \left\{ N_q, \left\lfloor \frac{RT_{NP}}{\ell} \right\rfloor \lim_{\tau \rightarrow \infty} L_{RSP}(\tau) \right\}, & \text{for RSP} \\ \min \left\{ N_q, \left\lfloor \frac{RT_{NP}}{\ell} \right\rfloor \lim_{\tau \rightarrow \infty} L_{NSP}(\tau) \right\}, & \text{for NSP} \end{cases} \quad (2.39)$$

where the distributions of $L_{RSP}(\tau)$ and $L_{NSP}(\tau)$ are characterized by Eqs. (2.15) and (2.18), respectively. Thus, we obtain the aggregate throughput, denoted by η , as follows:

$$\eta = \frac{E[N_s]\ell}{T_S}. \quad (2.40)$$

Since the average queue length, denoted by L_q , of the packets for any given SU is the first moment of N_q , we have

$$L_q = \left. \frac{d}{dz} P_q(z) \right|_{z=1} = L^+ - \bar{y}\rho + \frac{\lambda^2 \Psi^{(2)}(1)}{2\bar{y}\rho}, \quad (2.41)$$

where L^+ is derived by Eq. (2.36). According to Little's law, the queuing delay, denoted by W_q , for a given SU can be derived by

$$W_q = \frac{L_q T_S}{\lambda}, \quad (2.42)$$

where T_S is the length of the time slot. Thus, the average packet transmission delay, denoted by W_s , for a given SU is derived as:

$$W_s = W_q + E[V]T_S = \left(\frac{L_q}{\lambda} + u \right) T_s, \quad (2.43)$$

where $E[V]T_S$ is the service delay.

Table I. The parameters for our proposed opportunistic multi-channel cognitive MAC protocol.

RTS	44 Bytes	The length of RTS packet
CTS	38 Bytes	The length of CTS packet
ℓ	250 Bytes	The length of the data packet
T_{ms}	9 μ s	Mini-slot interval
T_S	1.89 ms	The length of time slot
SIFS	15 μ s	Short inter-frame space
DIFS	34 μ s	DCF inter-frame space
p	0.01	The prob. of sending a packet
R	1 Mbps	Data rate of the licensed channel

F. Performance Evaluations

The parameters for our proposed schemes are summarized in Table I. These parameters ensure that Eq. (2.10) is satisfied, which suggests that at least one SU can successfully send RTS packet during the negotiating phase with a high probability.

We first investigate the time spent by the negotiation-based sensing policy to attain the desired state, where 1) if the number (u) of SUs is larger or equal to the number (n) of licensed channels, all the channels are sensed by the SUs, 2) otherwise, each channel is sensed by no more than one SU. Fig. 7 plots the time spent to attain the desired state against the number of SUs with different γ 's and n 's. Each point in Fig. 7 is the mean of the results of 500 simulations. Note that the length of the time slot is typically very short.¹ The negotiation-based sensing policy can quickly attain the desired state even in the worst case where $n = 10$ with $\gamma = 0.6$, as shown

¹For example, the time-slot length of GSM cellular network is 577 μ s.

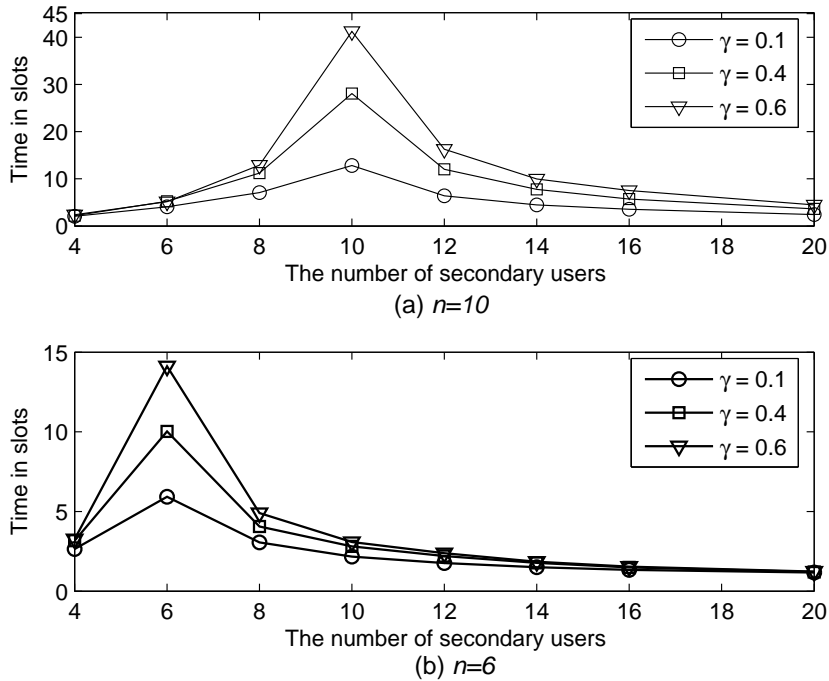


Fig. 7. The time spent to attain the desired state by the negotiation-based sensing policy against the number of SUs with different γ 's. (a) The case with $n = 10$. (b) The case with $n = 6$.

in Fig. 7. We also observe that the time spent to attain the desired state gets longer if the number u of SUs becomes closer to the number n of channels. This is because i) when u is much smaller than n , it is less likely that the channels sensed by two SUs are the same in the initial state, which will only take several more steps (in slots) to attain the desired state; and ii) when u is much larger than n , Fact 2 shows that most channels are sensed by the SUs in the initial state, which is also close to the desired state. In addition, we notice that it will take more time to attain the desired state if the channel utilization (γ) by the PUs gets larger.

By using the analytical model developed in Section D-2, we obtain the numerical results for the *saturation throughput* achieved by two different channel-sensing policies under different situations with $n = 10$, as shown in Fig. 8. Given γ and u , the

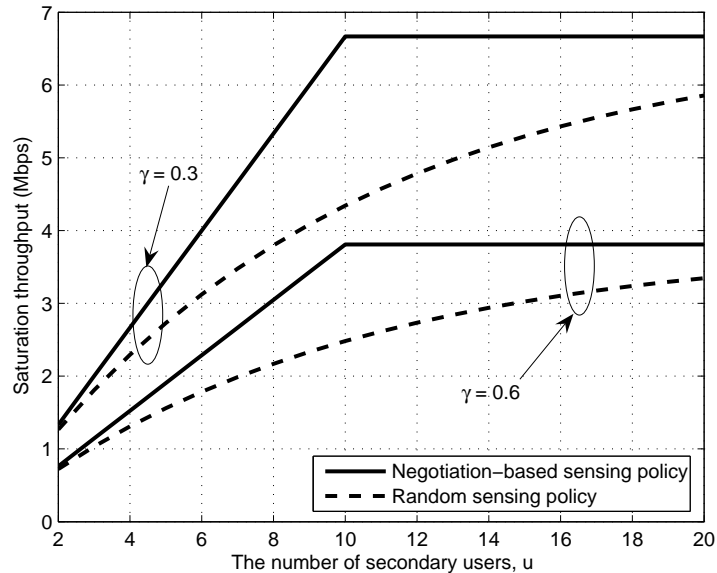


Fig. 8. The saturation throughput achieved by two different channel-sensing policies against the number (u) of SUs with different γ 's when the number (n) of licensed channels is 10.

saturation throughput achieved by the negotiation-based sensing policy is higher than that by the random sensing policy. When the number of SUs is equal to the number of channels, the improvement achieved by the negotiation-based sensing policy over that achieved by the random sensing policy reaches to the maximum. When the number of SUs is less than the number of channels, the saturation throughput achieved by the negotiation-based sensing policy increases linearly as the number of SUs increases. However, the saturation throughput achieved by the negotiation-based sensing policy becomes the constant after the number of SUs is larger than the number of channels. This is expected because all the vacant channels are perceived by the SUs when the number of SUs is larger than or equal to the number of channels, as discussed in Section C-3. From Fig. 8, we also observe that the larger the channel utilization by the PUs (γ), the lower saturation throughput the SUs can achieve for both channel

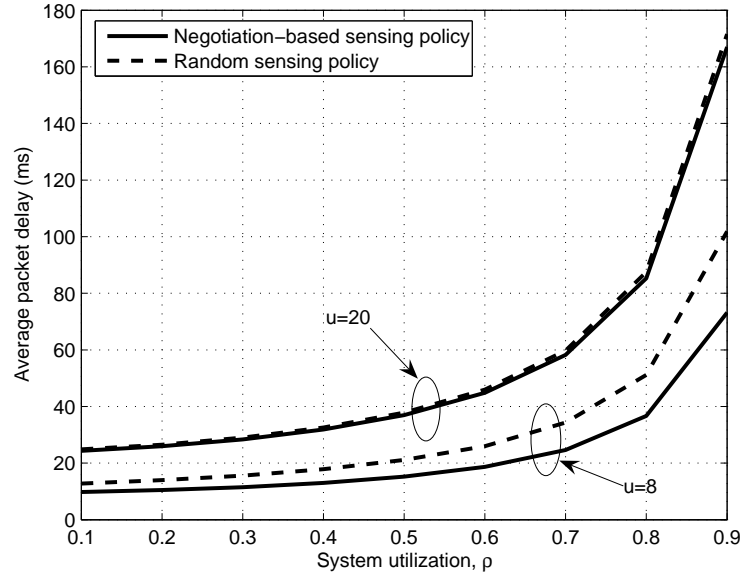


Fig. 9. The average packet transmission delay (W_s) against the system utilization (ρ) of SUs with different number of SUs (u) when the channel utilization (γ) of PUs is 0.6. The number (n) of licensed channels is 5. The solid lines represent the average packet transmission delay under negotiation-based sensing policy, and the dashed lines represent the average packet transmission delay under the random sensing policy.

sensing policies, which makes sense because the higher the channel utilization (γ), the less the channels can be used by the SUs.

Now, we investigate the performance of our proposed MAC protocols in the *non-saturation network* case, where the number (n) of licensed channels is set to 5. Using Eqs. (2.41) through (2.43), Fig. 9 plots the average packet transmission delay against the system utilization (ρ) of SUs when the number of SUs (u) is set to 8 and 20, respectively, while the channel utilization (γ) of PUs is fixed at 0.6. As the system utilization increases, the average packet transmission delay gets larger for both the negotiation-based sensing policy and the random sensing policy. Also, the average packet transmission delay increases much faster when the system utilization ρ gets

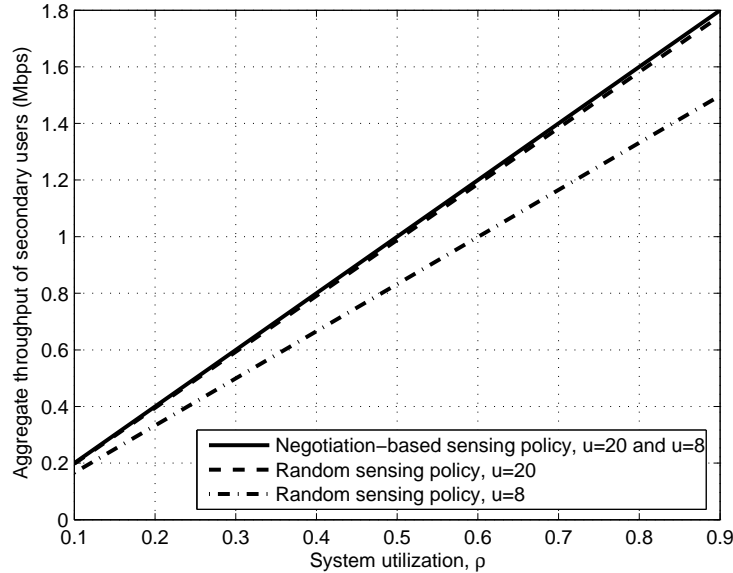


Fig. 10. The aggregate throughput (η) of SUs against different system utilization (ρ) of SUs when the number (u) of SUs is equal to 20 and 8. The channel utilization (γ) of PUs is 0.6, and the number (n) of licensed channels is 5. The solid line represents the negotiation-based sensing policy for both $u = 8$ and $u = 20$, the dashed line represents the random sensing policy with $u = 20$, the dashdotted line represents the random sensing policy with $u = 8$.

larger. From Fig. 9, we observe that the average packet transmission delay achieved by the negotiation-based sensing policy is smaller than that achieved by the random sensing policy for the same ρ and u . In particular, when the number of SUs is close to the number of licensed channels, the delay achieved by the negotiation-based sensing policy is much smaller than that achieved by the random sensing policy. However, the delays achieved by the negotiation-based sensing policy and the random sensing policy are virtually the same when the number of SUs is much larger than the number of licensed channels, which verifies Fact 2.

Using Eq. (2.40), Fig. 10 plots the aggregate throughput against the system utilization under both the negotiation-based sensing policy and random sensing policy.

Note that under the negotiation-based sensing policy the aggregate throughput of $u = 20$ is the same as that of $u = 8$. This is because based on the negotiation-based sensing policy, the SUs are aware of all channels' states in both $u = 20$ and $u = 8$ cases, and thus these two cases have the same total packet arrival rates under the same system utilization. The aggregate throughput increases linearly with the system utilization. The reason is that under the fixed γ , the increase of the system utilization (ρ) leads to the increase of the packet arrival rate (λ), which implies that more packets are sent under the non-saturation network case. From Figs. 9 and 10, we observe that there is a tradeoff between the aggregate throughput and average packet transmission delay. That is, as the system utilization increases, the aggregate throughput increases, while the average packet transmission delay also becomes larger.

Now, we investigate the impact of the channel utilization (γ) of the PUs on the performance of our proposed MAC protocols. Using Eqs. (2.41)-(2.43) and Eq. (2.40), Figs. 11 and 12 plot the average packet transmission delay against the channel utilization (γ) of the PUs and the aggregate throughput of the SUs against the channel utilization of PUs, respectively. The system utilization (ρ) of SUs is set as a constant of 0.1. The number (n) of licensed channels is set to 5. From Fig. 11, we observe that the average packet transmission delay increases monotonically with γ . The increasing rate of the average packet transmission delay becomes larger as the channel utilization (γ) of PUs increases. From Fig. 12, we find that the aggregate throughput decreases as the channel utilization of PUs increases. That is expected because the number of vacant licensed channels which can be utilized by the SUs decreases, as the channel utilization of PUs gets larger. When the number of SUs is small, the performance improvement of the negotiation-based sensing policy over the random sensing policy gets larger in terms of throughput and delay. On the other hand, when the number of SUs gets large, the performance achieved by the simple random sensing policy is

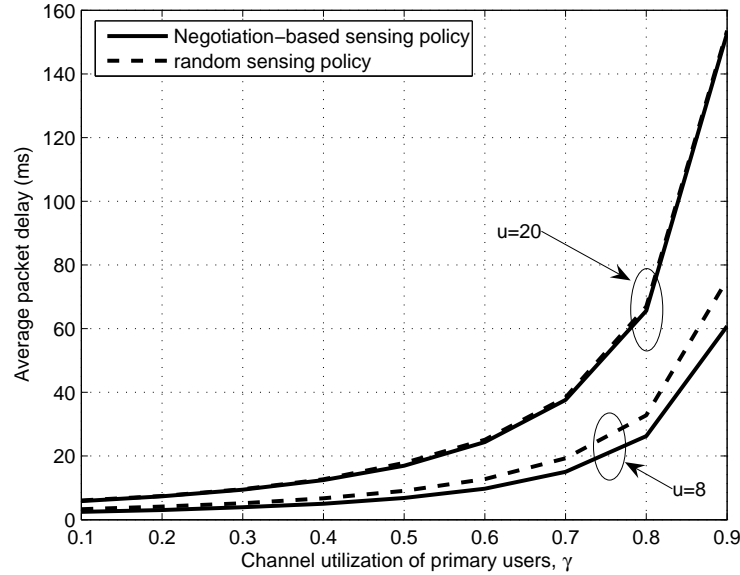


Fig. 11. The average packet transmission delay (W_s) against the channel utilization (γ) of PUs with different number of SUs (u) when the system utilization (ρ) of SUs is 0.1. The number (n) of licensed channels is 5. The solid lines represent the negotiation-based sensing policy, and the dashed lines represent the random sensing policy.

very close to that achieved by the negotiation-based sensing policy.

Using Eqs. (2.41)-(2.43), Fig. 13 plots the impact of different combinations of γ and λ on the average packet transmission delay under the negotiation-based sensing policy, when the number (n) of licensed channels is 5 and the number (u) of SUs is 20. Under the same channel utilization of PUs, the higher the packet arrival rate, the larger the packet transmission delay. Furthermore, the impact of the packet arrival rate on the packet transmission delay gets higher when the channel utilization of PUs becomes larger. When the channel utilization of PUs is high, even the small increase of packet arrival rate can result in the significant increase of packet transmission delay. These observations provide practically important guidelines to derive the different desired parameters, such as packet arrival rate, the channel utilization of PUs, and

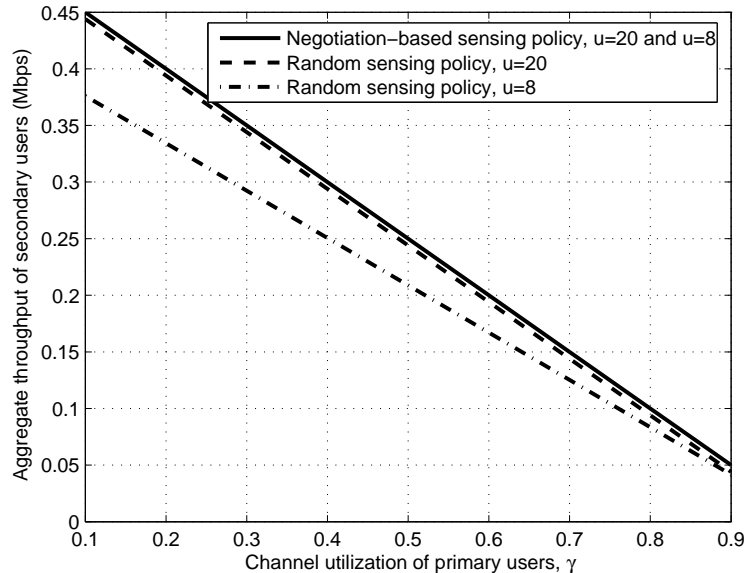


Fig. 12. The aggregate throughput (η) of SUs varies with different channel utilization (γ) of PUs when the number (u) of SUs is equal to 20 and 8. The system utilization (ρ) of SUs is 0.1 and the number (n) of licensed channels is 5. The solid line represents the negotiation-based sensing policy for both $u = 8$ and $u = 20$, the dashed line represents the random sensing policy with $u = 20$, the dashdotted line represents the random sensing policy with $u = 8$.

the number of SUs, etc., for the QoS-provisioning over the cognitive radio wireless networks.

G. Summary

We proposed and analyzed the opportunistic multi-channel MAC protocols for the cognitive radio-based wireless ad hoc networks. Specifically, the cognitive MAC protocols enable the SUs to identify and utilize the available frequency spectrum without causing harmful interference to the PUs. To detect the availabilities of the vacant licensed channels, we proposed two different channel sensing policies: the random sensing policy and the negotiation-based sensing policy. Our proposed cognitive radio-

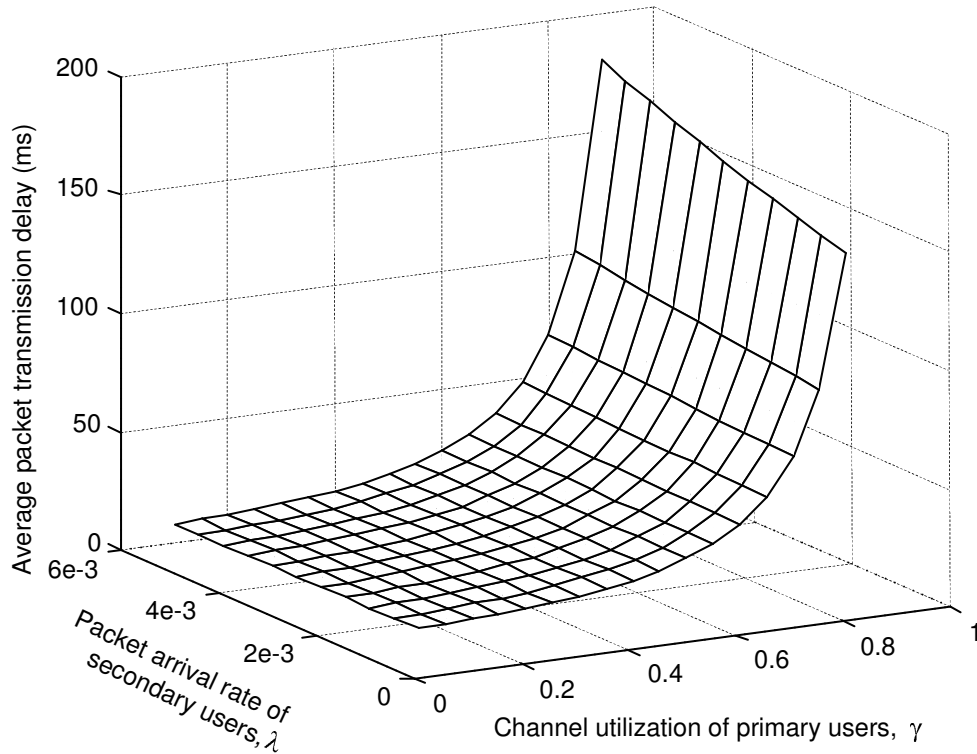


Fig. 13. The average packet transmission delay (W_s) varies with different γ 's and λ 's under negotiation-based sensing policy. The number (n) of licensed channels is 5 and the number (u) of SUs is 20.

based MAC protocols do not need any centralized controllers, since the negotiation between the sender and receiver of the SUs is conducted using the CSMA/CA-based algorithm. Applying the Markov chain model and the $M/G^Y/1$ queueing model, we develop analytical models to evaluate the performance of our proposed protocols with two channel sensing policies for both the saturation network case and non-saturation network case, respectively. Our analyses also reveal the tradeoff between throughput and delay, which provides the guidelines to support the different QoS requirements over cognitive radio based wireless networks.

CHAPTER III

CHANNEL-HOPPING BASED SINGLE TRANSCEIVER MAC FOR
SYNCHRONOUS COGNITIVE RADIO NETWORKS

A. Introduction

In Chapter II, we proposed the cross-layer based multi-channel opportunistic MAC protocol for synchronous cognitive radio networks, which requires each SU to be equipped with two sets of radios. However, in some hardware-constrained cognitive radio networks, it may be difficult to equip each SU with two sets of radios, especially in cognitive radio-based wireless sensor networks. Thus, in this chapter we propose a channel-hopping based *single transceiver* cognitive MAC protocol for synchronous cognitive radio networks. Under our proposed protocol, each SU is equipped with *only one* SDR-based cognitive transceiver that can dynamically utilize the licensed channels to receive/transmit the SUs' packets. Our proposed protocol enables the SUs to exchange the negotiation packets (e.g., ready-to-send/clear-to-send, i.e., RTS/CTS packets) at multiple rendezvous such that no dedicated control channel is required. In particular, in our proposed channel-hopping MAC protocol, the SUs switch across the licensed channels with their distinct channel-hopping sequences. When an SU sender wants to send packets to its intended SU receiver, the SU sender changes its hopping schedule and follows the hopping sequence of the intended receiver to conduct the negotiation and then transmit data packets if the channel is not currently used by PUs.

The main advantages of our proposed scheme include the followings: 1) no extra control channel is needed; 2) it overcomes the single control channel bottleneck problem; and 3) one transceiver is sufficient. In addition, our proposed protocol

does not need any centralized controllers. We also rigorously model and analyze the performance of our MAC protocol in terms of aggregate throughputs.

The rest of this chapter is organized as follows. Section B describes the PUs' channel-usage model and develops our proposed cognitive MAC protocol. Applying the Markov chain based analytical model, Section C models and analyzes the throughput of our proposed cognitive MAC protocol. Using this Markov chain model, Section D evaluates our multi-channel MAC protocol. The chapter concludes with Section E.

B. Our Proposed Channel-Hopping Cognitive MAC Protocol

1. The PUs' Channel-Usage Model

The PUs' channel-usage model considered in this chapter is similar to that in Chapter II. In particular, we consider there are two non-cooperating types of users, namely PUs and SUs. The PUs, for example, TVs, cellular phones, or wireless microphones, are those to which an amount of wireless spectrum is licensed. On the other hand, the SUs are referred to those without pre-assigned wireless spectrum. However, the SUs equipped with the cognitive radios can transmit their own packets by seizing the opportunities that the PUs do not use the licensed wireless spectrum. In this chapter, the wireless spectrum accessible to the SUs is further divided into a number of channels, each with a fixed amount of frequency bandwidth.

Suppose that a spectrum licensed to the PUs consists of M channels, as depicted in Fig. 2 in Chapter II. We assume that for each channel, the channel usage pattern of the PUs follows independent and identically distributed (i.i.d.) ON/OFF random process, as shown in Fig. 3 in Chapter II. An ON-period represents that the channel is occupied by the PUs. An OFF-period represents that the channel is vacant and thus

can be opportunistically used by the SUs. Suppose that the ON- and OFF-periods on each channel are independent. Note that the average ON- and OFF-periods depend on the channel usage pattern of the PUs. In this chapter, we assume that the length of ON- and OFF-periods for i -th licensed channel follows exponential distribution with means equal to α_i and β_i , respectively. If we denote γ_i as the probability that i -th channel is occupied by the PUs, then we have

$$\gamma_i = \frac{\alpha_i}{\alpha_i + \beta_i}, \quad (3.1)$$

where $1 \leq i \leq M$. Note that γ_i also represents the channel utilization of i -th channel with respect to PUs.

2. The Protocol Description

Our proposed protocol does not employ a common control channel as the rendezvous where the SUs exchange the control packets for multi-channel resource reservation. Each SU has its own hopping sequence and switches across the channels following the hopping sequence. Each SU hops across all M licensed channels according to its own pseudo-random (PR) hopping sequence. SUs decide on their own PR hopping sequence based on their unique ID (e.g., their MAC address) and share the same hopping sequence generating algorithm. The hopping sequence is fixed for a given SU. As shown in Fig. 14, if a source SU, A , wants to send packets to its intended receiver, B , A follows the B 's hopping sequence to meet with it and exchange the negotiation packets if the channel is not used by the PUs.

Unlike the conventional channel hopping MAC protocol [89–91], at the beginning of each time slot, to guarantee that the SUs do not interfere with the PUs or the ongoing communication pairs of SUs, the SUs need to keep their transmitters quiet for a predefined period, called the *quiet period*. During the quiet period, if an SU

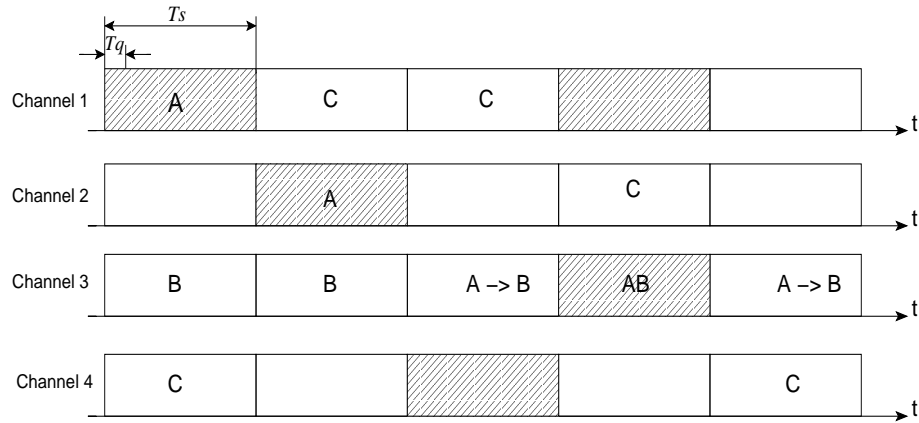


Fig. 14. Illustrations of our proposed opportunistic MAC protocol. The shadowed rectangles represent the time slots during which the PUs are active. The empty rectangles represent the unused time slots. Let A , B , and C be three SUs. If A wants to send packets to B , A follows the B 's hopping sequence to meet with it and exchange the negotiation packets if the channel is unused by the PUs.

does not detect any signal on its current operating channel, it assumes that no PU is present in the current time slot and it is safe for SUs to use the channel. The channel operations for the SUs can be categorized as three types: *advertising*, *negotiation*, and *data exchange*. Note that in each time slot, all of these operations can be performed by the SUs only if there are no PUs' signals detected during the quiet period.

The Advertising Operations: Each SU periodically broadcasts its own hopping sequence over an unused channel to let its neighbors know such that the neighbors can follow its hopping sequence to communicate with. When an SU is entering the network, it discovers its neighbors and adds them to its neighbors list table. The SU needs to send its ID so that its neighbors can know its home hopping sequence which is only decided by the SU's unique ID. When an SU receives any packet, if the sender is a new neighbor, the SU records the sender's home hopping signature consisting the time stamp and the unique ID of the sender. Whenever a new neighbor is discovered,

the receiver sends an extra packet with its own hopping sequence to accelerate the advertising process. The SUs can also ask their neighbors for a list of their known neighbors.

The Negotiation Operations: Before exchanging any data packets, the sender and receiver of SUs have to hop to the same channel at the same time slot to negotiate for the data transmission. In our proposed protocol, SUs can conduct the negotiations at different channels simultaneously. In other words, multiple pairs of senders and receivers can transmit or negotiate at the same time, which is different from the dedicated control channel based cognitive MAC protocols where only one pair of sender and receiver can conduct negotiation at the same time. In this sense, the proposed cognitive protocol can alleviate negotiation bottleneck.

Under our proposed protocol, each SU keeps one packet queue per destination to avoid head-of-line blocking. At the beginning of each time slot, if the SU has no data to send, it will follow its home hopping sequence and monitor on that channel. If the SU has packets to send, it allows itself to temporarily deviate from its home hopping sequence and transmit to a receiver on another channel. Otherwise, it simply stays on the current channel. The sender deviates from its home hopping sequence at the beginning of the time slot to monitor the receiver's status. After the sender hops to the receiver's channel, it needs to wait for the predefined quiet period. If during the quiet period, there are no signals detected, it sends a negotiation message to the receiver with a randomized delay. After receiving the acknowledgment from the receiver, the sender starts transmitting data packets, which means the negotiation is successful.

The Data Exchange: After a pair of SUs successfully negotiate for the channel, they start exchanging data packets. If they cannot finish the data packets in a time slot. They continue exchanging data over the same channel at the next time slot.

If the channel is occupied by PUs, then the pair of SUs wait on the same channel until the channel is vacant again. If the channel is occupied by PUs for consecutive 5 times, the pair of SUs gives up the data exchanging, which means that the data exchange fails.

C. Throughput Analysis

For our proposed cognitive MAC protocols, there are four sets of SUs in the t -th time slot, denoted by \mathcal{C}_t , \mathcal{R}_t , \mathcal{I}_t , and \mathcal{N}_t , respectively, where t indexes the time slots, as shown in Fig. 15. \mathcal{C}_t is the set of SUs that exchange data during the t -th time slot. \mathcal{R}_t is the set of SUs that is ready to transmit or receive data at the beginning of the t -th time slot. \mathcal{I}_t is the set of SUs that is idle during t -th time slot. \mathcal{N}_t is the set of SUs that have buffered data packets and contend for transmitting negotiating packets during the t -th time slot. As shown in Fig. 15, the set of \mathcal{R}_t includes two parts: i) all the SUs in \mathcal{R}_{t-1} , and ii) a fraction of \mathcal{C}_{t-1} SUs that finish the data exchange. We assume that each SU in \mathcal{R}_t generates a packet at the beginning of t -th time slot with probability λ . The destination address of the generated packet is arbitrarily chosen among all the SUs. The SUs that generate packets (i.e., \mathcal{N}_t) contend for the right of transmission on the unused licensed channels. If an SU in \mathcal{N}_t successfully negotiates with its intended secondary receiver, then it can exchange data packet in the t -th time slot.

To make the model tractable, we mainly focus on the scenarios where all SUs utilize the licensed channels used by the same set of PUs. This implies that the licensed channel availability information sensed by each SU is consistent among all SUs. Furthermore, let the same γ apply to all licensed channels, i.e., $\gamma = \gamma_i = \gamma_j$ for $1 \leq i, j \leq M$. We assume that the data packet length in terms of the time-slot

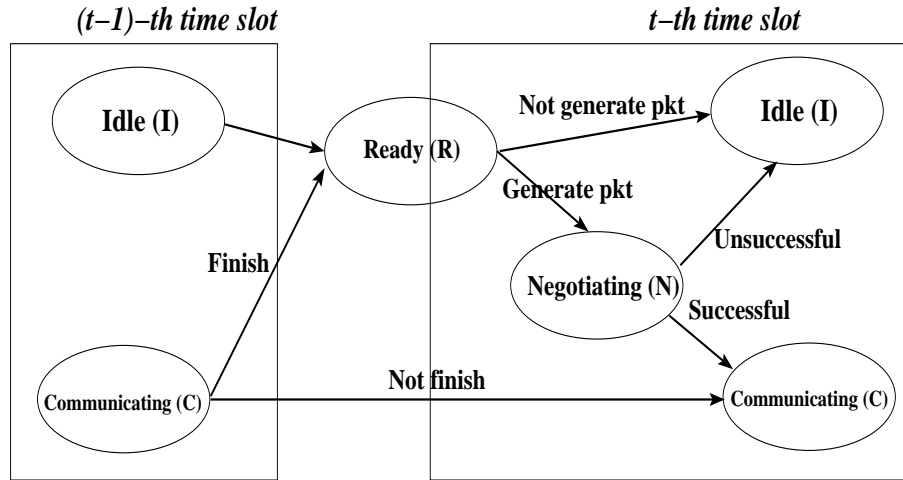


Fig. 15. The diagram of node states transition from $(t - 1)$ -th time slot to t -th time slot. \mathcal{I} , \mathcal{C} , \mathcal{R} , and \mathcal{N} imply the sets of idle nodes, communicating nodes, nodes that are ready to transmit/receive, buffered nodes, respectively.

length follows the geometrical distribution, i.e., the probability that a data packet has length ℓ is

$$P(L = \ell) = \mu(1 - \mu)^{\ell-1}. \quad (3.2)$$

It will take ℓ time slots to complete the transmission of data packet with a length of ℓ . If we denote the data transmission rate, the length of time slot, and the length of quiet period by R_d , T_s , and T_q , respectively, then the average packet length, denoted by \bar{L} , in bytes is obtained by:

$$\bar{L} = \frac{(T_s - T_q)R_d}{\mu}. \quad (3.3)$$

Clearly, at any given beacon interval, the system state at every interval beacon can be characterized by the number of communicating pairs of nodes during the corresponding time slot (i.e., $|\mathcal{C}|/2$). We proceed to analyze the proposed protocol by using a discrete-time Markov chain to analyze the network throughput. A transition in the Markov chain from one state to another occurs if i) at least one communicating

pairs finishes the data transmission, or (and) ii) at least one communicating pairs begins the data transmission.

For convenience, we summarize the key parameters for protocol modeling as Table II. The number of nodes, denoted by N_r , that is ready to transmit or receive at the beginning of the t -th time slot can be written as:

$$N_r = |\mathcal{R}_t| = N - 2(k - v), \quad (3.4)$$

where k and m with $0 \leq k, m \leq C \triangleq \min\{M, \lfloor N/2 \rfloor\}$ are the number of communicating pairs of SUs at $(t-1)$ -th time slot and t -th time slot, respectively. Because the geometrical distribution is memoryless and the given licensed channel is occupied by the PUs with probability of γ , the probability that each communicating pair in \mathcal{C}_{t-1} finishes the data at the end of $(t-1)$ -th time slot is $\mu(1-\gamma)$. Given the number k of communicating pairs in the $(t-1)$ -th time slot, the number v of communicating pairs that become ready at the beginning of t -th time slot follows the binomial distribution, i.e.,

$$p(v|k) = \binom{k}{v} [\mu(1-\gamma)]^v [1 - \mu(1-\gamma)]^{k-v}, \quad (3.5)$$

where $0 \leq v \leq k$. Also, the number w of nodes that has buffered packets to send in the t -th time slot follows the binomial distribution conditioning on v and k , i.e.,

$$p(w|k, v) = \binom{N_r}{w} \lambda^w (1-\lambda)^{N_r-w}, \quad (3.6)$$

where $0 \leq w \leq N_r$.

Denote by $p(c|k, v, w)$ the conditional probability mass function (pmf) of the number (c) of channels to which only one buffered SU hops given that there is w buffered SUs. $p(c|k, v, w)$ is the same as the probability that c out of M urns contain exactly one ball after we throw w balls independently and uniformly in M urns. We

Table II. The parameters for channel-hopping cognitive MAC protocol modeling

N	The number of SUs in the system.
N_r	The total number of SUs in \mathcal{R}_t , i.e., $ \mathcal{R}_t $.
u	The number of pairs of SUs that successfully negotiate, i.e., $ \mathcal{N}_t \cap \mathcal{C}_t $.
v	The number of communicating pairs of SUs that finish data exchange at the end of $t - 1$ time slot and become ready at the beginning of the t -th time slot, i.e., $ \mathcal{C}_{t-1} \cap \mathcal{R}_t /2$.
c	The number of exclusive channels which has only one SU in t -th time slot user that has packets to send.
e	The number of the idle channels in t -th time slot.
d	The number of the idle and exclusive channels in t -th time slot.
k	The number of communicating pairs that communicate in the $(t - 1)$ -th time slot, i.e., $ \mathcal{C}_{t-1} /2$.
m	The number of communicating pairs that is communicate in the t -th time slot, i.e., $ \mathcal{C}_t /2$.
w	The number of SUs that have packets to send in the t -th time slot, i.e., $ \mathcal{N}_t $.
λ	Probability that an idle SU generates a packet.
μ	Probability that a pair of SUs finish the data exchange and release the channel.

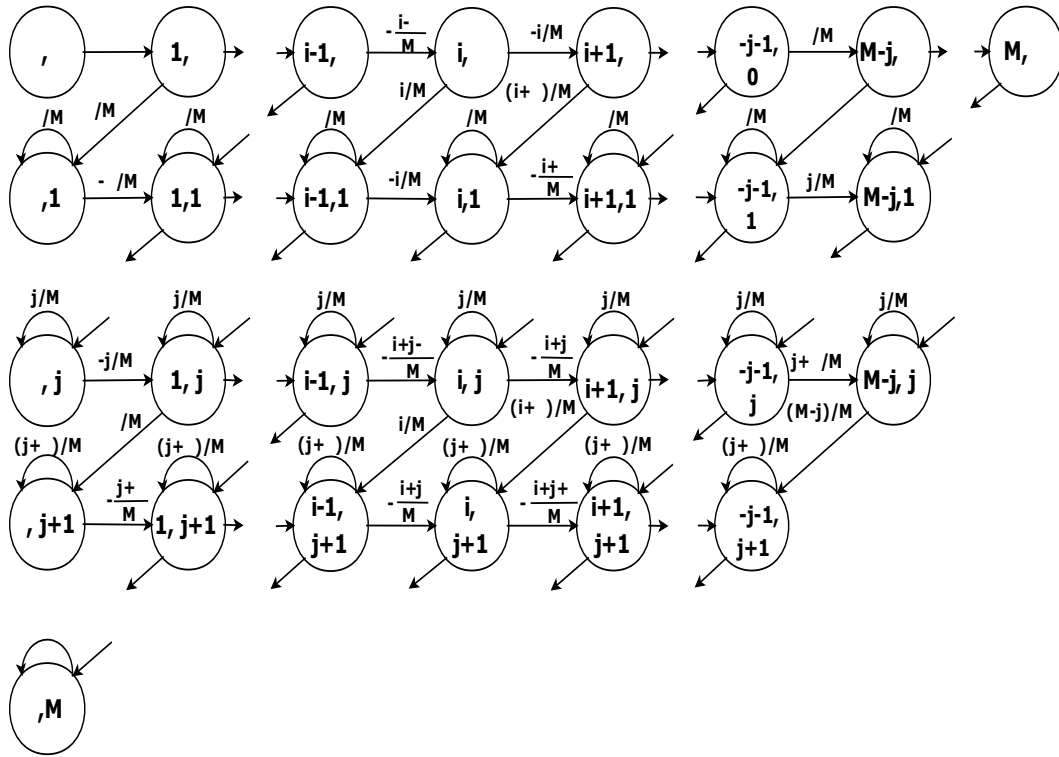


Fig. 16. The two-dimensional Markov chain for the number of exclusive channels in a given time slot.

can use a two-dimensional discrete-time Markov chain to derive $p(c|k, v, w)$. Let $o(w)$ be the stochastic process representing the number of channels each of which is selected by exactly one buffered SU (i.e., the exclusive channels) given there are w buffered SUs. Clearly, this process is non-Markovian. We also denote $n(w)$ as the stochastic process representing the number of channels each of which is selected by at least two SUs. Then, we get a two-dimensional process $\{o(w), n(w)\}$ that is a discrete-time Markov chain as shown in Fig. 16. Thus, we get the one-step transition probabilities

as follows:

$$\begin{cases} p(i, j|i, j) = \frac{j}{M}, & 0 \leq i, j \leq M \\ p(i+1, j|i, j) = 1 - \frac{i+j}{M}, & 0 \leq i \leq (M-1), j \geq 0 \\ p(i-1, j+1|i, j) = \frac{i}{M}, & 1 \leq i \leq M, 0 \leq j \leq (M-1) \\ p(x, y|i, j) = 0, & |x-i| \geq 2 \text{ or } |y-j| \geq 2 \end{cases} \quad (3.7)$$

where $(i+j) \leq M$ holds. Then, we can construct the two-dimensional transition probability matrix $\{p(x, y|i, j)\}_{0 \leq x, y, i, j \leq M}$. We further convert this two-dimensional matrix into an one-dimensional transition probability matrix, denoted by \mathbb{Q} , as follows:

$$\mathbb{Q} = \{q_{m,n}\}_{\frac{(M+2)(M+1)}{2} \times \frac{(M+2)(M+1)}{2}} \quad (3.8)$$

where $q_{m,n} = p(x, y|i, j)$ with m and n satisfying the follows:

$$\begin{cases} m = \frac{(2M-i+3)i}{2} + j \\ n = \frac{(2M-x+3)x}{2} + y \end{cases} \quad (3.9)$$

Then, we can obtain the conditional pmf of the number (c) of exclusive channels given w , k , and v as:

$$p(c|k, v, w) = p(c|w) = \sum_{t=(2M-c+3)c/2}^{(2M-c+3)c/2+M-c} \mathbb{Q}^w|_{(0,t)} \quad (3.10)$$

where $0 \leq c \leq w$ and $\mathbb{X}|_{(i,j)}$ represents the element of matrix \mathbb{X} located at the i -th line and the j -th column.

Denote by $p(d|k, v, w, e, c)$ the conditional pmf of the number (d) of the idle and exclusive channels given e idle channels and c exclusive channels. Based on the

combinatorial rules, $p(d|k, v, w, e, c)$ can be expressed as:

$$p(d|k, v, w, e, c) = \frac{\binom{e}{d} \binom{M-e}{c-d}}{\binom{M}{c}} \quad (3.11)$$

where $0 \leq d \leq c$. If we denote by $p(e|k, v, w, c)$ the conditional pmf of the number (e) of the idle channels given that there are k communicating pairs in $(t-1)$ -th time slot and there are v pairs of SUs that finished communications at the end of $(t-1)$ -th time slot, then we get

$$p(e|k, v, w, c) = p(e|k, v) = \binom{M-k+v}{e} \gamma^{M-k+v-e} (1-\gamma)^e. \quad (3.12)$$

Combining Eqs. (3.12) and (3.11), we obtain:

$$\begin{aligned} p(d|k, v, w, c) &= \sum_{e=1}^{M-k+v} p(d|k, v, w, e, c) p(e|k, v, w, c) \\ &= \sum_{e=1}^{M-k+v} \frac{\binom{e}{d} \binom{M-e}{c-d}}{\binom{M}{c-d}} \binom{M-k+v}{e} \gamma^{M-k+v-e} (1-\gamma)^e. \end{aligned} \quad (3.13)$$

Given k, v, w , and d , the pmf, denoted by $p(u|k, v, w, d)$, of the number of SUs' pairs (u) of that successfully negotiate at t -th time slot can be written as follows:

$$p(u|k, v, w, d) = \binom{d}{u} \left(\frac{N_r - w}{N - 1} \right)^u \left(\frac{N_r - w}{N - 1} \right)^{d-u} \quad (3.14)$$

where $\frac{N_r - w}{N - 1}$ is the probability that a given secondary transmitter can find its intended secondary receiver. Since $u = m - (k - v)$, we can rewrite Eq. (3.14) as:

$$\begin{aligned} p(m|k, v, w, d, c) &= p(m|k, v, w, d) \\ &= \binom{d}{m - (k - v)} \left(\frac{N_r - w}{N - 1} \right)^{(m-k+v)} \left(\frac{N_r - w}{N - 1} \right)^{(d-m-k+v)}. \end{aligned} \quad (3.15)$$

By using Eqs. (3.5), (3.6), (3.10), (3.13), (3.15) together, the conditional pmf, denoted by $p(m|k)$, of the number (m) of SUs' pairs communicating in t -th time slot

given that there are k pairs of SUs communicating in $(t - 1)$ -th time slot can be written as:

$$p(m|k) = \sum_{v=0}^k \sum_{w=0}^{N-2(k-v)} \sum_{c=0}^w \sum_{d=0}^c p(m|k, v, w, d, c) \times p(d|k, v, w, c)p(c|k, v, w)p(w|k, v)p(v|k) \quad (3.16)$$

where $0 \leq k, m \leq C$. Using the transition probabilities obtained from Eq. (3.16), we can calculate the probability for steady state of the number of communicating pairs that is denoted by π_k with $0 \leq k \leq C$. Since the SUs in set of $\mathcal{C}_{t-1} \cap \mathcal{C}_t$ may not send data during t -th time slot due to the presence of the PUs, we need to differentiate the old communicating pairs of SUs ($\mathcal{C}_{t-1} \cap \mathcal{C}_t$) and the new joining communicating pairs of SUs ($\mathcal{R}_t \cap \mathcal{C}_t$). All of the new joining communicating pairs of SUs in t -th time slot can exchange data. At the same time, given k and v , the average number, denoted by $\bar{N}_c(k, v)$, of old communicating pairs of SUs that can exchange data in t -th time slot can be written as:

$$\bar{N}_c(k, v) = \sum_{i=0}^{k-v} i \binom{k-v}{i} \gamma^{k-v-i} (1-\gamma)^i \quad (3.17)$$

where $0 \leq v \leq k \leq C$. Then, the average aggregate throughput, denoted by ϕ , can be written as:

$$\phi = \frac{R_d(T_s - T_q)}{T_s} \sum_{k=0}^C \sum_{m=0}^C \sum_{v=0}^k p(k, v, m) [N_c(k, v) + m - (k - v)] \quad (3.18)$$

where T_s and T_q are the lengths of time slot and quiet period, respectively, $p(k, v, m)$ is the joint pmf of k , v , and m , and it can be obtained by

$$p(k, v, m) = p(v, m|k)\pi_k = p(v|k, m)p(m|k)\pi_k = p(v|k)p(m|k)\pi_k. \quad (3.19)$$

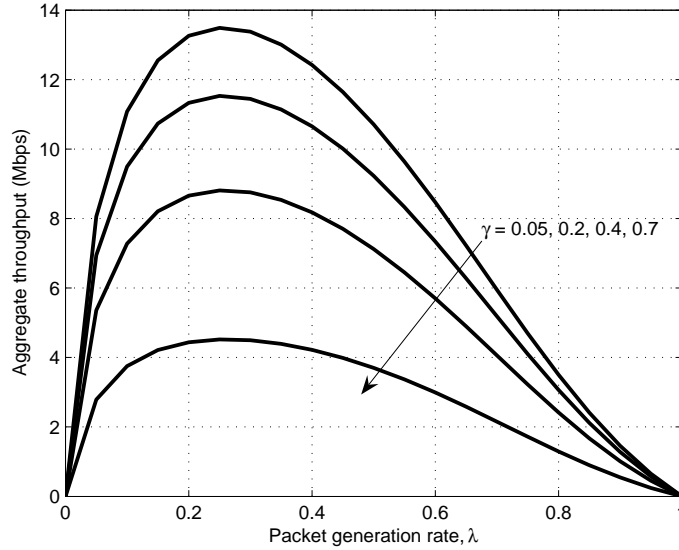


Fig. 17. The aggregate throughput of SUs against the packet generation rate. The average packet size is set to 170 bytes. The number of SUs $N = 20$. γ is set to 0.05, 0.2, 0.4 and 0.7, respectively.

D. Performance Evaluations

The parameters used to evaluate our proposed cognitive MAC protocol are set as follows: $R_d = 5$ Mbps, $T_s = 200 \mu\text{s}$, $T_q = 9 \mu\text{s}$, and $M = 6$. Using Eq. (3.18) in Section C, we obtain the aggregate throughput of SUs against packet generation rate (λ), channel utilization of PUs (γ), and average packet size (\bar{L}), respectively, when $N = 20$, as shown in Fig. 17. We first investigate the impact of the packet generation rate (λ) on the aggregate throughput with variant channel utilizations of PUs against packet generation rate when the average packet size is 170 Bytes (or equivalent to $\mu=0.7$), as shown in Fig. 17. Under the same packet generation rate, the less the channel utilization of PUs, the higher the aggregate throughput achieved. Regardless of the channel utilization of PUs, the aggregate throughput is 0 when $\lambda = 0$ or 1. When $\lambda = 0$, no packet is generated, the aggregate throughput is therefore zero. On

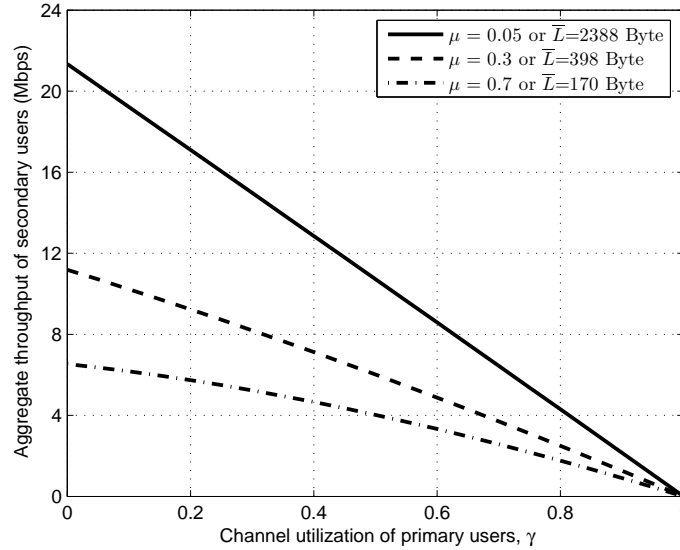


Fig. 18. The aggregate throughput of SUs against the channel utilization of PUs. The packet generation rate $\lambda = 0.5$. The number of SUs $N = 20$. The average packet size is set to 2388, 398 and 170 bytes, respectively.

the other hand, when $\lambda = 1$, all the idle SUs attempt to transmit, resulting in no sender that can find an idle receiver. Furthermore, we observe that given average packet size and the number of SUs, the utilization of PUs has hardly impact on the optimal packet generation rate that achieve the highest aggregate throughput.

Fig. 18 shows the impact of the channel utilization (γ) of PUs on aggregate throughput of SUs. As γ decreases, the aggregate throughputs become lower. It is clear because larger γ means fewer unused licensed channels that can be used by the SUs, leading to lower throughput. Given a fixed γ , with larger average packet size, the SUs can achieve higher aggregate throughput. The reason is that the large average packet size is equivalent to the small μ , which means that the SUs tend to stay in the same licensed channel for a longer time, and thus they don't need to frequently negotiate for the channels. Consequently, the SUs can utilize the licensed channels once the channels are unused by PUs. This impact of the average packet size on the

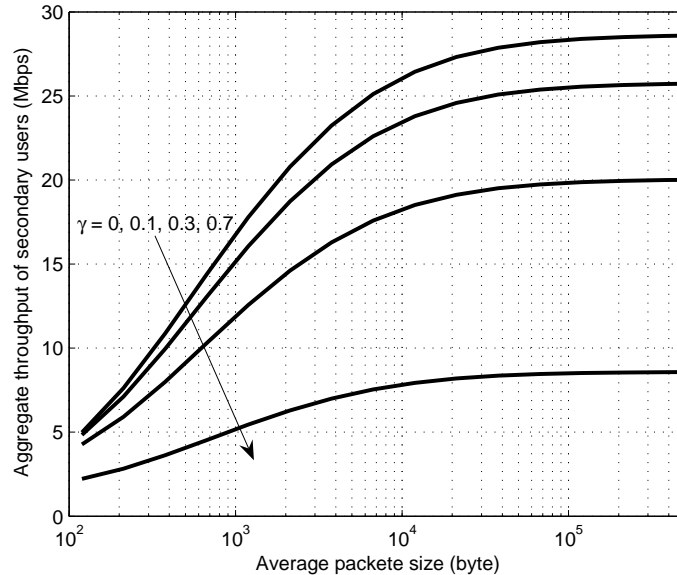


Fig. 19. The aggregate throughput of SUs against the average packet size. The packet generation rate $\lambda = 0.5$. The number of SUs $N = 20$. γ is set to 0, 0.1, 0.3 and 0.7, respectively.

aggregate throughput can be further studied in Fig. 19, which plots the aggregate throughput versus the average packet size. As average packet size increases, the aggregate throughputs of SUs get larger. Given a fixed γ , when the average packet size is 200 Kbytes, the aggregate throughput of SUs can almost fully utilize all the licensed channels that are unused by the PUs. Although the large average packet size can improve channel utilization, it reduces the probability that the idle SUs acquire channels, which leads to high packet transmission delay. Hence, there exists a tradeoff between the channel utilization and the packet transmission delay.

Fig. 20 shows the aggregate throughput versus the packet generation rate when the number (N) of SUs is 20 and 30, respectively. Given the average packet size, the highest aggregate throughput achieved by $N = 30$ is larger than that by $N = 20$. For $\bar{L} = 995$ bytes, when $\lambda < 0.4$, the aggregate throughput achieved by $N = 30$ is

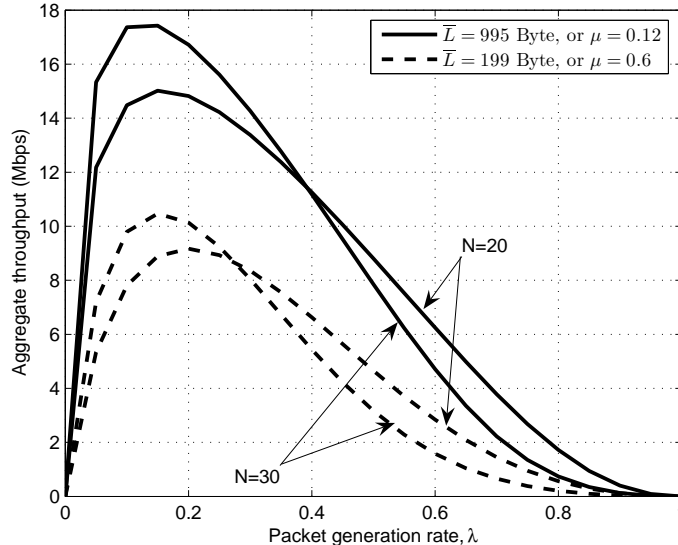


Fig. 20. The aggregate throughput against the packet generation rate with $\gamma = 0.1$ when $N = 20$ and 30 , respectively.

higher than that by $N = 20$. On the other hand, When $\lambda > 0.4$, smaller number of SUs achieves better throughput. The similar situation happens when $\bar{L} = 199$ bytes. That is expected because when λ is small, more SUs can provide more pairs of SUs that successfully utilize the vacant licensed channels. At the same time, when λ is large, larger number of SUs means that more buffered SUs cannot successfully negotiate for channels.

E. Summary

We proposed and analyzed the channel-hopping based cognitive MAC protocol. Under the proposed MAC protocol, each SU, which is equipped only one SDR based transceiver, seizes the opportunity where unused licensed channels are available to exchange their own packets while not causing any interference to the PUs. Each SU generates its own channel-hopping pattern with the unique sequence generating seed.

A SU follows its own channel-hopping pattern when it doesn't have packets to send, while it follows its intended receiver's channel-hopping pattern if it wants to send packets to the intended receiver. In this way, our proposed cognitive MAC protocol needs neither the dedicated control channel nor centralized controllers. We developed a Markov chain based analytical model to analyze the performance of our proposed cognitive MAC protocol in terms of aggregate throughput. We also identified the tradeoff between the channel utilization and the packet transmission delay.

CHAPTER IV

CREAM-MAC: COGNITIVE RADIO-ENABLED MULTI-CHANNEL MAC
PROTOCOL FOR ASYNCHRONOUS COGNITIVE RADIO NETWORKS

A. Introduction

In this chapter, we concentrate on the asynchronous cognitive radio networks, where the SUs are not synchronized with the PUs. The transmit duration of the PUs is not fixed. The design of MAC protocols for the asynchronous cognitive radio networks is more challenging than that for the synchronous cognitive radio networks we study in Chapters II and III. Besides all the problems encountered in the synchronous cognitive radio networks, in the asynchronous cognitive radio networks, when transmitting/receiving the SUs are not aware whether/when the PUs become active due to the half-duplex nature of the wireless spectrum-medium. Thus, the SUs in the asynchronous cognitive radio networks may inevitably cause interference to the PUs. How the SUs limit the interference caused to the PUs to an acceptable level is the critical problem in the design of MAC protocols for asynchronous or non-time-slotted cognitive radio networks. Moreover, the problems become more complicated when there are no centralized controllers and each SU is equipped with only a single transceiver.

To tackle the aforementioned problems, in this chapter we propose an efficient Cognitive Radio-EnAbleD Multi-channel MAC protocol, called CREAM-MAC protocol, which integrates the cooperative sequential spectrum sensing at physical layer and packet scheduling at MAC layer, over the wireless DSA networks. Under the CREAM-MAC protocol, each SU is equipped with a SDR-based transceiver that can dynamically utilize one or multiple licensed channels to receive/transmit the SUs' packets, and multiple sensors that can detect multiple licensed channels simultane-

ously. The proposed cooperative sequential spectrum sensing scheme aims at improving the accuracy of spectrum sensing to decrease the interference imposed to the PUs. The CREAM-MAC protocol enables the SUs to dynamically utilize the unused licensed frequency spectrum in a way that confines the level of interference to the range the PUs can tolerate. With the help of the four-way handshakes of control packets, the CREAM-MAC protocol with a single transceiver can efficiently handle the traditional hidden terminals and the multi-channel hidden terminals.

We also rigorously model and analyze the performance metrics, including the aggregate throughput delay and packet transmission delay, of our proposed scheme for the saturation network and the non-saturation network cases, respectively. First, in the saturation network case, where the SUs always have *non-empty* queues, we analyze the aggregate throughput for the CREAM-MAC protocol with the cooperative spectrum sensing scheme. Second, using the $M/G^Y/1$ queueing theory, we also develop an analytical model to study non-saturation network case, in which the packet arrivals are characterized by a Poisson process. The average aggregate throughput and the average delay analyses we have derived for non-saturation network case can help appropriately devise the important parameters, such as the packet arrival rate, to support the QoS requirements for wireless DSA networks.

The rest of this chapter is organized as follows. Section B describes the system models. Section C develops the CREAM-MAC protocol with the cooperative sequential spectrum sensing scheme. Section D develops the analytical model to study the CREAM-MAC protocol with the cooperative spectrum sensing scheme in the saturation network case. Applying the $M/G^Y/1$ queueing model, Section E analyzes the packet transmission delay and throughput of the proposed CREAM-MAC protocol in the non-saturation network case. Section F evaluates our proposed multi-channel MAC protocol by using our developed analytical models and simulation experiments.

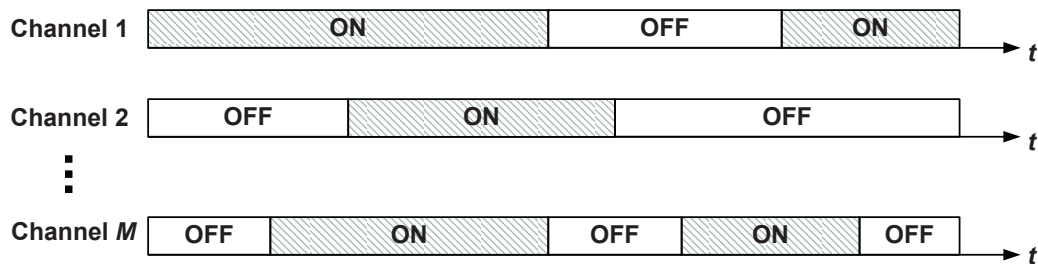


Fig. 21. Illustration of PUs' channel utilization in cognitive-radio based DSA networks. There are M licensed channels. The ON and OFF states of PUs operating at different licensed channels are unsynchronized.

The chapter concludes with Section G.

B. The System Models

We consider the scenario where there are two non-cooperating types of users, namely PUs and SUs. The PUs, for example, TVs, cellular phones, or wireless microphones, are those to which an amount of wireless spectrum is licensed. On the other hand, the SUs are referred to those without pre-assigned wireless spectrum. However, the SUs equipped with the cognitive radios can transmit their own packets by seizing the opportunities that arise when the PUs do not use the licensed wireless spectrum. In this chapter, the wireless spectrum accessible to the SUs is further divided into a number of channels, each with a fixed amount of frequency bandwidth.

1. Primary Users' Behaviors

Our system model focuses on the asynchronous cognitive-radio based DSA networks, which impose more challenges as compared with the synchronous cognitive-radio based DSA networks. In particular, we consider a scenario where a spectrum licensed to the PUs consists of M channels, as depicted in Fig. 21, in which the PUs operating at different channels are unsynchronized. We assume that for each channel,

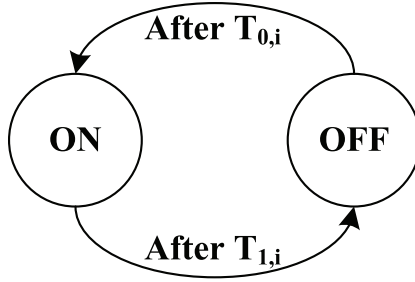


Fig. 22. The ON/OFF channel model for the i -th licensed data channel.

the channel usage pattern of the PUs follows independent and identically distributed (i.i.d.) ON/OFF renewal process, as shown in Fig. 22. An ON state represents that the channel is occupied by the PUs. An OFF state represents that the channel is vacant and thus can be opportunistically used by the SUs. Note that the average ON- and OFF-periods depend on the channel usage pattern of the PUs.

In the viewpoint of the SUs, the channel is alternating between ON and OFF states. We refer a spectrum access cycle for the SUs as a ON state followed by an OFF state. For an alternating renewal channel, let random variables $T_{1,i}$ and $T_{0,i}$ represent the sojourn times of ON and OFF states, respectively, for the i -th licensed channel. Without loss of generality, we assume that $T_{1,i}$ is independent of $T_{0,i}$. Denote $f_{T_{1,i}}(s)$ and $f_{T_{0,i}}(s)$ as the probability density functions (pdf) for the durations of the i -th licensed channel's ON state and OFF state, respectively. Then, we can derive the probability, denoted by γ_i , that the channel is in its ON state at an arbitrary time instance as follows:

$$\gamma_i = \frac{\int_0^\infty s f_{T_{1,i}}(s) ds}{\int_0^\infty s f_{T_{1,i}}(s) ds + \int_0^\infty s f_{T_{0,i}}(s) ds} = \frac{\bar{T}_{1,i}}{\bar{T}_{1,i} + \bar{T}_{0,i}}, \quad (4.1)$$

where $\bar{T}_{1,i}$ and $\bar{T}_{0,i}$ are the mean sojourn times of ON and OFF states, respectively, for i -th channel utilization. Note that in fact γ_i is the i -th channel utilization w.r.t. PUs.

We assume that the PUs' channel utilization pattern is homogeneous, i.e., $\bar{T}_{1,i} = \bar{T}_{1,j}$ and $\bar{T}_{0,i} = \bar{T}_{0,j}$, $\forall i \neq j$.

2. The Spectrum Sensing Model

The spectrum sensing scheme plays an important role in cognitive-radio based DSA networks. There are several signal detection techniques used for spectrum sensing, such as the energy detection, feature detection, and matched filter, for the SUs to detect the presence of the PUs [32]. We mainly focus on the energy detection approach in this chapter because the energy detection approach is efficient and simple to be implemented in hardware, and more importantly, it does not require the knowledge of signal features of the PUs, which typically may not be known by the SUs. We assume that all channels experience Rayleigh fading. If a PU is active and its sent signal is s with the transmit power E_s , then the received signal at a given SU's side, denoted by r , is

$$r = hs + \omega, \quad (4.2)$$

where h is the instantaneous amplitude gain of the channel between the PU and the given SU and follows Rayleigh distribution, and ω is the additive white Gaussian noise (AWGN) that has zero mean and variance of σ^2 . The instantaneous signal-to-noise ratio (SNR), denoted by ν , is equal to $(E_s|h|^2/\sigma^2)$. If the PU is idle, then only the thermal noise can be found at the receiver of the SUs. Thus, the objective of spectrum sensing is to decide between the following two hypotheses:

$$r = \begin{cases} hs + \omega, & \mathcal{H}_1 \\ \omega, & \mathcal{H}_0 \end{cases} \quad (4.3)$$

where \mathcal{H}_1 is the hypothesis stating that the given licensed channel is in ON state, and \mathcal{H}_0 is the hypothesis stating that the given licensed channel is in OFF state.

When the SUs perform the spectrum sensing, all of the SUs need to keep their radios silent for τ_s time units in order to obtain an accurate sensing outcome. During this silent period, no transmissions can be made. Since the sender and the receiver may have different sensing outcomes due to the relatively different locations to the PUs and the wireless fading channels, the SUs cooperatively exchange the sensing outcomes to make the more accurate decisions based on the overall sensing results.

3. Channel Aggregating Technique

After the SUs sense the licensed channels for a period of time, they have the information of the licensed channel conditions. By using this information, the SUs can opportunistically utilize multiple unused channels simultaneously. However, in most cases, the unused channels are discontinuous. Fortunately, the orthogonal frequency division multiplexing access (OFDMA) has been introduced to help the SUs aggregate the discontinuous channels. In particular, the cognitive radios with OFDMA can enable or suppress the corresponding subcarriers based on the channel availability, and thus access the multiple continuous/discontinuous unused channels simultaneously.

C. The Proposed CREAM-MAC Protocol

1. Protocol Overview

There are many challenges imposed on the design of MAC protocols for the DSA networks. Among them, the following three problems are most important: (i) the problem when to transmit data packets in a way that limits the interference on the PUs, (ii) synchronization between the SU sender and the SU receiver due to the

difference of the channel availability between them, and (iii) the traditional hidden terminal problem and the multi-channel hidden terminal problem.¹ Keeping these in mind, we start to develop the CREAM-MAC protocol under which the SUs can dynamically utilize the vacant licensed channels.

The CREAM-MAC protocol employs a *common control channel* as the rendezvous where the SUs exchange the control packets for multi-channel resource reservation. The control channel can be either statically assigned or dynamically selected. Under the static case, the control channel can use either the dedicated channel licensed to the SUs or the unlicensed spectrum band (e.g., 2.4GHz spectrum for IEEE 802.11b/g). On the other hand, for the dynamical case, the control channel can select the most reliable one from the unused channels which are licensed to the PUs [45]. In this chapter, we do not delve into which way the control channel is selected. Instead, we assume that control channel is *always* reliable and available.

Under the CREAM-MAC protocol, each SU is equipped with n sensors, such that at most n licensed channel can be sensed simultaneously. After sensing the licensed spectrum for a period of time, each SU has the information of the channel states in these spectrum bands. Then, the SUs can opportunistically access the vacant channels which are not being occupied by the PUs. Since the interference from SUs' transmission must be constrained to a modest level the PUs can tolerate, we limit each channel access time of SUs to be no more than the maximum tolerable interference period, denoted by T_d^{\max} . Thus, the constraint that each opportunistic access of the SUs does not exceed T_d^{\max} time units ensures that the PUs only experience the acceptable and limited interference imposed by the SUs. Moreover, the CREAM-

¹In multi-channel systems, especially those with only one single transceiver, the multi-channel hidden terminal problem emerges. The reason is that a single transceiver may operate on only one channel, which makes it difficult to use virtual carrier sensing to handle the hidden terminals [92].

MAC protocol employs the cooperative sequential spectrum sensing scheme for the CREAM-MAC protocol to improve the spectrum sensing accuracy, and thus further protect the PUs by reducing the interference caused by SUs.

One of the important components for the CREAM-MAC protocol is to employ the four types (two pairs) of control packets, namely, Ready-to-Send/Clear-to-Send (RTS/CTS) and Channel-State-Transmitter/Channel-State-Receiver (CST/CSR) packets, to implement the *channel negotiation* which is a process for multiple SUs to compete for the vacant licensed channels. All of the above four types of control packets are exchanged over the control channel. First, the functions of the RTS/CTS control packets include: (i) reserving the control channel, and (ii) solving the hidden terminal problem. The SU sender sends the RTS packet over the control channel based on the contention-based mechanism. Without loss of generality, we adopt the binary exponential backoff based IEEE 802.11 Distributed Coordination Function (DCF) [82] as the contention algorithm. The RTS/CTS handshakes can prevent the neighboring SUs from selecting the same channels to transmit data, guaranteeing no collisions between the SUs. Thus, exchanging the RTS/CTS control packets can efficiently solve the hidden terminal problem. Second, the function of the CST/CSR handshakes aims to synchronize the vacant channel information between the SU sender and the SU receiver, and thus to prevent the collisions between the SUs and the PUs. The CST packet includes the lists of the vacant channels at the transmitter's side, while the CSR packet includes the lists at the receiver's side. The exchange of the CST/CSR packets ensures that the SU sender and the SU receiver select the set of the vacant channels, which are shared by both of them. In summary, the objective of the RTS/CTS control packets is to prevent the collisions among the SUs, while the objective of the CST/CSR control packets is to avoid the collisions between the SUs and the PUs. We will detail the process on how the control packets are exchanged

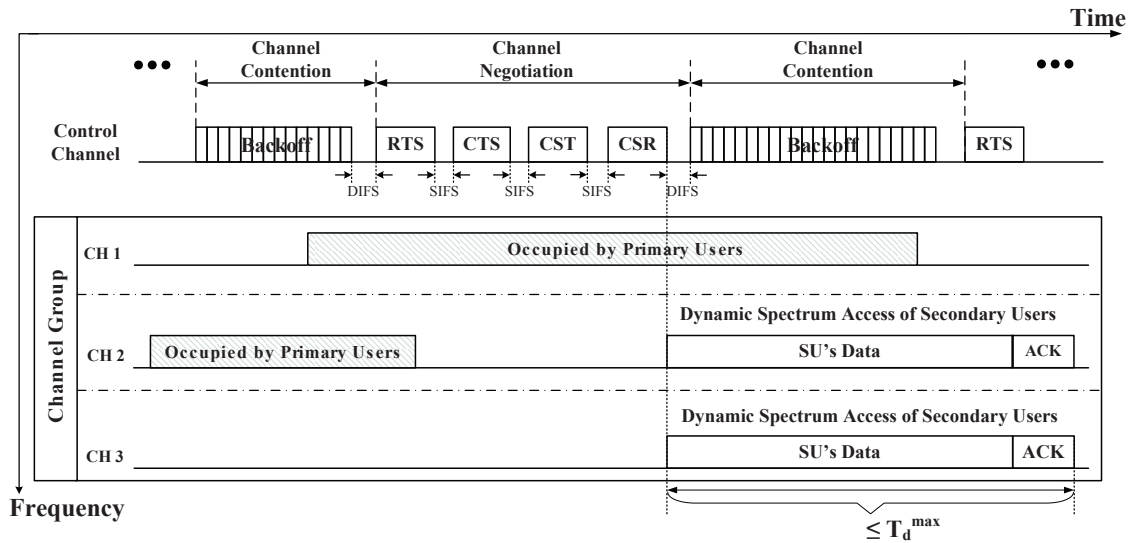


Fig. 23. Illustrations of the CREAM-MAC protocol for an example case with 1 control channel and 3 data channels (CH 1, CH 2, CH 3) which form a Channel Group.

over the control channel in Section C-4 and Section C-5.

To better understand the CREAM-MAC protocol, Fig. 23 illustrates an example case with 1 control channel and 3 data channels (CH 1, CH 2, CH 3) which form a Channel Group (to be detailed in Section C-3). In this particular example, when an SU sender wants to communicate with an SU receiver through the cognitive-radio based DSA network, the SU sender contends for the data channels via the control channel by going through the binary exponential backoff algorithm as described in the above. After the successful *backoff* stage, the SU sender conducts the *channel negotiation* with the SU receiver by exchanging RTS/CTS/CST/CSR control packets over the control channel. Since the common idle licensed channels for the SU sender and SU receiver are CH 2 and CH 3 (CH 1 is being occupied by PUs) at this time point, after the successful channel negotiation, the SU sender utilizes CH 2 and CH 3 simultaneously to send the data to the SU receiver. Upon successfully receiving the data, the SU receiver responds with two ACK packets to the SU sender over CH 2 and

CH 3, respectively. Note that the channel negotiation over the control channel and the opportunistic data transmission over the licensed data channels can be performed simultaneously by different pairs of SU senders and SU receivers. As shown in Fig. 23, because the licensed CH 1 becomes idle during the time when the SU sender and SU receiver exchange data over the licensed CH 2 and CH 3, another SU sender can start its own channel negotiation by sending the RTS packet.

2. The Maximum Allowable Transmission Duration for SUs

Before transmitting packets, the SUs need to sense the licensed channel and detect the presence of the PUs. Due to the half-duplex characteristic of the wireless radio, SUs cannot sense the channel while transmitting their own signals, which implies that the SUs cannot accurately know when the PUs become active again, especially when the SUs are not synchronized with PUs. The SUs may inevitably cause harmful interference to PUs. We have to limit the duration of interference that is caused by SUs. Particularly, we apply the interference constraint in time domain by limiting the amount of time when the SUs and PUs transmit simultaneously.

In this chapter, we assume the duration of each OFF state ($T_{0,i}$) of the i -th data channel follows the exponential distribution. Let t_{sp} and t_{ls} be time that the channel switches from an ON state to an OFF state and the most recent time that the channel state is sensed, respectively. If the channel is in an OFF state at t_{ls} , then there is still a positive probability that the channel remains OFF for a certain period, and thus it is possible for the SUs to opportunistically access the spectrum. Let τ_t be the transmit duration of SUs. Given that the channel is in an OFF state at t_{ls} , we can derive the probability that the SUs will interfere with the PUs in a given channel

during the transmission as follows:

$$I_1(\tau_t) = \Pr\{T_{0,i} < t_{ls} - t_{sp} + \tau_t | T_{0,i} > t_{ls} - t_{sp}\} = 1 - e^{-\frac{\tau_t}{\bar{T}_{0,i}}}. \quad (4.4)$$

In our proposed scheme, the SUs are allowed to utilize up to n licensed channels during a transmission. Then, we obtain the probability that at least a channel is interfered by the SUs as follows:

$$I_n(\tau_t) = 1 - (1 - I_1)^n = 1 - e^{-\frac{\tau_t}{n\bar{T}_{0,i}}}. \quad (4.5)$$

It is clear that the probability $I_n(\tau_t)$ is a monotonically increasing function of τ_t . For the given predefined interference constraint, denoted by I_{th} , we can derive the maximum allowable transmission duration $T_{d,i}^{max}$ for the i -th data channel as follows:

$$T_{d,i}^{max} = \operatorname{argmax}_{\tau_t > 0} \{I_n(\tau_t) < I_{th}\}. \quad (4.6)$$

Since we assume that the PUs' channel utilization pattern is homogeneous, i.e., $\bar{T}_{0,i} = \bar{T}_{0,j}$, $\forall i \neq j$, we have $T_d^{max} = T_{d,i}^{max}$, $\forall i$. In other words, the maximum allowable transmission durations for all channels are the same, and thus in the rest of chapter we use T_d^{max} only.

3. The Selection of Licensed Channels

Since the licensed channels are sometimes utilized by the PUs unevenly, some licensed channels may be utilized more than the others. Because the SUs can only sense a limited number of licensed channels simultaneously, to fully utilize the licensed channels, the SUs need to select the licensed channels which are used less intensively to sense. At the beginning, the SUs randomly select a number ($\leq n$) of channels to sense. They can update the statistical utilization information of licensed channels in either the non-cooperation way or the cooperation way. In the non-cooperation way (e.g., the

POMDP scheme [13]), the SUs update its channel by themselves without exchanging information. On the other hand, the cooperation based channel selection allows the SUs to exchange information such that the SUs can learn the global channel states. Compared with the non-cooperation based schemes, the cooperation based schemes allow the SUs to obtain the updated channel states more accurately and quickly, but need more communication overheads. We adopt the cooperation-based scheme for our CREAM-MAC protocol. In particular, the channel state information is embedded in the control packets. Thus, the SUs can obtain the neighbors' channel state information by overhearing the control packets. After obtaining the statistical utilization information of the licensed channels, the SUs select n of the licensed channels, which form a *channel group* (see Fig. 23 for an example), to sense by using the n sensors.

4. Channel Contention

Under the CREAM-MAC protocol, to decrease the collision probability of the control packets, the SU sender, which attempts to send an RTS packet, selects a backoff counter within a contention window and maintains the contention window size. At the initial state, the contention window size is set to be equal to a predefined value, denoted by CW_{\min} . The counter is deducted by one after a time slot during which both the control channel and at least one data channel in the channel group are idle. Otherwise, the counter remains the same. When the backoff counter reaches zero, the SU sender tries to reserve the control channel by sending RTS to the SU receiver. The binary exponential backoff algorithm is employed when the collisions occur. In other words, the collided SUs double their contention window size to lower the probability of further collision. Fig. 23 demonstrates when/where the channel contention occurs.

5. Channel Negotiation

The CREAM-MAC does not require global synchronization among all the PUs and SUs. Under the CREAM-MAC, the contention mechanism over the control channel is similar to IEEE 802.11 DCF. The SU sender reserves time for the following transmission operations within the neighborhood through the control channel by exchanging RTS/CTS control packets with the SU receiver. In particular, after the backoff counter of the SU sender reaches zero, the SU sender senses the control channel for a duration equal to the DCF interframe space (DIFS). If the control channel remains idle after the DIFS duration, the SU sender sends RTS packet including its channel group list to the SU receiver through the control channel. Upon receiving the RTS packet, if at least one data channel in the channel group is currently not used by its neighboring SUs, the SU receiver replies to the SU sender with a CTS packet after a duration equal to the short interframe space (SIFS). In the meantime, the SU receiver uses its sensors to detect the channel group indicated in the RTS packet. The other neighboring SUs overhear the RTS/CTS control packets to update the available channel list.

After SU sender and SU receiver reserve the control channel by successfully exchanging RTS/CTS packets, they negotiate on the licensed channels which are vacant for both the transmitter and the receiver. More precisely, the SU sender first sends the CST packet which includes the vacant channel list at the transmitter's side. Upon receiving the CST packet, the SU receiver replies with the CSR packet telling the SU sender which common channels are vacant and how long the communication will last over these common channels. Since the communication interval can be less than or equal to T_d^{\max} , the other neighboring SUs can overhear the CST/CSR packets to precisely predict when the channels used by this pair of SUs will be released. The

above channel negotiations operations are also illustrated in an example given in Fig. 23.

The handshakes of RTS/CTS can only solve the traditional hidden terminal problem, but not the multi-channel hidden terminal problem. Specially, the SUs which just finished the data transmission over the licensed channels may miss their neighbor's control packets while their transceivers worked over the licensed data channels. They will probably win the control channel contention, and then enter the licensed channels over which its neighbors are receiving data. Consequently, these SUs become the hidden terminals interrupting their neighbors' ongoing communications. To prevent this from happening, we need to put additional rules on CREAM-MAC. In particular, the SUs which just finished the data transmission can only select the same channel group which they just released within a *waiting* interval of T_d^{\max} . After the waiting period, these secondary can select any other channel groups to use. It allows these SUs to have enough time to observe the current spectrum activities before they start packet transmissions and to prevent them from interfering the neighbors' ongoing communications, since the maximum time interval that the SUs can occupy the licensed channels each time is T_d^{\max} . During the waiting period, if these SUs receive any control packets, they can obtain the updated channel state from the control packets. Otherwise, it is safe for these SUs to assume that all the licensed channels are not being used by any SUs after the waiting period, which can efficiently solve the multi-channel hidden terminal problem. Note that the same rules also apply to the new SUs which first join the network.

6. Data Transmissions

Totally, there are six-way handshakes in a successful data exchange between the SU sender and the SU receiver. Besides the four-way handshakes of the control packets

over the control channel, there are another two-way handshakes of Data/ACK over the licensed data channels. In particular, after the successful four-way handshakes of the control packets over the control channel, the SU sender starts transmitting data to the SU receiver over the channel group's idle channels. The SU receiver sends ACK to the SU sender after successful receiving the data packets from the SU sender. The above data transmissions operations are also illustrated in Fig. 23 for an example. Data transmissions over multiple idle channels in a channel group (see CH 2 and CH 3 in Fig. 23) can be implemented by using the OFDMA-based channel aggregating technique as described in Section B-3. Also, each SU data transmission only lasts for a variable duration less than or equal to T_d^{\max} , as shown in Fig. 23.

7. The Distributed Spectrum Sensing Scheme

As described in Section B, we adopt the energy detection approach. A typical *energy detector* consists of a bandpass filter which chooses the center frequency and bandwidth of interest, a squaring device which calculates the energy of the signal samples, and an integrator which controls the observation intervals. Let Y be the output of the integrator in the energy detector. Following the work in [93], given that the PUs are present (i.e., \mathcal{H}_1) and instantaneous SNR is ν , we have the conditional pdf, denoted by $f_{Y|\nu, \mathcal{H}_1}(y)$, of Y , which follows the non-central chi-square distribution, i.e.,

$$f_{Y|\nu, \mathcal{H}_1}(y) = \frac{1}{2} \left(\frac{y}{2\nu} \right)^{\frac{m-1}{2}} e^{-\frac{2\nu+y}{2}} I_{m-1} \left(\sqrt{2\nu y} \right), \quad (4.7)$$

where m denotes the integer number of samples measured and $I_\nu(\cdot)$ denotes the ν -th order modified Bessel function of the first kind. Since the channel gain is assumed to follow the Rayleigh distribution, the SNR ν follows the exponential distribution with

the mean SNR equal to \bar{v} . Thus, taking into account the fading factor, we have

$$f_{Y|\mathcal{H}_1}(y) = \int_0^\infty f_{Y|v,\mathcal{H}_1}(y) \frac{1}{\bar{v}} e^{-\frac{v}{\bar{v}}} dv = \frac{(1+\bar{v})^m e^{-\frac{y}{2(1+\bar{v})}}}{2(1+\bar{v})^2 \bar{v}^{m-1}} \left[1 - \frac{\Gamma\left(m-1, \frac{\bar{v}y}{2(1+\bar{v})}\right)}{\Gamma(m-1)} \right] \quad (4.8)$$

where $\Gamma(\cdot)$ is the complete gamma function, and $\Gamma(a, z) = \int_z^\infty t^{a-1} e^{-t} dt$ is the upper incomplete gamma function.

On the other hand, suppose that the PUs do not occupy the spectrum (i.e., \mathcal{H}_0), then the output of the integrator in the energy detector can be characterized by the central chi-square distribution as follows:

$$f_{Y|\mathcal{H}_0}(y) = \frac{1}{2^m \Gamma(m)} y^{m-1} e^{-\frac{y}{2}} \quad (4.9)$$

Then, we obtain its cumulative distribution function (cdf), denoted by $F_{Y|\mathcal{H}_1}(y)$, of Y given \mathcal{H}_1 as follows:

$$\begin{aligned} F_{Y|\mathcal{H}_1}(y) &= \int_0^y f_{Y|\mathcal{H}_1}(t) dt \\ &= \frac{\Gamma(m-1, 0) - \Gamma\left(m-1, \frac{y}{2}\right)}{\Gamma(m-1)} + \left(\frac{1+\bar{v}}{\bar{v}}\right)^{m-1} \left[1 - e^{-\frac{y}{2(1+\bar{v})}} - \frac{\Gamma\left(m-1, 0\right)}{\Gamma(m-1)} \right. \\ &\quad \left. + e^{-\frac{y}{2(1+\bar{v})}} \frac{\Gamma\left(m-1, \frac{\bar{v}y}{2(1+\bar{v})}\right)}{\Gamma(m-1)} \right] \end{aligned} \quad (4.10)$$

Similarly, we can get the cdf, denoted by $F_{Y|\mathcal{H}_0}(y)$, of Y given \mathcal{H}_0 as follows:

$$F_{Y|\mathcal{H}_0}(y) = \int_0^y f_{Y|\mathcal{H}_0}(t) dt = 1 - \frac{\Gamma\left(m, \frac{y}{2}\right)}{\Gamma(m)} \quad (4.11)$$

Because in the cognitive systems the PUs have the higher priority in spectrum access than the SUs, the missed detection probability of the PUs' presence should be limited to a small value. However, based on the traditional single-threshold energy-detection method [94], decreasing the missed detection probability is equivalent to increasing the false alarm probability, which consequently decreases the spectrum ac-

cess opportunities for SUs. It is contradicted to decrease the missed detection probability while decreasing the false alarm probability. To overcome the contradiction, we propose to use the *two-threshold based sequential sensing policy*, which can decrease the false alarm probability while confining the missed detection probability to a predefined threshold, denoted by P_{MD}^{th} . The basic idea of our proposed spectrum sensing policy is to collect PUs' signal samples sequentially in multiple uncorrelated sensing rounds to enhance the decision process. In particular, we design two thresholds, denoted by β_1 and β_2 , with $\beta_1 < \beta_2$, for the two hypotheses, \mathcal{H}_1 and \mathcal{H}_0 , respectively. Our proposed policy can be described as follows: 1) When the energy (Y) of the detected signal is larger than β_2 , then we claim that the PUs are active; 2) When Y is less than β_1 , we claim that the PUs are inactive; 3) Otherwise, if $\beta_1 < Y < \beta_2$, the SUs need to take one more sensing round to collect PUs' signal samples after a duration equaling the channel's coherence time until $Y > \beta_2$ or $Y < \beta_1$.

Then, we define and derive the *missed detection probability*, denoted by P_{MD} , as follows:

$$P_{MD} \triangleq \Pr\{Y < \beta_1 | \mathcal{H}_1\} = F_{Y|\mathcal{H}_1}(\beta_1) \quad (4.12)$$

where $F_{Y|\mathcal{H}_1}(\cdot)$ is specified in Eq. (4.10). Similarly, we define and derive the *false alarm probability*, denoted by P_{FA} , as follows:

$$P_{FA} \triangleq \Pr\{Y > \beta_2 | \mathcal{H}_0\} = 1 - F_{Y|\mathcal{H}_0}(\beta_2) \quad (4.13)$$

where $F_{Y|\mathcal{H}_0}(\cdot)$ is specified in Eq. (4.11). Fig. 24 illustrates $f_{Y|\mathcal{H}_0}(y)$, $f_{Y|\mathcal{H}_1}(y)$, P_{MD} , P_{FA} , β_1 , and β_2 . Fig. 24 also shows how β_1 and β_2 impact the missed detection probability P_{MD} and the false alarm probability P_{FA} , respectively. In the two-threshold sensing policy, the missed detection and false alarm probabilities are controlled by two separated parameters, namely, β_1 and β_2 , respectively. As shown in Fig. 24,

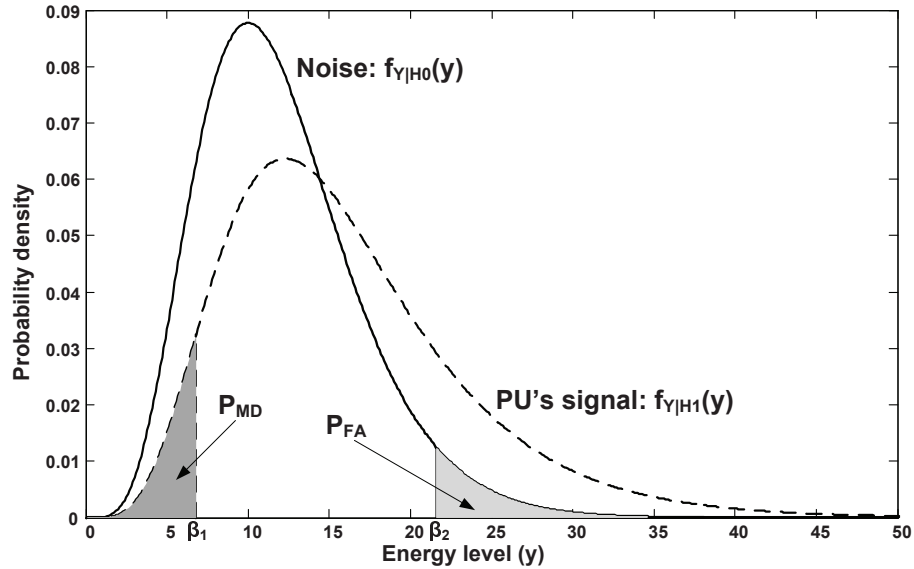


Fig. 24. The illustration of the relationship between the P_{FA} and P_{MD} in the two-threshold sequential sensing. The two thresholds β_1 and β_2 control P_{MD} and P_{FA} , respectively.

decreasing β_1 and increasing β_2 at the same time can decrease both the missed detection and false alarm probabilities, which, however, may also increase the number of required uncorrelated sensing rounds because the probability that the sensed signal's energy level falls between the two thresholds becomes larger. Hence, we proceed to study the impact of β_1 and β_2 on the average number of required sensing rounds by deriving the probability, denoted by q , that the detected signal energy falls between the two thresholds as follows:

$$q = [F_{Y|\mathcal{H}_1}(\beta_2) - F_{Y|\mathcal{H}_1}(\beta_1)] \gamma + [F_{Y|\mathcal{H}_0}(\beta_2) - F_{Y|\mathcal{H}_0}(\beta_1)] (1 - \gamma), \quad (4.14)$$

where γ is the PUs' channel utilization of any given licensed channel. The number of sensing rounds that need to be taken during the i -th spectrum sensing follows the geometry distribution, i.e.,

$$\Pr\{N_s = n\} = q^{n-1}(1 - q).$$

Thus, the average number, denoted by \bar{N}_s , of the sensing rounds that need to be taken during the i -th spectrum sensing is given by

$$\bar{N}_s = \frac{1}{1 - q}. \quad (4.15)$$

It is clear that there is a tradeoff between the number of uncorrelated sensing rounds and false alarm probability while the missed detection probability is upper-bounded. When the missed detection probability is given, β_1 is determined. The larger the value of \bar{N}_s , the smaller the value of β_2 , and thus the smaller the false alarm probability. It is interesting to note that the single-threshold sensing policy is a special case of our sequential sensing policy. Specifically, when setting $\bar{N}_s = 1$, we have $\beta_1 = \beta_2$, which implies that our proposed sequential sensing policy reduces to the single-threshold based sensing policy.

D. Throughput Analysis for the Saturation Network Case

In this section, we develop an analytical model to analyze the aggregate throughput of our proposed CREAM-MAC protocol under the saturation network case, where each SU has always an infinite amount of data packets to send.

1. The Analysis for the Licensed Data Channels

Suppose that there are M licensed data channels and each SU is equipped with n sensors. Based on the CREAM-MAC protocol, the SUs can reserve at most n licensed channels, and utilize all of them with the help of channel aggregating technique if n licensed channels are free. There are $\lfloor M/n \rfloor$ channel groups that can be utilized by the SUs.

Denote a discrete random variable H as the number of vacant channels in a

specified channel group with n licensed channels. To make the model tractable, we assume that each channel is evenly utilized by the PUs. Thus, we apply the same γ to all licensed channels, i.e., $\gamma = \gamma_i = \gamma_j$ for $1 \leq i, j \leq M$, where γ_i is given in Eq. (4.1). Since the channel states among different channels are independent with each other, we get the probability that the number H of vacant channels in a specified channel group is equal to i following the binomial distribution as follows:

$$\Pr\{H = i\} = \binom{n}{i} [1 - \gamma(1 - P_{FA})^2]^i [\gamma(1 - P_{FA})^2]^{n-i}, \quad (4.16)$$

where the term $(1 - P_{FA})^2$ is due to the available-channel list synchronizing between the SU sender and SU receiver. Thus, we can derive the average number, denoted by the expectation $\mathbb{E}[H]$, of vacant channels as follows:

$$\mathbb{E}[H] = \sum_{i=0}^n i \Pr\{H = i\} = n [1 - (1 - P_{FA})^2 \gamma]. \quad (4.17)$$

2. The Analysis for the Control Channels

In order to analyze the saturation network throughput of the proposed CREAM-MAC, we need to study the contention behavior over the control channel where the control packets are transmitted based on the IEEE 802.11 DCF. We develop the analytical model based on the works of [95, 96], which uses a Markov chain model to analyze the backoff operations for IEEE 802.11 DCF. Following the previous works, if we denote the probability that a given SU transmits in a randomly chosen time slot by τ , and the probability that a transmitted packet collides by p , respectively, then we obtain the following equations:

$$\begin{cases} \tau = \frac{2(1-2p)}{(1-2p)(CW_{min}+1)+CW_{min}p[1-(2p)^m]} \\ p = 1 - (1 - \tau)^{u-1} \end{cases} \quad (4.18)$$

where m is the maximum backoff stage, u is the number of the contending SUs, CW_{\min} is the initial contention backoff window size. Note that τ is the function of p while p is also the function of τ . Solving simultaneously the two equations in Eq. (4.18), we can obtain the numerical solutions for τ and p . Obviously, $\tau, p \in (0, 1)$. Observing Eq. (4.18), we can learn that p only depends on the number of the contending SUs (u), the maximum backoff stage (m), and the initial contention backoff window size (CW_{\min}).

Let P_{tr} be the probability that there is at least one transmission in a given time. Since each contending SU transmits with probability τ at any given time, given that there are u contending SUs, we get that P_{tr} can be expressed as:

$$P_{tr} = 1 - (1 - \tau)^u. \quad (4.19)$$

Then, we can derive the probability, denoted by P_s , that an SU transmits successfully without collisions, given that at least one SU transmits, as follows:

$$P_s = \frac{u\tau(1 - \tau)^{u-1}}{P_{tr}} = \frac{u\tau(1 - \tau)^{u-1}}{1 - (1 - \tau)^u}. \quad (4.20)$$

Denote the duration of a time slot by σ . Under the IEEE 802.11 DCF, the backoff counter of the contention node decreases by 1 when the sensed channel is idle in a time slot. However, it should be noted that under the CREAM-MAC protocol, only when both the control channel and at least one data channel in the channel group are idle, the backoff counters of the contending SUs decrease by 1. In other words, if all of channels in the channel group are busy, the backoff counter should remain the same until the time slot in which control channel and at least one data channel in channel group are idle, which is different from the backoff mechanism in traditional IEEE 802.11 DCF. Therefore, we introduce a new parameter, namely the effective duration of a time slot, denoted by σ' , which represents the average duration of a

time slot after taking the above descriptions into account. The effective duration of a time slot includes the duration of the normal time slot and the average duration of time slots where the backoff counter remains the same due to all the channels in the channel group being busy. Thus, we can derive σ' as follows:

$$\sigma' = \sigma(1 + \mathbb{E}[N_{\text{busy}}]), \quad (4.21)$$

where N_{busy} is the random number of time slots in which all the channels in a channel group are busy between the two consecutive time slots where the backoff counter decreases, and $\mathbb{E}[N_{\text{busy}}]$ is the mathematical expectation of N_{busy} . Since the channel states in different time slots are independent, N_{busy} follows the geometric distribution, and thus we can obtain its probability mass function (pmf) as follows:

$$\Pr\{N_{\text{busy}} = i\} = P_{\text{busy}}^i(1 - P_{\text{busy}}), \quad (4.22)$$

where $P_{\text{busy}} = \Pr\{H = 0\}$ is the probability that all the channels in a channel group are busy. According to Eq. (4.16), we have $\Pr\{H = 0\} = [\gamma(1 - P_{FA})^2]^n$. Then, we can get $\mathbb{E}[N_{\text{busy}}]$ by

$$\mathbb{E}[N_{\text{busy}}] = \sum_{i=0}^{\infty} i \Pr\{N_{\text{busy}} = i\} = \frac{[\gamma(1 - P_{FA})^2]^n}{1 - [\gamma(1 - P_{FA})^2]^n}. \quad (4.23)$$

Hence, substituting Eq. (4.23) into (4.21), we can calculate the effective duration (σ') of a time slot.

Let T_{succ} and T_{coll} be the time used for successful transmission and the time spent when collisions happen, respectively. Then, T_{succ} and T_{coll} can be expressed as:

$$\begin{cases} T_{\text{succ}} = \frac{\text{RTS} + \text{CTS} + \text{CST} + \text{CSR}}{R_c} + 3 \times \text{SIFS} + \text{DIFS}, \\ T_{\text{coll}} = \frac{\text{RTS}}{R_c} + \text{DIFS}, \end{cases} \quad (4.24)$$

where R_c is the transmission rate of control channel, SIFS is the duration of the short

interframe space, DIFS is the duration of DCF interframe space, RTS, CTS, CST, and CSR are the sizes of RTS, CTS, CST, CSR control packets, respectively. Then, we can derive the average time, denoted by $\mathbb{E}[T_c]$, spent for the successful four-way handshakes of RTS/CTS/CST/CSR (i.e., the channel negotiation) as follows:

$$\begin{aligned}\mathbb{E}[T_c] &= \frac{(1 - P_{tr})\sigma' + P_s P_{tr} T_{succ} + P_{tr}(1 - P_s)T_{coll}}{P_s P_{tr}} \\ &= T_{succ} + \frac{1 - P_{tr}}{P_s P_{tr}}\sigma' + \frac{1 - P_s}{P_s}T_{coll}.\end{aligned}\quad (4.25)$$

3. The Aggregate Throughput

For convenience of presentation, Table III lists the important parameters for the design and analysis of our proposed CREAM-MAC protocol. Let N_c be the maximum number of SUs that successfully reserve the licensed channel groups during the length of T_d^{max} on average. Clearly N_c is inversely proportional to $\mathbb{E}[T_c]$, and thus we obtain:

$$N_c = \frac{T_d^{max}}{\mathbb{E}[T_c]}.$$

Note that there are at most $\lceil N_c \rceil$ SUs that can opportunistically transmit data over the licensed data channels at the same time from the global viewpoint. Comparing the value of $(N_c + 1)$ and the number $\lfloor M/n \rfloor$ of channel groups, we can determine whether the control channel gets saturated.

On one hand, if $(N_c + 1) \leq \lfloor M/n \rfloor$, then there are always vacant channel groups that can accommodate the SUs successfully conducting channel negotiation. As a result, the control channel gets saturated and is the bottleneck to the aggregate throughput. Fig. 25(a) shows an example of the saturated control channel case where the number $\lfloor M/n \rfloor$ of channel groups is equal to 4 and $3 < N_c + 1 < 4$. As shown in Fig. 25(a), the SUs can always find the idle channel group to transmit data whenever

Table III. The parameters for design and analysis of the CREAM-MAC protocol.

RTS	20 Bytes	The size of RTS packet
CTS	20 Bytes	The size of CTS packet
CST	20 Bytes	The size of CST packet
CSR	20 Bytes	The size of CSR packet
σ	9 μs	Mini-slot interval
SIFS	15 μs	Short interframe space
DIFS	34 μs	DCF interframe space
R_c	1 Mbps	Transmission rate of the control channel
R_d	1 Mbps	Transmission rate of a licensed channel
n		The number of sensors each SU has
u		The number of contending SUs
γ		Channel utilization of PUs
M		The number of licensed channels
$\mathbb{E}[T_c]$		Avg. time for successful four-way handshakes
T_d^{max}		Max. tolerable interference-time of PUs
CW_{min}		The minimum size of contention window
β_1		Threshold that determines the missed detection probability
β_2		Threshold that determines the false alarm probability
ν		Instantaneous SNR of PUs' signal at the side of the SU

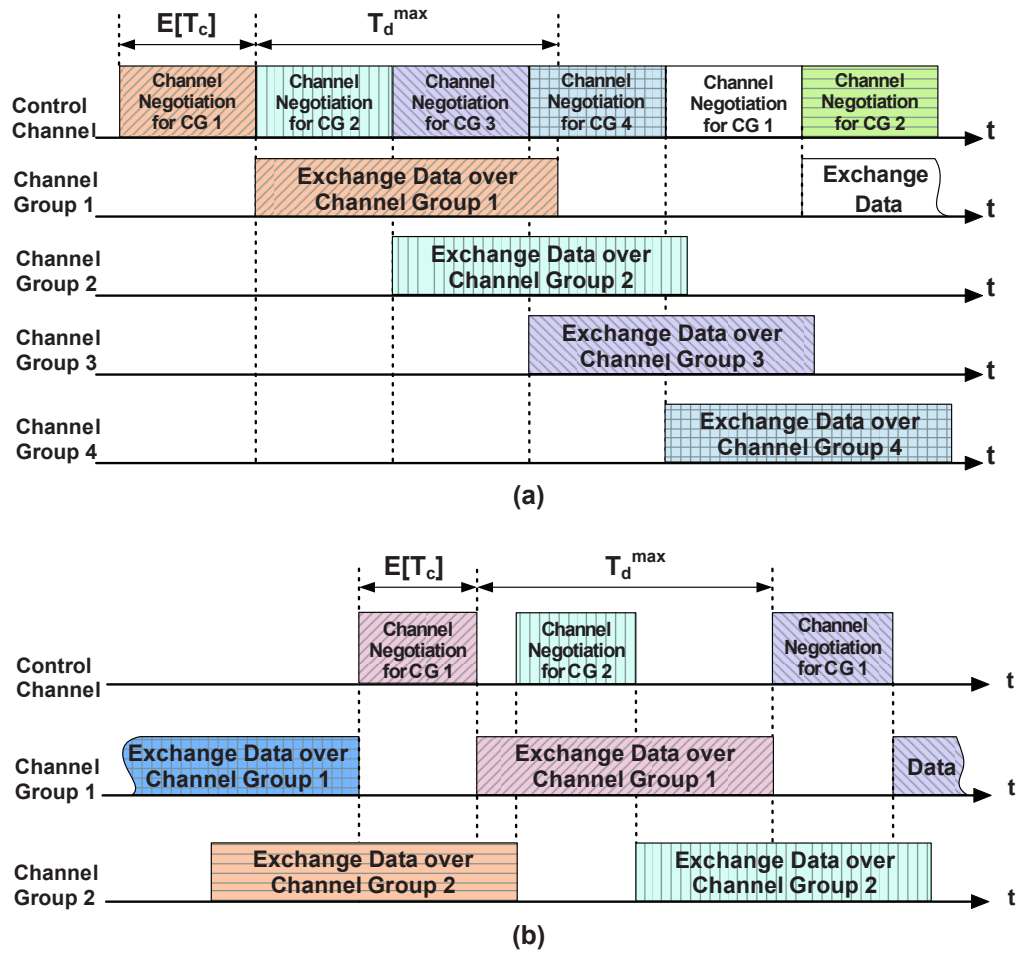


Fig. 25. Illustrations of the CREAM-MAC protocol for the saturation network case. (a) The case where the number of channel group is 4 and the *control channel gets saturated*. (b) The case where the number of channel group is 2 and the *control channel does not get saturated*, implying that the data channels get saturated. Here CG i represents Channel Group i . The channel occupation blocks drawn with the *same* filling pattern and color in either Fig. 25(a) or Fig. 25(b) represent that the control-channel and data-channel resources are occupied by the *same* pair of SU sender and SU receiver. The average duration of the channel negotiation is equal to $E[T_c]$ and the duration for the exchange data block is equal to T_d^{\max} .

the SUs successfully complete the channel negotiation over the control channel. On the other hand, if $(N_c + 1) > \lfloor M/n \rfloor$, then there is always an idle period between the two consecutive channel negotiations on the control channel because the data channels in each channel group become saturated. Fig. 25(b) shows an example of this case where the number $\lfloor M/n \rfloor$ of channel groups is equal to 2 and $N_c + 1 > 3$. As shown in Fig. 25(b), due to the requirements of the CREAM-MAC protocol, the SUs cannot start channel negotiation until at least one channel group becomes idle, which results in an idle period between two consecutive channel negotiations.

Based on whether the control channel gets saturated or not, we derive the aggregate throughput in two different cases, respectively. First, for the case where the control channel gets saturated, as shown in Fig. 25(a), on average, the SUs can transmit data for T_d^{\max} time units at the cost of $\mathbb{E}[T_c]$ time units. Note that in the saturation network case, all the SUs that win the channel reservation use up all of the transmission time T_d^{\max} to transmit packets. Consequently, we derive the aggregate throughput, denoted by η_c , when the control channel becomes saturated as follows:

$$\eta_c = \frac{T_d^{\max} \mathbb{E}[H] R_d}{\mathbb{E}[T_c]} \quad (4.26)$$

where R_d is the data rate of a licensed channel, $\mathbb{E}[H]$ is the average number of vacant channels and is given by Eq. (4.17). Second, when $(N_c + 1)$ is larger than the number $\lfloor M/n \rfloor$ of channel groups, as shown in Fig. 25(b), for every channel group, the SUs can effectively transmit for T_d^{\max} time units within each $(\mathbb{E}[T_c] + T_d^{\max})$ time units. Hence, we can derive the aggregate throughput, denoted by η_d , when the control channel is not saturated as follows:

$$\eta_d = \left\lfloor \frac{M}{n} \right\rfloor \frac{T_d^{\max} \mathbb{E}[H] R_d}{\mathbb{E}[T_c] + T_d^{\max}} \quad (4.27)$$

where the term $\lfloor M/n \rfloor$ represents the number of data channel groups. Therefore,

combining Eqs. (4.26) and (4.27) together, we obtain the general expression of the aggregate throughput, denoted by η , for the saturation network as follows:

$$\eta = \frac{T_d^{\max} N_d \mathbb{E}[H] R_d}{\mathbb{E}[T_c] + T_d^{\max}} = \frac{T_d^{\max} N_d n [1 - \gamma(1 - P_{FA})^2] R_d}{\mathbb{E}[T_c] + T_d^{\max}}, \quad (4.28)$$

where

$$N_d = \min \left\{ (N_c + 1), \left\lfloor \frac{M}{n} \right\rfloor \right\} \quad (4.29)$$

which distinguishes between the control-channel saturation (if $N_d = N_c + 1$) and data-channel saturation (if $N_d = \lfloor M/n \rfloor$).

E. Performance Analysis for the Special Non-Saturation Network Case

In this section, we analyze the performance of the CREAM-MAC protocol, including the network throughput, queueing delay, and service delay (or packet transmission delay), for the non-saturation-network case, where the SUs may have the empty queues. To make the model tractable, we consider the case where the number of licensed channels is equal to the number of equipped sensors, i.e., $M = n$. As a result, there is only one channel group for the SUs. Without loss of generality, we suppose that the packets of the SUs arrive according to the Poisson process with a mean arrival rate λ and the size of each data packet is equal to $R_d T_d^{\max}$. Every time the SUs successfully reserve the licensed data channels, they occupy the licensed channels for a period of T_d^{\max} to transmit their data packets. For convenience of presentation, we call the procedure, during which an SU successfully reserves the data channels and transmits data packets, a *service procedure*, or simply, a *service*, in the following discussions.

Utilizing the channel-aggregating technique, the SUs can send multiple data

packets simultaneously after they successfully exchanged the control packets. Note that the number of data packets that an SU can send depends on the number of common unused channels, which is a random variable, between the SU sender and SU receiver. This implies that the service capacity for the SUs *varies* from time to time. Therefore, similar to the non-saturation-network case in Chapter II, for the non-saturation-network case of the proposed CREAM MAC protocol, we also use the single-server bulk-service queueing model, $M/G^Y/1$, to characterize the network throughput, queueing delay, and service delay, where Y stands for the variable service capacity.

We first obtain the equilibrium-state distribution of the number of buffered packets in the queue for any given SU at any random points in order to derive the queueing delay and network throughput. We start with studying the random number, N_α^+ , $\alpha = 0, 1, 2, \dots$, where α is used to index the services, of packets in the system for a given SU immediately after the α -th service. The probability, denoted by P_j^+ , that the system has j packets in the equilibrium state can be expressed as:

$$P_j^+ = \lim_{\alpha \rightarrow \infty} \Pr\{N_\alpha^+ = j\}. \quad (4.30)$$

Denote by Y_α , $\alpha = 0, 1, 2, \dots$ the service capacity during the α -th service, i.e., the maximum number of data packets the given SU can send during the α -th service. Since each data packet is transmitted over an unused channel and the size of each data packet is equal to $R_d T_d^{max}$, the service capacity is equal to the maximum number of unused channels in the channel group. Thus, we obtain Y_α 's distribution as follows:

$$\Pr\{Y_\alpha = i\} = \Pr\{H = i\} = \binom{n}{i} [1 - \gamma(1 - P_{FA})^2]^i [\gamma(1 - P_{FA})^2]^{n-i}, \quad (4.31)$$

where n is the number of sensors equipped in each SU and equal to the number of licensed channels. Then, the pmf, denoted by y_i , that the given SU sends i data

packets during a service at the equilibrium state, can be determined by

$$y_i = \lim_{\alpha \rightarrow \infty} \Pr\{Y_\alpha = i\}. \quad (4.32)$$

Since the sequence of $\{y_i\}$ is independent of the arrival process of the packets for a given SU, we can get average number, denoted by \bar{y} , of packets that an SU can send during a service as follows:

$$\bar{y} = \mathbb{E}[\Pr\{Y_\alpha = i\}] = n [1 - \gamma(1 - P_{FA})^2]. \quad (4.33)$$

Let us define the following two equations:

$$\begin{cases} \phi_j \triangleq \sum_{m=j}^n y_m, \\ \Phi_j(z) \triangleq \sum_{m=j}^n y_m z^m, \end{cases} \quad (4.34)$$

where $j = 0, 1, 2, \dots$, and note that $\Phi_0(z)$ is the probability generating function (PGF) for $\{y_i\}$ and $\Phi_0(1) = \phi_0$.

For a given SU, a service period consists of four components: (i) the successful transmission time of packets sent by itself, (ii) the successful transmission time of packets sent by other SUs, (iii) the backoff time, and (iv) the time spent due to collisions. Since the sum of components (iii) and (iv) is much smaller than the components (i) and (ii), we only focus on the components (i) and (ii) to derive the service period. The successful transmission time, denoted by D , of a node includes the time spent by transmitting control packets and data packets, i.e.,

$$D = T_{succ} + T_d^{\max}. \quad (4.35)$$

Let p_s be the probability that a given SU successfully reserves the data channels given that a successful reservation occurs during a contention period, and V be the random number of other nodes' transmissions between two successfully transmissions

of a given node plus its own successful transmission (i.e., the service period in terms of the number of successful transmissions), respectively. Then, we obtain [86]

$$p_s = \frac{1}{\rho(u-1) + 1}, \quad (4.36)$$

where ρ is the system utilization. Then, the service period in terms of the number of successful transmissions (V) follows the geometric distribution, which has the following pmf:

$$\Pr\{V = v\} = p_s(1 - p_s)^{v-1}, \quad (4.37)$$

where $v = 1, 2, \dots$. Thus, we can get the average service period in terms of the number of successful transmissions, denoted by \bar{v} for a given SU as follows:

$$\bar{v} \triangleq \mathbb{E}[V] = \frac{1}{p_s} = \rho(u-1) + 1. \quad (4.38)$$

According to the definition of the system utilization, ρ can also be written as

$$\rho \triangleq \frac{\lambda D \bar{v}}{\bar{y}}, \quad (4.39)$$

where \bar{y} is given by Eq. (4.33). Consequently, solving Eqs. (4.38) and (4.39) simultaneously, we can obtain

$$\rho = \frac{\lambda D}{\bar{y} - \lambda(u-1)D}. \quad (4.40)$$

For the equilibrium-state probability distribution to exist, ρ should be less than 1.

Denote ψ as the random number of arrived packets for a given SU during the α -th service. Note that the packet arrivals follow the Poisson process. Given that the length of the service period is vD , we can obtain the probability that the number of

arrived packets is j as follows:

$$\Pr\{\psi = j|V = v\} = \frac{e^{-\lambda Dv}(\lambda Dv)^j}{j!}. \quad (4.41)$$

By removing the conditioning on variable V in Eq. (4.41), we get the probability that the number of arrived packets is j as follows:

$$\begin{aligned} \Pr\{\psi = j\} &= \sum_{v=1}^{\infty} \Pr\{\psi = j|V = v\} \Pr\{V = v\} \\ &= \sum_{v=1}^{\infty} \frac{e^{-\lambda Dv}(\lambda Dv)^j}{j!} [p_s(1-p_s)^{v-1}]. \end{aligned} \quad (4.42)$$

Then, we get the PGF, denoted by $\Psi(z)$, of $\Pr\{\psi = j\}$ as follows:

$$\Psi(z) = \sum_{j=0}^{\infty} \Pr\{\psi = j\} z^j = \frac{p_s e^{\lambda D(z-1)}}{1 - (1-p_s)e^{\lambda D(z-1)}}. \quad (4.43)$$

Let us denote N_s as the average number of packets that SUs send during a service period at the equilibrium state. We can obtain:

$$N_s = \min \left\{ N_q, \lim_{\alpha \rightarrow \infty} Y_\alpha \right\}, \quad (4.44)$$

where Y_α is the service capacity at α -th service. Thus, we obtain the network throughput, denoted by θ , as follows:

$$\theta = \mathbb{E}[N_s] T_d^{\max} R_d. \quad (4.45)$$

Following the work in [87, 88], we can obtain the average queue length, denoted by L_q , of the packets for any given SU is the first moment of N_q as follows

$$\begin{aligned} L_q &= \frac{(\lambda D)^2 \Psi^{(2)}(1) + \Phi_0^{(2)}(1)}{2\bar{y}(1-\rho)} + \frac{1-n+\rho(n-\rho\bar{y})}{1-\rho} \\ &\quad + \sum_{i=1}^{n-1} (1-z_i)^{-1} - \bar{y}\rho + \frac{(\lambda D)^2 \Psi^{(2)}(1)}{2\bar{y}\rho}, \end{aligned} \quad (4.46)$$

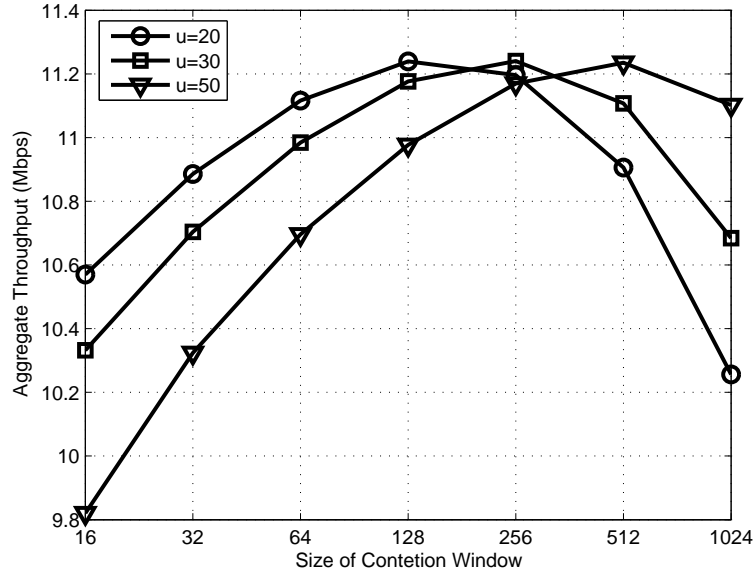


Fig. 26. The aggregate throughput against the size of contention window (CW_{min}). The number (n) of sensors is set to be 4. The channel utilization (γ) of PUs is set to be 0.5. R_c and R_d are set to be 1 Mbps.

where $f^{(i)}(\cdot)$ indicates the i -th derivative of $f(\cdot)$, and z_i with $1 \leq i \leq n - 1$ are the $(n - 1)$ roots of $\Psi(z)\Phi_0(z^{-1}) = 1$, which are located inside the unit circle [88]. Using the Little's law, we can derive the queueing delay, denoted by W_q , for a given SU as follows:

$$W_q = \frac{L_q}{\lambda}. \quad (4.47)$$

Finally, we can derive the service delay, or the average packet transmission delay, denoted by W_s , for a given SU as follows:

$$W_s = W_q + \bar{v}D = \frac{L_q}{\lambda} + [\rho(u - 1) + 1]D. \quad (4.48)$$

F. Performance Evaluations

The parameters used to evaluate the CREAM-MAC protocol are summarized in Table III. We first investigate the aggregate throughput for the saturation network case. Let the number n of sensors of each SU be 4, the channel utilization γ of PUs be fixed at 0.5, and R_c be equal to 1 Mbps. By tuning the thresholds β_1 and β_2 in the spectrum sensing scheme, the false alarm probability and missed detection probability are set to 10^{-3} and 10^{-4} , respectively. Using Eq. (4.28), we plot the aggregate throughput η against the size of the contention window CW_{min} in Fig. 26. In Fig. 26, we observe that the optimal CW_{min} , denoted by CW_{min}^* , which achieves the highest aggregate throughput, changes with the different number (u) of contending SUs. This is expected because given that there are sufficient licensed channels, the aggregate throughput only depends on the time spent to accomplish the RTS/CTS/CST/CSR four-way handshakes over the control channel, which is ultimately determined by the IEEE 802.11 DCF parameters, such as CW_{min} and R_c . If we can obtain the number of contending SUs in advance, we can pre-select the optimal CW_{min} which achieves the highest aggregate throughput. On the other hand, if the number of contending SUs dynamically fluctuates, we can adopt the algorithms proposed in [96] to dynamically adjust the value of CW_{min} . In the rest of our chapter, we assume that in each scenario the number of contending SUs is fixed, and thus we can pre-select CW_{min}^* for different scenarios with different u 's.

After setting the optimal CW_{min}^* to be 256 for the case where $u = 30$, we use Eq. (4.28) to get numerical results of the aggregate throughput against the channel utilization of PUs as shown in Fig. 27. The aggregate throughput (η) decreases as the channel utilization (γ) of PUs increases, which implies that the SUs get less opportunities to transmit their own packets if the PUs utilize the licensed channels

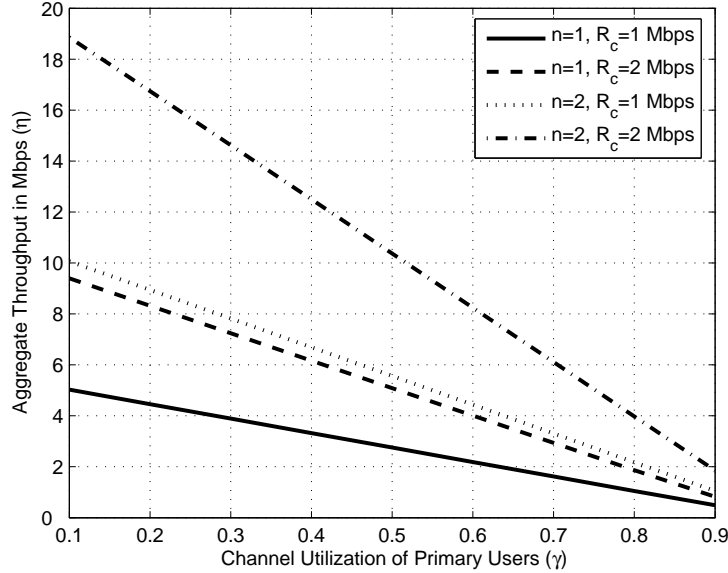


Fig. 27. The aggregate throughput against the channel utilization of PUs, when the number (M) of licensed channels is set to be 30, the number (u) of contending SUs is set to be 30, and $CW_{min} = 256$.

more intensively. From Fig. 27, we also observe that a larger number of sensors equipped in an SU can lead to a higher aggregate throughput. However, the larger number of sensors equipped with in each SU, the higher the hardware cost. An alternative way to improve the aggregate throughput with the stringent hardware-cost constraint is to increase the data rate of the control channel. For example, consider Scenario I where each SU is equipped with a sensor and the data rate of the control channel is 2 Mbps and Scenario II where each SU is equipped with two sensors and the data rate of the control channel is 1 Mbps. From Fig. 27, the aggregate throughputs achieved by Scenario I and Scenario II are close to each other regardless of the channel utilization of PUs.

Then, we evaluate our proposed CREAM-MAC protocol in the saturation network case using a customized simulator. Fig. 28 shows the simulation and analytical

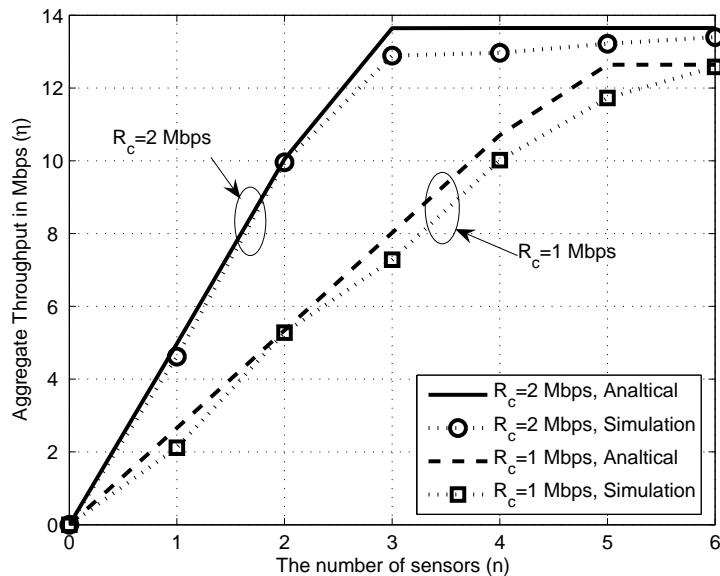


Fig. 28. The aggregate throughput against the number of sensors in each SU, when the channel utilization (γ) of the PUs is set to be 0.5, the number (M) of licensed channels is set to be 30, the number (u) of contending secondary is set to be 30, and $CW_{min} = 256$.

results, given that the number (M) of licensed channels is 30. Each point in the simulation plots of Fig. 28 is the mean of the results of 500 simulations. Fig. 28 shows that the simulation results agree well with the analytical results. We also observe that the aggregate throughput linearly increases as the number of sensors equipped in an SU increases before they reach the state where all the licensed channels are saturated. This is expected by Eqs. (4.29) and (4.28). More precisely, when the SUs can only access a small number of channels simultaneously with fewer sensors, there are sufficient channel groups for the SUs to access. As a result, the control channel becomes saturated, which implies that the average number of winning SUs during a fixed amount of time is constant. Thus, increasing the number of sensors can efficiently increase the aggregate throughput. On the other hand, when the num-

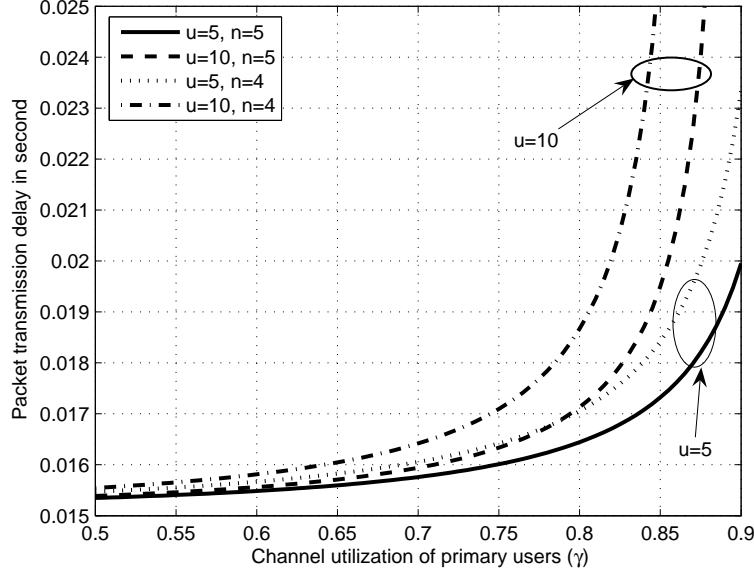


Fig. 29. The packet transmission delay against the channel utilization of PUs with the combinations of the number (u) of contending SUs being set to be 5 or 10 and the number (n) of licensed channels being set to be 4 or 5.

ber of sensors equipped with in each SU is large enough, the licensed data channels become saturated before the control channel gets saturated, which implies that the control channel is not the bottleneck any more. Thus, further increasing the number of sensors cannot increase the aggregate throughput any more. However, as shown in Fig. 28, we can still increase the aggregate throughput by increasing the data rate of the control channel because the higher control-channel data rate implies the less time spent to accomplish the RTS/CTS/CST/CSR four-way handshakes.

We further proceed to the non-saturation network case. Using Eq. (4.48), we plot the packet transmission delay against the channel utilization of PUs when the packet arrival rate is set to be a constant of 0.049, as shown in Fig. 29. The packet transmission delay increases as the channel utilization (γ) of PUs gets larger. In particular, when γ is larger than 0.83, the packet transmission delay for $u = 10$

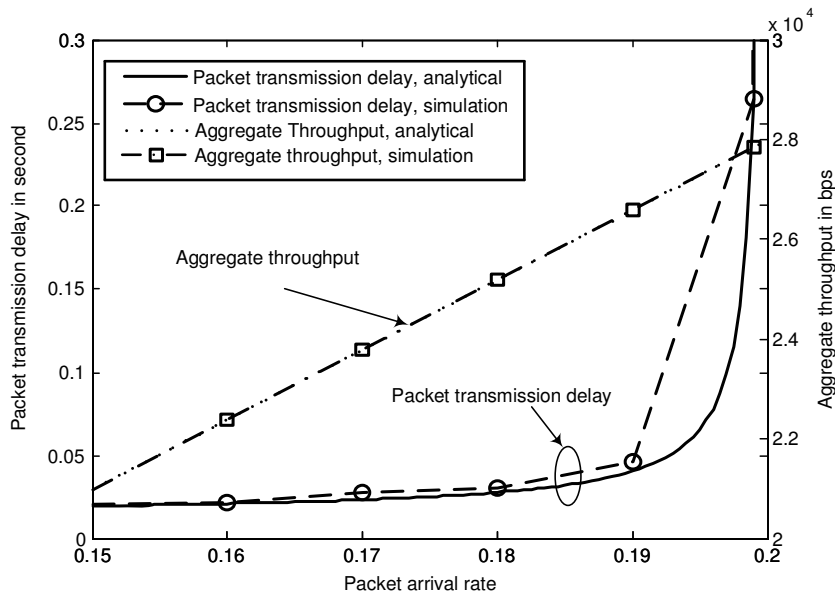


Fig. 30. Analytical and simulation results for the non-saturation network case when the packet arrival rate varies. The number (u) of contending SUs is set to be 10, the number (n) of licensed channels is set to be 4, the channel utilization (γ) of PUs is set to be 0.5.

increases much faster than that for $u = 5$. This is because when γ is larger than 0.83, the system utilization ρ for $u = 10$ approaches to 1, implying that the packet transmission delay goes to infinity. Fig. 29 shows that when the number of contending SUs is fixed, the packet transmission delay decreases by utilizing more channels.

Also, we conduct simulations to verify the analytical model for the non-saturation network case. Fig. 30 shows the analytical and simulation results of the aggregate throughput and the packet transmission delay, denoted by the two Y-axes, respectively. The number of licensed channels is set to be 4 and the channel utilization of PUs is set to be 0.5. Fig. 30 illustrates that the simulation results agree well with the analytical results for both the aggregate throughput and packet transmission delay, verifying the correctness and accuracy of our developed analytical models. When the packet arrival rate is less than 0.19, the packet transmission delay increases slowly

with the packet arrival rate. However, as the packet arrival rate is larger than 0.19 and approaches to 0.2, the system utilization gets close to 1, causing the queue of each SU to build up quickly. Consequently, the packet transmission delay increases rapidly. On the other hand, since the system utilization is less than 1, there are enough vacant channels to serve the SUs' packets, and thus the aggregate throughput can increase proportionally to the packet arrival rate.

G. Summary

We proposed and analyzed the CREAM-MAC protocol with cooperative sequential spectrum sensing scheme for the cognitive radio wireless networks. Under the CREAM-MAC protocol, each SU, which is equipped with a cognitive radio and multiple sensors, seizes the opportunity whenever the vacant licensed channels are available to exchange their own packets while only causing the acceptable interference to the PUs. Without using any centralized controllers, our proposed CREAM-MAC protocol can still solve both the traditional and multi-channel hidden terminal problems by introducing the four-way handshakes of control packets over the control channel. Our developed cooperative sequential spectrum sensing scheme can enhance the accuracy of spectrum sensing to reduce the interference imposed to the PUs. Applying the IEEE 802.11 DCF based model and the $M/G^Y/1$ queueing model, we developed analytical models to accurately evaluate the performance of our proposed CREAM-MAC protocol for both the saturation network case and non-saturation network case. The simulation results also verify the analytical models and analyses.

CHAPTER V

ADAPTIVE CDMA-BASED UPLINK MAC FOR ASYNCHRONOUS
COGNITIVE RADIO NETWORKS

A. Introduction

This chapter focuses on the uplink communications of asynchronous cognitive radio networks. The critical design criteria for asynchronous cognitive radio networks is to maintain a balance between the two contradictory goals: i) minimizing the interference imposed onto the PUs and ii) maximizing the overall spectrum utilization. On one hand, by allowing opportunistic spectrum access, the overall spectrum utilization can be improved. On the other hand, transmissions by SUs inevitably introduce harmful interference to PUs in the asynchronous cognitive radio networks. Therefore, there is a tradeoff between the interference caused to the PUs by the SUs and the overall spectrum utilization.

As discussed in Section A-2 of Chapter I, it is clear that there exist both advantages and disadvantages for the intrusive spectrum sharing mode (i.e., the interweave spectrum sharing mode) and non-intrusive spectrum sharing mode (i.e., the underlay spectrum sharing mode), respectively. In particular, the non-intrusive spectrum sharing scheme is more conservative than the intrusive spectrum sharing scheme in terms of power constraints, and thus causes the less interference to the PUs. On the other hand, the intrusive spectrum sharing scheme can utilize the entire vacant spectrum without considering any interference temperature constraint for PUs, if the channel is sensed and found to be idle. However, when the SUs perform the channel sensing, all of the SUs should keep their radios silent in order to obtain an accurate sensing outcome. During this silent period, no transmissions can be made, which

implies that the channel sensing is an overhead for the system. The sensing overhead is considerable, especially when the more accurate sensing is required. Moreover, the intrusive spectrum sharing scheme may cause the direct interference to PUs if the PUs become active and re-utilize their spectrum when SUs are transmitting.

To achieve the optimal tradeoff between the interference imposed onto the PUs and the overall spectrum utilization, in this chapter we propose the opportunistic spectrum sharing schemes for the adaptive CDMA MAC in the uplink cognitive radio networks, which combines the intrusive and non-intrusive spectrum sharing schemes together. In particular, under our proposed schemes, the SUs can adaptively select either the intrusive spectrum sharing or non-intrusive spectrum sharing schemes to transmit data based on the channel utilization, traffic load, and interference constraints. Our proposed schemes take into consideration the joint channel sensing and data transmissions, and power and rate allocations.

The rest of this chapter is organized as follows. Section B presents the system models. Section C addresses power and rate allocations of CDMA uplink communications and develops our proposed adaptive spectrum sharing schemes for cognitive MAC. Section D evaluates the performance of our proposed schemes. The chapter concludes with Section E.

B. The System Models

1. The Network Model

We consider a single-hop cognitive radio network as shown in Fig. 31. The cognitive radio network consists of a set of SUs and a secondary base station (SBS). There is a primary network located adjacent to the cognitive radio network. In the primary network, a primary base station (PBS) broadcasts packets to the PUs through the

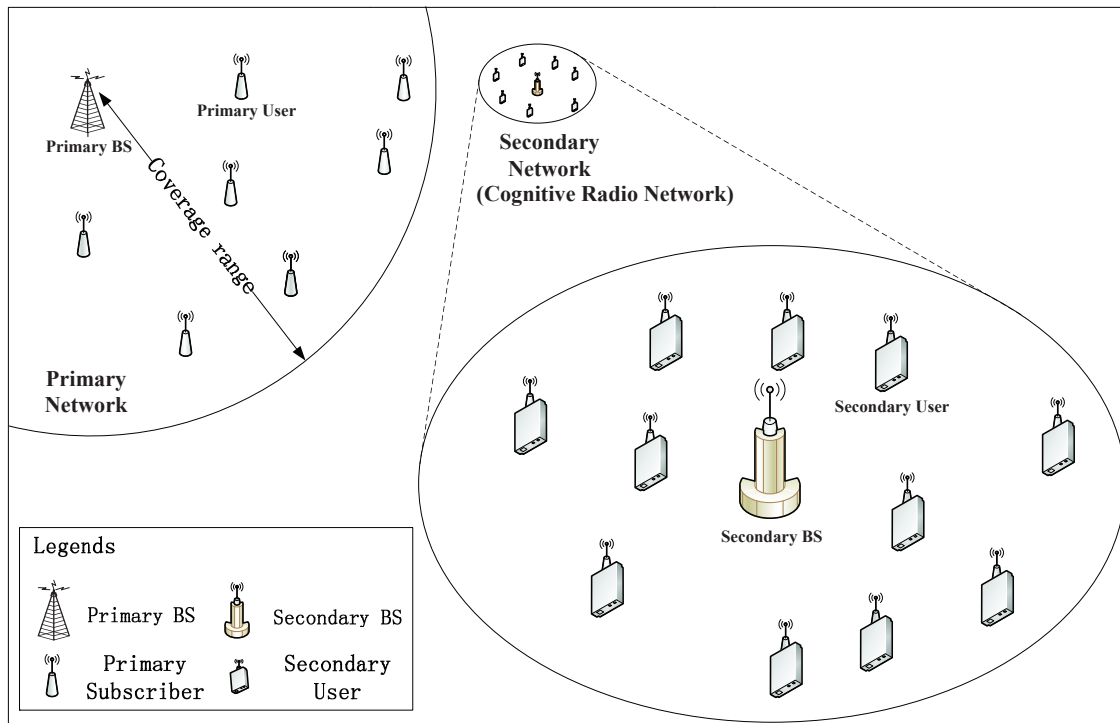


Fig. 31. Illustration of the CDMA-based secondary (users) network. The sub-figure on the bottom right corner shows the detailed topology of the secondary (users) network. The secondary (users) network consists of a set of SUs and a secondary base station (SBS). The SUs transmit data to the SBS by opportunistically accessing the licensed spectrum of the PUs in the primary (users) network.

downlink channel over a licensed spectrum band. In this chapter, we mainly focus on the primary networks consisting of the stationary PBS and PUs, and thus assume that the secondary network has *a priori* knowledge about the locations of the stationary PBS and the stationary PUs, which is common and reasonable in many existing practical cases¹, especially with the increasing support for cognitive radio networks

¹As one of examples, the location of the stationary PBS and PUs in New York City can be found in <http://www.city-data.com/city/New-York-New-York.html>. For another example, in the fixed-WiMAX based last-hop broadband access networks, the locations for the stationary WiMAX basestation (i.e., PBS) and the stationary subscribed WiMAX end-users (i.e., PUs) can be known by inquiring the telecommunication carriers.

by the governmental authority. In addition, we assume that the SBS has the dedicated downlink channel to communicate with the SUs without interfering the PUs. Thus, we do not need to consider the interference from the SBS to the PUs.

The PBS does not always occupy the channel. Due to the radio signal path loss and the PBS's frequent vacancy, the SUs may opportunistically utilize the licensed spectrum to access the SBS by using the intrusive/non-intrusive spectrum sharing modes. We assume that the distance between the PBS and SBS is larger than the effective transmission range of the PBS. Under this assumption, the PBS has little interference on the uplinks of the cognitive radio network. The SUs communicate with the SBS through CDMA uplinks. As shown in Fig. 31, the PUs on the boundary, which is specified by the *coverage range* (see Fig. 31) of the primary network, between the primary network and the secondary network can be interfered by the SUs during the intrusive spectrum sharing mode operated by the cognitive radio network. We need to upper-bound the transmit power levels of the SUs to protect the right of the boundary PUs.

The downlink and uplink communications of the cognitive radio network is implemented in a time division manner. For the cognitive radio network, the time is partitioned into frames. Each frame includes a downlink subframe and an uplink subframe. During the downlink subframe, the SBS broadcasts the power allocations, and the decisions of operation modes to the SUs. Then, during the following uplink subframe, the SUs transmit packets with the assigned transmit power. The uplink communication is based on CDMA. Following the CDMA power allocations, the SBS can receive and correctly decode the SUs' packets simultaneously.

2. The Primary Channel Model

The licensed primary channel is modeled as an alternating renewal process which switches between ON and OFF states. The On (or OFF) state represents that the PBS is (or is not) broadcasting packets to the PUs. The licensed channel state switches between ON and OFF states based on the PUs' activity. For an alternating renewal channel, let random variables τ_1 and τ_0 represent the sojourn times of ON and OFF states, respectively. Without loss of generality, we assume that τ_1 is independent of τ_0 . Denote $A_{\tau_1}(s)$ and $A_{\tau_0}(s)$ as the probability density functions (pdf) for the durations of the licensed channel's ON state and OFF state, respectively. Then, we can get the probability, denoted by u , that the channel is in its ON state at an arbitrary time instance as follows:

$$u = \frac{\int_0^{\infty} s A_{\tau_1}(s) ds}{\int_0^{\infty} s A_{\tau_1}(s) ds + \int_0^{\infty} s A_{\tau_0}(s) ds} = \frac{\bar{\tau}_1}{\bar{\tau}_1 + \bar{\tau}_0}, \quad (5.1)$$

where $\bar{\tau}_1$ and $\bar{\tau}_0$ are the mean sojourn times of ON and OFF states, respectively. Note that in fact u is the channel utilization with respect to (w.r.t.) PUs. The empirical spectrum measurement data [97, 98] already showed that the heavy-tailed distributions or exponential-tailed distributions are appropriate to characterize the duration of the licensed channel's ON/OFF state. In this chapter, to better analyze our proposed scheme, we consider the *gamma* distribution and the two heavy-tailed distributions, namely, the *pareto* and *lognormal* distributions for the ON/OFF duration distribution of the primary networks.

3. Channel Sensing and Data Transmission Models

When the SUs perform the channel sensing, all of the SUs should keep their radios silent for a certain amount of time in order to obtain an accurate sensing outcome.

During this silent period, no transmissions can be made. All of the SUs and SBS can participate in channel sensing so that the collaborative channel sensing can decrease the missed detection probability and false alarm probability.

Based on the selection of operation modes and sensing results, the SBS assigns power and rate to the active SUs that request to transmit packets to the SBS. The SUs transmit data to the SBS simultaneously by using different CDMA codes according to the assigned power and rate. Denote by \mathcal{N} the index set of the active SUs that request for uplink communications. Denote W and R_i as the channel bandwidth and data rate for SU i , respectively. Thus, the processing gain for SU i is W/R_i . Let P_i be the transmit power of SU i . Also, let $G_{j,0}^{ss}$ be the channel gain between SU j and the SBS. Thus, the signal to interference-plus-noise ratio (SINR), denoted by γ_i^s , of SU i 's signal at the SBS can be obtained by [99]

$$\gamma_i^s = \frac{WG_{i,0}^{ss}P_i}{R_i \left(\frac{2}{3R_c} \sum_{j \in \mathcal{N} \setminus \{i\}} G_{j,0}^{ss}P_j + N_0 \right)} \quad (5.2)$$

where R_c is the CDMA chip rate that is inversely proportional to the duration of a CDMA chip and N_0 is the power spectral density of a constant background noise.

C. Our Proposed Opportunistic Spectrum Sharing Schemes for Uplink Cognitive MAC

1. The Overview of Our Proposed Opportunistic Spectrum Sharing Schemes

Our proposed opportunistic spectrum sharing schemes, which aims at achieving the high spectrum utilization for cognitive radio networks, are the key components of the CDMA-based uplink cognitive MAC protocol. In our proposed scheme, the SUs can operate in two transmission modes: intrusive spectrum sharing mode and non-

intrusive spectrum sharing mode. In the mode of non-intrusive spectrum sharing, the SUs can “share” the licensed spectrum with the PUs simultaneously by adapting the transmit power so that the interference caused by the SUs’ transmissions is below the noise floor of the spectrum. The SBS makes the power and rate allocations with the constraint of PUs’ interference constraints. In the intrusive spectrum sharing mode, the SUs sense the channel before transmitting. If the channel is idle, then the SBS can assign power to SUs without taking the PUs’ interference constraints. We design *rewarding functions* to determine which spectrum sharing operation should be used by the SUs based on the channel utilization, the number of active SUs, and the interference constraints.

2. Power and Rate Allocations

We first focus on the power and rate allocations in CDMA uplink communications for the *non-intrusive* and the *intrusive* spectrum sharing schemes (modes) which are detailed in the following two cases, respectively.

CASE 1: Intrusive Spectrum Sharing Mode

Suppose that the power vector for the SUs are given. That is, the SINR of each SU before despreading at the SBS is fixed. We search for the optimized processing gain. For the convenience of presentation, rewriting Eq. (5.2), we have the SINR, denoted by γ_i^s , of the received power of SU i at the SBS as follows:

$$\gamma_i^s = \frac{WG_{i,0}^{ss}P_i}{R_i \left(\frac{2}{3R_c} \sum_{j \in \mathcal{N} \setminus \{i\}} G_{j,0}^{ss}P_j + N_0 \right)} = \frac{s_i W}{R_i} \quad (5.3)$$

where s_i is the SINR of SU i before despreading and is defined as

$$s_i \triangleq \frac{G_{i,0}^{ss}P_i}{\frac{2}{3R_c} \sum_{j \neq i} G_{j,0}^{ss}P_j + N_0}. \quad (5.4)$$

Note that $\gamma_i^s \geq s_i$ because $(W/R_i) \geq 1$.

Let ℓ be the length of a packet. Let κ_i be the instantaneous user-priority weighting factor for SU i . The larger the κ_i for the SU i is, the higher priority SU i has. We will elaborate on the determination of κ_i in Section C-7. The goodput, denoted by η_i , of SU i can be written as:

$$\eta_i = \kappa_i R_i [1 - Y(\gamma_i^s)]^\ell = \kappa_i \frac{s_i W}{\gamma_i^s} [1 - Y(\gamma_i^s)]^\ell \quad (5.5)$$

where $Y(\cdot)$ is the bit error rate (BER) function, which is the function of SINR. The form of function $Y(\cdot)$ depends on the modulation and coding scheme used in the system. Our goal is to maximize the weighted goodput over all SUs. The optimization problem is formulated as follows:

$$\mathbf{P0} : \max \sum_{i \in \mathcal{N}} \kappa_i \eta_i \quad (5.6)$$

$$\text{s.t. } 0 \leq P_i \leq P_i^{\max}, \forall i \in \mathcal{N} \quad (5.7)$$

where \mathcal{N} is the index set of the active SUs which request for uplink communications.

To solve the problem **P0**, let us first concentrate on η_i of a single SU i in Eq. (5.5). On one hand, the first component, $\kappa_i s_i W / \gamma_i^s$, of the second equation in Eq. (5.5) is a decreasing function with γ_i^s . On the other hand, $Y(\gamma_i^s)$ is a decreasing function of γ_i^s . Thus, the second component, $[1 - Y(\gamma_i^s)]^\ell$, of the second equation in Eq. (5.5) is an increasing function of γ_i^s . To find the value of γ_i^s that achieves an extrema of η_i , we take the first-order derivative of η_i given in Eq. (5.5) w.r.t. γ_i^s :

$$\begin{aligned} \frac{d\eta_i}{d\gamma_i^s} &= -\kappa_i s_i W \left\{ \frac{1}{(\gamma_i^s)^2} [1 - Y(\gamma_i^s)]^\ell + \frac{\ell}{\gamma_i^s} Y'(\gamma_i^s) [1 - Y(\gamma_i^s)]^{\ell-1} \right\} \\ &= \frac{-\kappa_i s_i W [1 - Y(\gamma_i^s)]^{\ell-1}}{(\gamma_i^s)^2} [1 - Y(\gamma_i^s) + \ell \gamma_i^s Y'(\gamma_i^s)] \end{aligned} \quad (5.8)$$

where $Y'(\cdot)$ is the derivative of the BER function $Y(\cdot)$. If setting Eq. (5.8) to 0, then

we have

$$1 - Y(\gamma_i^s) + \ell \gamma_i^s Y'(\gamma_i^s) = 0. \quad (5.9)$$

The roots of Eq. (5.9) are the extremas of η_i . The number of possible roots depends on the BER function $Y(\cdot)$ and ℓ only. Thus, the root for SU i is also the root for any other SUs. Without loss of generality, let $\gamma_i^s = \gamma_0$, with $\gamma_0 > 0$, be one of the solutions, which achieves the local maximum of η_i . Since the processing gain should be less than or equal to 1, we have $W s_i / \gamma_0 \leq W$, resulting in $s_i \leq \gamma_0$. Thus, the optimal goodput for SU i is

$$\eta_i = \begin{cases} \frac{\kappa_i s_i W}{\gamma_0} [1 - Y(\gamma_0)]^\ell, & s_i \leq \gamma_0 \\ \kappa_i W [1 - Y(s_i)]^\ell, & s_i > \gamma_0. \end{cases} \quad (5.10)$$

Based on Eq. (5.10), when $s_i > \gamma_0$, η_i is not a linear function of s_i . We set $[1 - Y(s_i)]^\ell$ to be a constant value. In this sense, η_i is the linear function of s_i , implying that maximizing the objective function in **P0** is equivalent to maximize $\sum_{i \in \mathcal{N}} \kappa_i s_i$ since we have the constant W and γ_0 for each SU. Then, we have the following new power-allocation optimization problem.

In the intrusive spectrum sharing mode, the power-allocation optimization problem, denoted by **P1**, can be formulated as follows:

$$\mathbf{P1} : \max \sum_{i \in \mathcal{N}} \kappa_i s_i \quad (5.11)$$

$$\text{s.t. 1). } 0 \leq P_i \leq P_i^{\max}, \forall i \in \mathcal{N} \quad (5.12)$$

$$2). \quad s_i \leq \gamma_0, \forall i \in \mathcal{N} \quad (5.13)$$

By solving **P1**, we can derive the optimal SINR $s_i^{\mathbf{P1}}$ of SU i . Then, substituting $s_i^{\mathbf{P1}}$ into Eq. (5.10), we can obtain the optimal goodput $\eta_i^{\mathbf{P1}}$ for SU i under the intrusive spectrum sharing mode. It is worth noting that Eq. (5.11) is convex in each

component (P_i), but it is not convex over the entire power vector, which suggests that the Karush-Kuhn-Tucker conditions are not sufficient for optimality. That is, taking partial derivatives cannot guarantee global optimality of a solution. Consequently, we have to optimize the non-convex function in a very large space. Thus, we need to further analyze **P1**.

Proposition 3. *The optimal solution to the objective function given by Eq. (5.11) lies on the surface of the polyhedron defined by the constraints given by Eqs. (5.12) and (5.13).*

Proof. We derive the second-order derivative of the objective function with respect to P_i as follows:

$$\frac{\partial^2(\sum_{i \in \mathcal{N}} \kappa_i s_i)}{\partial P_i^2} = \sum_{j \in \mathcal{N} \setminus \{i\}} \frac{\kappa_j G_{j,0}^{ss} P_j}{\left(\sum_{k \in \mathcal{N} \setminus \{j\}} G_{k,0}^{ss} P_k + \frac{3R_c N_0}{2}\right)^3}. \quad (5.14)$$

It is clear that the second-order derivative of the objective function is always larger than 0. Therefore, the objective function is convex w.r.t. P_i and the optimal solution lies on the boundary, which completes the proof. \square

Proposition 3 characterizes the relationships among the given SU's transmit power, throughput, the interference that the SU imposes to the entire system, and the aggregate throughput over all SUs. By increasing a given SU's power, it increases its own data transmission rate while the data transmission rates of the other SUs decrease due to the additional Multiple Access Interference (MAI) caused by the given SU. In contrast, the decrease of a given SU's transmit power can lead to the increase of data transmission rates of the other SUs because the MAI contributed by the given SU becomes smaller. Based on Proposition 3, when a given SU increases its transmit power, the objective function (i.e., weighted system data rate) maybe initially declines with the loss of data rate because the additional MAI impairs the increase of data

rate caused by the new SU. However, when the SU keeps increasing transmit power, the benefit contributed by the SU eventually offsets the loss of data rate caused by the augmented MAI. Using Proposition 3, we can observe the following facts.

Fact 3. *If $\max_{i \in \mathcal{N}}(\gamma_i^s) < \gamma_0$, then the optimal power allocation scheme for the intrusive spectrum sharing mode (i.e., **P1**) is as follows:*

$$P_i \in \{0, P_i^{\max}\}, \forall i \in \mathcal{N}. \quad (5.15)$$

Fact 4. *The objective function (Eq. (5.11)) of **P1** is convex w.r.t. each component of the power vector. However, The objective function is not convex w.r.t. the entire power vector.*

For the special case where $\kappa_i = \kappa_j, \forall i \neq j \in \mathcal{N}$, we can have a simple way to obtain the solution to **P1**. Without loss of generality, we suppose that

$$\kappa_i G_{i,0}^{ss} P_i^{\max} < \kappa_j G_{j,0}^{ss} P_j^{\max}, \forall i < j \quad (5.16)$$

Let $|\mathcal{N}|$ be the number of elements in \mathcal{N} . We can sort $|\mathcal{N}|$ active SUs based on the criteria given by Eq. (5.16) in the decreasing order of the weighted received power ($\kappa_i G_{i,0}^{ss} P_i^{\max}$). We call the first n SUs in \mathcal{N} as the *preferred* n SUs, which are the best SUs in terms of weighted received power at the SBS. Denote \mathcal{N}_{opt} , with $\mathcal{N}_{opt} \subset \mathcal{N}$ as the set of SUs that transmit at their maximum power for maximizing objective function Eq. (5.11). There exists an n_{opt} , with $0 < n_{opt} < |\mathcal{N}|$, such that the optimal solutions can be achieved with $\mathcal{N}_{opt} = \{1, 2, \dots, n_{opt}\}$. That is, the optimal solution is achieved for the first n_{opt} preferred SUs. Thus, for the case where $\kappa_i = \kappa_j, \forall i \neq j \in \mathcal{N}$, we can derive the optimal power allocation as follows: given the weights κ_i and channel gain $G_{i,0}^{ss}$, we sort the SUs based on Eq. (5.16). Then, we need to find the objective function achieved by the n_{opt} preferred SUs. Letting \mathcal{N}_k be the set of the first k

preferred SUs, we can derive n_{opt} as follows:

$$n_{opt} = \arg \max_{1 \leq k \leq |\mathcal{N}|} \sum_{1 \leq i \leq k} \kappa_i \frac{3R_c}{2\gamma_0} \frac{G_{i,0}^{ss} P_i^{\max}}{\sum_{j \in \mathcal{N} \setminus \{i\}} G_{j,0}^{ss} P_j^{\max} + 3N_0 R_c / 2}. \quad (5.17)$$

CASE 2: Non-Intrusive Spectrum Sharing Mode

Compared with the intrusive spectrum sharing operation mode, the non-intrusive spectrum sharing counterpart needs to take into consideration the power interference imposed to the PUs. We need to put more stringent power constraints to guarantee that the interference caused by the SUs is below the acceptable noise level in the view point of PUs. In other words, we need add a constraint to guarantee that the SINR of the PUs in the interfering zone is higher than the pre-defined SINR threshold γ_{th}^p .

Let B be the transmit power of the PBS. Let $G_{j,i}^{sp}$ be the average channel gain between SU j and PU i . Let $G_{0,i}^{pp}$ be the average channel gain between the PBS and PU i . Since the information about the PBS and PUs is known to the secondary network, the average channel gain can be estimated based on the distance between the PBS and the PUs. Denote by \mathcal{I} the set of PUs that will be interfered by SUs' intrusive transmissions. Due to the presence of the SUs and the corresponding MAI, the SINR of PU j can be written as

$$\gamma_i^p = \frac{G_{0,i}^{pp} B}{\sum_{j \in \mathcal{N}} G_{j,i}^{sp} P_j + N_0} \quad (5.18)$$

where N_0 is the power spectral density of a constant background noise.

Hence, we can formulate the power and rate optimization for the non-intrusive

spectrum sharing operation as follows:

$$\mathbf{P2} : \max \sum_{i \in \mathcal{N}} \kappa_i s_i \quad (5.19)$$

$$\text{s.t. 1). } 0 \leq P_i \leq P_i^{\max}, \forall i \in \mathcal{N} \quad (5.20)$$

$$2). \quad s_i \leq \gamma_0, \forall i \in \mathcal{N} \quad (5.21)$$

$$3). \quad \gamma_i^p \geq \gamma_{th}^p, \forall i \in \mathcal{I} \quad (5.22)$$

Similar to **P1**, the objective function of **P2** is also not convex in the power vector. The solution to **P2** also lies on the boundary determined by the constraints. We can use a feasible-directions-based method [100] to solve the non-convex optimization problem of **P2**. Solving **P2**, we can derive the optimal SINR, denoted by $s_i^{\mathbf{P2}}$, of SU i under **P2**'s mode. Substituting $s_i^{\mathbf{P2}}$ to Eq. (5.10), we can get the optimal goodput, denoted by $\eta_i^{\mathbf{P2}}$, for SU i under **P2**'s mode. Note that when the distances between the SU transmitters and the PU receivers are far enough, the power and rate optimization problem **P2** for the non-intrusive spectrum sharing mode reduces to the power and rate optimization problem **P1** for the intrusive spectrum sharing mode.

3. The Interference Probability of Intrusive Spectrum Sharing Operations

Note that in the intrusive spectrum sharing operation, the SUs may interfere with the PUs because the SUs and PUs are not synchronized. We need to investigate the interfering probability of the intrusive spectrum sharing operations. Let t_{sp} be the most recent time when the channel switches from ON to OFF state and t_{ls} be the most recent time that the channel is sensed. If the channel is in OFF state at t_{ls} , then the probability that the channel remains OFF for a certain amount of time is non-zero, and thus it is possible for the SUs to perform intrusive spectrum operation. Let τ_s and τ_t be the durations needed by the SUs to sense the channel and transmit

data packets, respectively. Given that the SUs start sensing the channel at time t , during the channel sensing period, we can derive the probability, denoted by $I(t)$, that the channel keeps on being in OFF state as follows:

$$\begin{aligned}
I(t) &= \frac{\Pr\{\text{duration of OFF state} > t + \tau_s - t_{sp}\}}{\Pr\{\text{duration of OFF state} > t_{ls} - t_{sp}\}} \\
&= \frac{\int_{t+\tau_s-t_{sp}}^{\infty} A_{\tau_0}(s) ds}{\int_{t_{ls}-t_{sp}}^{\infty} A_{\tau_0}(s) ds} \\
&= \frac{1 - C_{\tau_0}(t + \tau_s - t_{sp})}{1 - C_{\tau_0}(t_{ls} - t_{sp})}, \tag{5.23}
\end{aligned}$$

where $C_{\tau_0}(s)$ is the cumulative distribution function (cdf) of the duration of the channel's OFF state.

During the entire duration of τ_s , if the channel is in OFF state, the SUs consider that the channel is idle and can be opportunistically utilized. In other words, if the channel remains idle after the channel sensing, based on our proposed spectrum sharing schemes, the SUs can perform the intrusive spectrum sharing operations. The SUs may interfere with the PUs if the PBS resumes broadcasting packets to PUs again (i.e., the channel transits from OFF to ON) during the SUs' transmissions. Denote by $Q(\tau_t, t)$ the probability that the SUs which send packets between t and $t + \tau_t$ will interfere with PUs, given that the channel is sensed idle at the beginning of SUs' attempt to access the channel. $Q(\tau_t, t)$ is equal to the probability that the channel state flips from OFF to ON during SUs' opportunistic transmission, which can be derived as:

$$\begin{aligned}
Q(\tau_t, t) &= 1 - \frac{\Pr\{\text{duration of OFF state} > (t + \tau_t - t_{sp})\}}{\Pr\{\text{duration of OFF state} > t - t_{sp}\}} \\
&= 1 - \frac{\int_{t+\tau_t-t_{sp}}^{\infty} A_{\tau_0}(s) ds}{\int_{t-t_{sp}}^{\infty} A_{\tau_0}(s) ds} \\
&= \frac{C_{\tau_0}(t + \tau_t - t_{sp}) - C_{\tau_0}(t - t_{sp})}{1 - C_{\tau_0}(t - t_{sp})} \tag{5.24}
\end{aligned}$$

and has the following property as described in Proposition 4.

Proposition 4. $Q(\tau_t, t)$ is a monotonically increasing function of τ_t .

Proof. Taking a derivation of $Q(\tau_t, t)$ w.r.t. τ_t , we get

$$\frac{\partial Q(\tau_t, t)}{\partial \tau_t} = \frac{A_{\tau_0}(t + \tau_t - t_{sp})}{1 - C_{\tau_0}(t - t_{sp})}. \quad (5.25)$$

Since $A_{\tau_0}(x) > 0$ and $0 \leq C_{\tau_0}(x) < 1$, $\forall x$, $Q(\tau_t, t)$ is a monotonically increasing function of τ_t . \square

As the transmission duration τ_t of the intrusive spectrum sharing mode increases, the probability that the SUs interfere with SUs increases.

4. The Optimal Transmission Duration of the Intrusive Spectrum Sharing Mode

Since the SUs are not synchronized with the PUs, the probability $Q(\tau_t, t)$ that the SUs interfere with PUs is non-zero, and thus the SUs may inevitably cause harmful interference imposed onto PUs in the intrusive spectrum sharing mode. We have to limit the maximum interference that is caused by SUs. We consider two interference constraints, such as power constraint and time constraint. In the non-intrusive spectrum sharing, we limit the transmit power of SUs so that the interference temperature is below PU's tolerable noise power, as specified in **P2**. For the intrusive spectrum sharing, we apply the constraint in time domain by limiting the amount of time when the SUs and PUs transmit simultaneously.

Define $\tau_f \triangleq t - t_{sp}$ as the duration elapsed from the most recent channel switching-time point to the time when SUs attempt to access the channel. Fig. 32 shows the relationship among the important notations and variables in the spectrum sharing schemes. Given that the channel is idle at the beginning of SUs' attempt to access channel and the channel-switch occurs during the transmission, we can obtain the

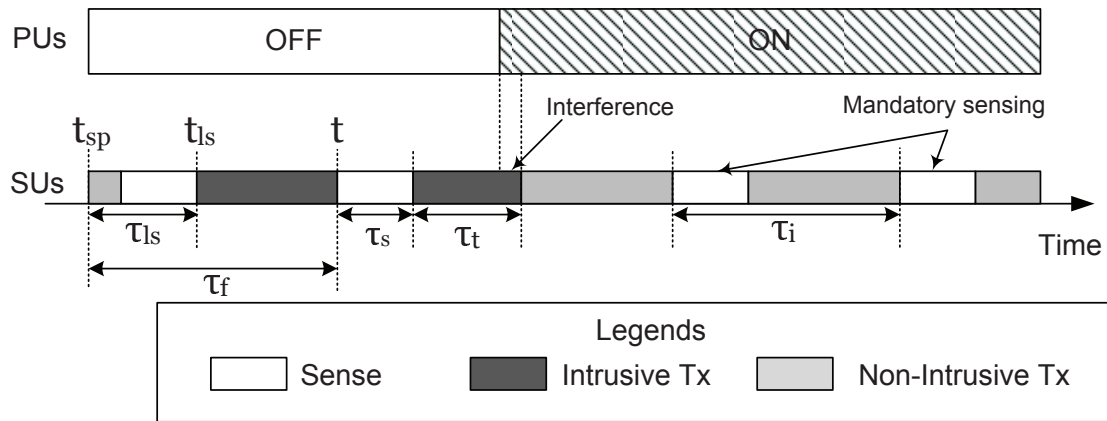


Fig. 32. Illustration of our proposed spectrum access schemes. The transmission duration τ_t depends on τ_f and the interference constraints. The SUs may interfere with the PUs when both the SUs and PUs access the spectrum.

pdf, denoted by $L_{\tau_t, \tau_f}(s)$, for the residual time of the PUs' OFF state given that the channel-switch occurs during the SUs' transmission as follows:

$$L_{\tau_t, \tau_f}(s) = \begin{cases} \frac{A_{\tau_0}(s+\tau_f)}{C_{\tau_0}(\tau_f+\tau_t) - C_{\tau_0}(\tau_f)}, & 0 < s \leq \tau_t \\ 0, & \text{otherwise} \end{cases} \quad (5.26)$$

Then, we can derive the average duration, denoted by $D(\tau_t, \tau_f)$, that the SUs interfere with the PUs as follows:

$$\begin{aligned} D(\tau_t, \tau_f) &= \int_0^{\tau_t} Q(\tau_t, t_{sp} + \tau_f) L_{\tau_t, \tau_f}(s) (\tau_t - s) ds \\ &= Q(\tau_t, t_{sp} + \tau_f) \left[(\tau_t + \tau_f) - \frac{1}{C_{\tau_0}(\tau_f + \tau_t) - C_{\tau_0}(\tau_f)} \int_{\tau_f}^{\tau_t + \tau_f} t A_{\tau_0}(t) dt \right] \\ &= \frac{1}{1 - C_{\tau_0}(\tau_f)} \left\{ (\tau_t + \tau_f) [C_{\tau_0}(\tau_f + \tau_t) - C_{\tau_0}(\tau_f)] - \int_{\tau_f}^{\tau_t + \tau_f} t A_{\tau_0}(t) dt \right\} \end{aligned} \quad (5.27)$$

where $Q(\tau_t, t_{sp} + \tau_f)$ is the probability that PUs are interfered by SUs' transmission in the intrusive spectrum sharing mode, and is given by Eq. (5.24). For different

distributions, we derive a set of closed-form expressions for Eq. (5.27) in Appendix B.

As time elapses, the probability that the SUs interfere with PUs changes. The transmission time τ_t of the SUs should be dynamically adjusted with the change of probability that the SUs interfere with PUs. Let D_{th} be the interference parameter for the intrusive spectrum sharing mode. Based on Eq. (5.27), let τ_t^* be the maximum allowable transmission time of the intrusive spectrum sharing mode given τ_f , i.e.,

$$\tau_t^* = \min\{\tau_t^{\max}, \max\{\tau_t : D(\tau_t, \tau_f) \leq D_{th}\}\} \quad (5.28)$$

where τ_t^{\max} is the pre-defined maximum transmission time. It is worth noting that the larger D_{th} suggests a longer transmission duration that the SUs can use, but also the more interference caused to the PUs.

In our proposed scheme, both the intrusive and non-intrusive spectrum sharing modes use the CDMA-based access technology and use the *same spectrum bandwidth* that is licensed to the primary network. These two sharing modes share most of the transmission and PHY designs. The major difference between the intrusive and non-intrusive spectrum sharing modes in terms of transmission parameters of the cognitive radio is the transmit power levels. Since the transmit power can be easily adjusted in cognitive radio, it is feasible to switch between the intrusive and non-intrusive sharing modes in a real-time manner. In particular, the transmit power adjustment of a cognitive radio can be implemented in a significantly shorter time period as compared with the operation periods of the intrusive and non-intrusive spectrum sharing modes. Thus, the power-switch time between the intrusive spectrum sharing mode (**P1**) and the non-intrusive spectrum sharing mode (**P2**) has virtually no impact on the performance of our proposed scheme.

5. The Selection Between the Intrusive Spectrum Sharing Mode and the Non-Intrusive Spectrum Sharing Mode

Under our proposed dynamic spectrum access schemes, the SUs can select between the non-intrusive spectrum access mode and the intrusive spectrum mode. This section describes how the SUs select operation modes. We proceed the descriptions in the following two cases, respectively.

Case (1): The primary channel is in ON state

Under the case where the primary channel is in ON state, the only available operation mode for the SUs is non-intrusive spectrum sharing mode. If the primary channel is sensed as ON state, the SUs use the non-intrusive spectrum sharing mode where the total transmit power of the SUs is below the noise floor for the PUs.

Case (2): The primary channel is in OFF state

In the case where the primary channel is in OFF state, the SUs can have two options in accessing the primary channel: intrusive or non-intrusive spectrum sharing modes. The selection principle is that the SUs choose the spectrum sharing mode which leads to higher goodput to transmit data packets to the SBS.

Because the intrusive spectrum sharing mode always starts with channel sensing and the sensing duration is constant, as the transmission time decreases, the communication overhead increases. When the transmission time keeps on decreasing, the goodput of the intrusive spectrum sharing mode will eventually be equal to that of the non-intrusive spectrum sharing mode, and then become lower than that of the non-intrusive spectrum sharing mode. Note that the non-intrusive spectrum sharing mode does not require to sense the channel before transmissions. Then, we can construct a rewarding function, denoted by $\zeta(t)$, in terms of goodput of the non-intrusive

spectrum sharing mode as follows:

$$\zeta(t) = \sum_{i \in \mathcal{N}} \eta_i^{\mathbf{P2}}, \quad (5.29)$$

where $\eta_i^{\mathbf{P2}}$ can be obtained by solving the optimization problem **P2** given in Section C-2, and n_t is the index of spectrum access of SUs at time t . We can construct another rewarding function, denoted by $\theta(t)$, in terms of the goodput of the intrusive spectrum sharing mode as follows:

$$\theta(t) = I(t) \left(\frac{\tau_t^*}{\tau_s + \tau_t^*} \right) \sum_{i \in \mathcal{N}} \eta_i^{\mathbf{P1}} + [1 - I(t)] \left(\frac{\tau_u - \tau_s}{\tau_u} \right) \zeta(t). \quad (5.30)$$

where $\eta_i^{\mathbf{P1}}$ is the optimal goodput of SU i under **P1**, which can be obtained by solving the optimization problem **P1** given in Section C-2, and τ_u is the maximum transmission duration in the non-intrusive spectrum sharing mode. As shown in Eq. (5.30), the goodput of the intrusive spectrum sharing mode is the sum of the following two terms. The first term on the right hand side of Eq. (5.30) represents that the SUs can use the higher transmit power to access the channel if the channel keeps idle after the channel sensing. In particular, $[\tau_t^*/(\tau_s + \tau_t^*)]$ in the first term on the right hand side of Eq. (5.30) suggests the overhead of the channel sensing. On the other hand, the second term on the right hand side of Eq. (5.30) indicates that the SUs have to use lower transmit power to share the spectrum with PUs if the channel is sensed as ON state.

Based on the outcome of $\zeta(t)$ and $\theta(t)$ at time t , the SBS selects the spectrum sharing mode which yields the higher goodput. If τ_t^* is a decreasing function of τ_f , then the SBS will always choose the non-intrusive spectrum sharing mode over the intrusive spectrum sharing mode when τ_f is larger than a certain threshold. In other words, the SUs will more likely choose the non-intrusive spectrum sharing mode

without channel sensing.

6. Mandatory Channel Sensing

Since the information about the channel switching-time point is critical to our proposed schemes, it is mandatory for the SUs to periodically sense the channel to detect/estimate the channel switching-time point in both cases where the primary channel is in ON or OFF states, which are detailed in the following two cases, respectively.

Case I: The primary channel is in ON state

Although the non-intrusive spectrum sharing mode does not require channel sensing, the periodical channel sensing is still necessary in the case where the primary channel is in ON state, because the SUs are required to have the knowledge of when the channel switches from ON to OFF state. The SUs must frequently sense the channel. Fig. 32 illustrates an example of the mandatory sensing when the primary channel is in ON state. The sensing period, denoted by τ_i , depends on the time elapsing from the last time when the channel switches from OFF to ON state.

Denote t'_{sp} and t_{sp} as the old channel switching-time point and the new estimated channel switching-time point between the two consecutive channel sensings, respectively. We can derive the probability, denoted by P_{cs} , that the channel-switch occurs between two consecutive channel sensings as follows:

$$P_{cs} = \frac{C_{\tau_1}(\tau_{ls} + \tau_i) - C_{\tau_1}(\tau_{ls})}{1 - C_{\tau_1}(\tau_{ls})} \quad (5.31)$$

where $\tau_{ls} \triangleq t_{ls} - t'_{sp}$ is the duration between the most recent sensing time and the most recent channel switching time, and $C_{\tau_1}(t)$ is the cdf of the licensed channel's ON state. If the channel-switch occurs between two successive channel sensings and τ_{ls} is given, we can derive the pdf, denoted by $p_{t_{sp}}(s, \tau_{ls})$, of the new channel switching-time

point as follows:

$$p_{t_{sp}}(s, \tau_{ls}) = \begin{cases} \frac{A_{\tau_1}(s + \tau_{ls})}{C_{\tau_1}(\tau_{ls} + \tau_i) - C_{\tau_1}(\tau_{ls})}, & 0 < s \leq \tau_i \\ 0, & \text{otherwise.} \end{cases} \quad (5.32)$$

The channel sensing frequency (or channel sensing period) determines the accuracy of the estimated channel switching-time point. From the view point of non-intrusive spectrum sharing, the channel sensing is not helpful and is thus considered as the pure overhead, which eventually results in degradation of the goodput. There is a tradeoff between the accuracy of the estimated channel switching-time point and the goodput. Specifically, if we have the higher channel sensing frequency, then we can have more accurate channel switching-time point, but lower goodput. In contrast, the lower channel sensing frequency leads to more estimation error of the channel switching-time point and higher goodput. Intuitively, when τ_{ls} is small, the probability that the channel switches from OFF to ON state is small. Thus, a low channel sensing frequency is good enough to estimate the channel switching-time point. On the other hand, when τ_{ls} is high, the probability that the channel switches from OFF to ON state is high, which implies that the high channel sensing frequency is necessary to accurately detect the channel switching-time point. In order to minimize the goodput degradation caused by the channel sensing while guaranteeing the accuracy of the estimated channel switching-time point, we introduce the mean squared estimation error for the channel switching-time point qualitatively to derive the channel sensing period τ_i based on the elapsed time τ_{ls} away from the last channel switching-time point. We derive the mean squared estimation error, denoted by $\epsilon(\tau_i, t_{sp})$, of t_{sp}

as follows:

$$\begin{aligned}
\epsilon(\tau_i, t_{sp}) &= \int_0^{\tau_i} (t_{sp} - t_{ls} - s)^2 p_{t_{sp}}(s, \tau_{ls}) ds \\
&= (t_{sp} - t'_{sp})^2 - \frac{2(t_{sp} - t'_{sp}) \int_{\tau_{ls}}^{\tau_{ls} + \tau_i} t A_{\tau_1}(t) dt - \int_{\tau_{ls}}^{\tau_{ls} + \tau_i} t^2 A_{\tau_1}(t) dt}{C_{\tau_1}(\tau_{ls} + \tau_i) - C_{\tau_1}(\tau_{ls})}
\end{aligned} \tag{5.33}$$

where $t_{ls} \leq t_{sp} \leq t_{ls} + \tau_i$, and $p_{t_{sp}}(s)$ is the pdf of t_{sp} given by Eq. (5.32). For different distributions, we derive a set of the closed-form expressions for Eq. (5.33) in Appendix B.

Let $t_{sp}^*(\tau_i)$ be the optimal t_{sp} that minimizes $\epsilon(\tau_i, t_{sp})$ given τ_i , which implies:

$$t_{sp}^*(\tau_i) = \arg \min_{0 \leq t_{sp} \leq \tau_i} \epsilon(\tau_i, t_{sp}). \tag{5.34}$$

Define ϵ_{th} as the pre-defined threshold for the mean squared error of estimated channel switching time. Thus, when the non-intrusive spectrum sharing mode is adopted, the optimal sensing period is

$$\tau_i^* = \max\{\tau_i : \epsilon(\tau_i, t_{sp}^*(\tau_i)) \leq \epsilon_{th}\}. \tag{5.35}$$

Case II: The primary channel is in OFF state

When the primary channel is in OFF state, we can use the intrusive spectrum sharing mode which requires the channel sensing before SUs' transmissions. In this case, the channel sensing is part of the channel accessing process. Essentially, the channel sensing frequency required by the intrusive spectrum sharing mode is higher than that required for channel switching-time point detection/estimation. In this sense, the mandatory channel sensing can be already covered by the channel sensing required in intrusive spectrum sharing mode.

7. The Fairness

Our proposed scheme takes into account the fairness. Since different SUs may have different service requirements, we employ a set of weighting factors ω_i to represent the different priorities of the SUs. Our proposed system aims at achieving the long-term fairness by updating the instantaneous user-priority weighting factor κ_i .

Definition 1. *The long-term fairness is said to be achieved if during a long duration of time, the ratios of the aggregated transmission rate to the weighting factor for all SUs are the same, i.e.,*

$$\lim_{n \rightarrow \infty} \frac{\sum_n R_i(n)}{\omega_i} = \lim_{n \rightarrow \infty} \frac{\sum_n R_j(n)}{\omega_j}, \quad \forall i \neq j \in \mathcal{S}, \quad (5.36)$$

where $R_i(n)$ is data rate of the SU i at the n -th round of spectrum-access and \mathcal{S} is the entire set of SUs.

To satisfy Eq. (5.36), we need to dynamically adjust the instantaneous weights that are used in the optimization problems including **P1** and **P2**. Let $S_i(n)$ be the average transmission rate for SU i during the pervious n times of attempting transmissions. The SBS updates $S_i(n)$ for SU i once the power allocation decision is made provided that SU i has a request for transmission. Note that the SBS does not update $S_i(n)$ for SU i at the round in which SU i does not have anything to send to SBS. We adopt the Exponential Moving Average (EMA) to update $S_i(n)$ as follows:

$$S_i(n) = \delta R_i(n) + (1 - \delta)S_i(n - 1) \quad (5.37)$$

where δ , with $0 \leq \delta \leq 1$, is a pre-defined constant smoothing factor. Under EMA, the weighting for the older transmission rate decreases exponentially, which implies that the unfairness caused by recent power allocations is more important than the unfairness contributed by older power allocations. In this sense, the fairness scheme will

put more efforts to compensate for the unfairness caused by recent power allocations. Thus, the instantaneous user-priority weighting factor κ_i for SU i at the $(n + 1)$ -th spectrum access attempt can be updated by setting:

$$\kappa_i = \frac{\omega_i}{S_i(n)}. \quad (5.38)$$

8. The Details of Our Proposed Scheme

Figure 33 shows the detailed pseudo-code of our proposed scheme. There are two important types of events occurring in our system: 1) the event of sensing and 2) the event of spectrum sharing mode selection. The objective of our proposed scheme is to handle these two types of events by repeatedly updating the parameters for the events. Let t_s and t_m be the triggers for the events of sensing and spectrum sharing mode selection, respectively. Initially, we set both of the last sensing time t_{l_s} and last channel switching-time point t_{sp} to negative infinity, the sensing trigger t_s to zero, and spectrum sharing mode selection trigger t_m to positive infinity.

If the current time is equal to t_s , then the sensing event is triggered. The SUs sense the channel for a duration of τ_s . If the channel switches states during the sensing, the SUs update t_{sp} to the channel switching-time point which the SUs have just detected. Otherwise, if the channel sensing result is different from the last sensing result, then the system calculates the new estimated t_{sp} based on Eq. (5.34). Then, based on the channel state, the systems choose the transmit power. If the channel is idle, the SUs transmit packets to the SBS by using the transmit power according to the optimal solution to **P1** with a duration of τ_t^* which is calculated by Eq. (5.28). In contrast, if the channel is busy, the SUs use a low transmit power given by the optimal solution to **P2** to access the channel. The SUs also need to update the new sensing trigger t_s and selection trigger t_m .

```

00. Initialize:  $t_{ls} = -\infty, t_{sp} = -\infty, t_s = 0, t_m = \infty$ 
01. while(1)
02.    $t :=$  current time
03.   if  $t = t_s$  //triggered by sensing event
04.     sense the channel for the duration of  $\tau_s$ 
05.     if channel switches states during sensing
06.       update  $t_{sp}$  to be the new channel switching-time point
07.     if channel state is different from the last sensing result
08.       calculate  $t_{sp}$  based on Eq. (5.34)
09.     update  $t := t + \tau_s, t_{ls} := t$ 
10.     calculate  $\tau_i$  based on Eq. (5.35)
11.     if channel is idle
12.       update  $\tau_f := t - t_{sp}$ 
13.       calculate  $\tau_t^*$ 
14.       update  $t_m := t + \tau_t^*, t_s := t + \tau_i$ 
15.       assign power and rate according to  $\eta_i^{\mathbf{P1}}$ 
16.       SUs send packets to SBS using intrusive mode for  $\tau_t^*$ 
17.     else
18.       update  $t_s := t + \tau_i$ 
19.       assign power and rate according to  $\eta_i^{\mathbf{P2}}$ 
20.       SUs send packets to SBS using non-intrusive mode
21.   if  $t = t_m$  //triggered by selection of spectrum sharing mode
22.     update  $\tau_f := t - t_{sp}$ 
23.     calculate  $\eta_i^{\mathbf{P1}}$  and  $\eta_i^{\mathbf{P2}}, \forall i \in \mathcal{N}$ 
24.     calculate  $\theta(t), \zeta(t)$ 
25.     if  $\theta(t) < \zeta(t)$ 
26.       assign power and rate according to  $\eta_i^{\mathbf{P2}}$ 
27.       SUs send packets to SBS using non-intrusive mode
28.       update  $t_m := \infty$ 
29.       //keep using non-intrusive until next mandatory channel sensing
30.     else
31.       update  $t_s := t$  //sense the channel immediately

```

Fig. 33. The pseudo code of our proposed schemes for the selection between the intrusive spectrum sharing mode and the non-intrusive spectrum sharing mode.

The event of selecting the spectrum sharing mode is triggered if the current time is equal to t_m . There are two options for the SUs: 1) trying to use the intrusive spectrum sharing mode by sensing the channel first, or 2) immediately sending packets to the SBS with a lower transmit power. The SBS calculates and compares $\zeta(t)$ with $\theta(t)$. On one hand, if $\theta(t)$ is larger, then the SUs use the non-intrusive spectrum sharing mode to access the channel. Furthermore, t_m is set to be infinity, which suggests that before the next mandatory channel sensing, the SUs keep on using the non-intrusive spectrum sharing mode. On the other hand, if $\zeta(t)$ is larger than $\theta(t)$, then the SUs will try to use the intrusive spectrum sharing mode by setting the sensing trigger t_s to be the current time.

D. Performance Evaluations

Our simulated primary and secondary networks have the similar wireless networks topologies as shown in Fig. 31. In particular, there is one primary channel with the bandwidth of 50 MHz licensed to the primary network. There are 1 PBS and 3 PUs in the primary network and there are 1 SBS and 10 SUs in the secondary network. The SUs form the wireless-network cell topology with the SBS being at the center position of the wireless-network cell. The average distance between the SUs and the SBS is 1 unit of distance. The average distance between PUs and the SBS is 4.3 units of distance. In the simulations, we set $G_{i,0}^{ss} = G_{j,0}^{ss}$ and $P_i^{\max} = P_j^{\max}$, $\forall i \neq j$. The sensing duration is 0.5 ms. The priority weighting factor ω_i for each SU is set to be $\omega_i = 1$, $\forall i \in \mathcal{S}$ (i.e., the equal-share fairness). Each SU is the persistent data source which always has data to send with the non-empty queue, implying that each SU always requests to transmit data to the SBS. For the convenience of presentation, we list the important parameters in Table IV.

Table IV. The parameters for design and analysis of our proposed adaptive uplink CDMA-based cognitive MAC scheme.

u	channel utilization of PUs
ω_i	priority weighting factor of SU i
$\bar{\tau}_1$	mean sojourn time of ON state
$\bar{\tau}_0$	mean sojourn time of OFF state
W	channel bandwidth
R_i	data rate of SU i
γ_i^s	SINR of SU i 's signal at SBS
γ_i^p	SINR of PU i 's receiving signal
κ_i	instantaneous user-priority weighing factor
η_i	goodput of SU i
τ_s	channel sensing duration
τ_t	SUs' transmission duration
t_{ls}	most resent channel sensing time
τ_{ls}	duration between sensing time and channel switching time
D_{th}	interference threshold
τ_t^*	max allowable tx time of intrusive spectrum sharing mode
t_{sp}	channel switching-time point
τ_i	sensing period
ϵ_{th}	estimation error threshold for channel switching time
δ	constant smoothing factor
t_s	trigger for sensing event
t_m	trigger for spectrum sharing mode selection event

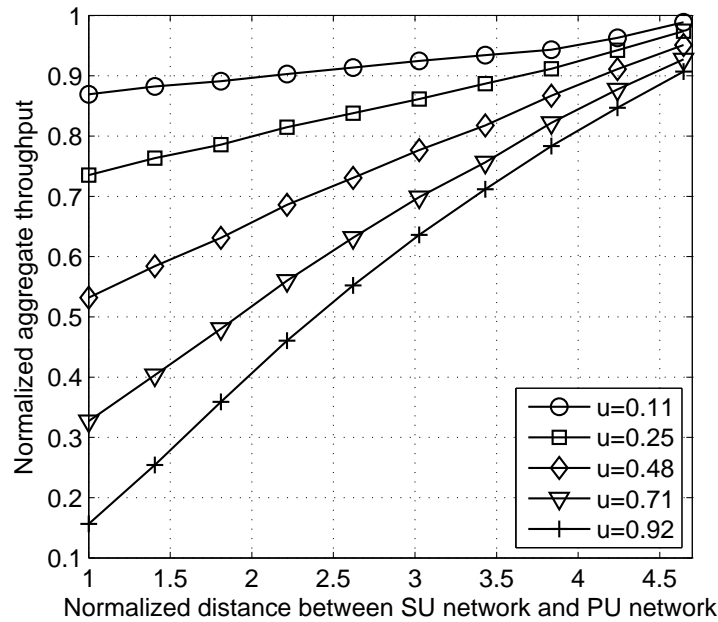


Fig. 34. The impact of distance between the secondary network and primary network on the normalized aggregate throughput of our proposed scheme when the PUs' traffic follows lognormal distribution.

We first study the impact of the distance between the primary network and secondary network on the throughput of our proposed scheme. Fig. 34 plots the normalized aggregate throughput of our proposed scheme against the normalized distance between the secondary network and primary network with different channel utilizations of PUs (u) when the PUs' traffic follows *lognormal* distribution. Note that the aggregate throughputs in this chapter are normalized by the throughput of the complete intrusive spectrum accessing mode with zero channel utilization of PUs. In addition, the distances between the SU and primary networks are normalized by the average distance between the SBS and SUs. As shown in Fig. 34, the normalized aggregate throughput increases as the normalized distance between the secondary network and primary network increases because the larger distance between the SU and primary networks leads to larger throughput of the non-intrusive spectrum shar-

ing mode. Furthermore, from Fig. 34, as the distance between the SU and primary networks increases, the difference of throughput between the higher channel utilization of PUs and lower channel utilization of PUs decreases, which is because of the following reasons. When the distance between the secondary network and primary network is small, the difference of the throughputs achieved by the intrusive and non-intrusive spectrum sharing modes is large, implying that with lower channel utilization of PUs, the SUs spending more time in non-intrusive spectrum sharing mode achieves much less throughput than the SUs with higher channel utilization of PUs. In contrast, when the distance between the secondary network and primary network is large, the throughput of the intrusive spectrum mode is close to the throughput of the non-intrusive spectrum sharing mode. As a result, the channel utilization of PUs has less impact on the throughput when the distance between the secondary network and primary network is larger.

Then, we evaluate the fairness performance of our proposed scheme using the Jain fairness index [101] (i.e., the equal-share attains the maximum Jain fairness index). Fig. 35 plots the Jain fairness index against the distance between the secondary network and primary network with the different numbers of SUs in the secondary network. The channel utilization of PUs is 0.17 and the PUs' traffic follows lognormal distribution. As shown in Fig. 35, our proposed scheme can achieve the desired fairness among SUs in the secondary network. In Fig. 35, for a given number of SUs, the Jain fairness index slightly increases as the distance between the secondary and primary networks increases, which is due to the following reasons. When the distance between the secondary network and primary network gets larger, the interference-level constraint on the secondary network becomes more relaxed. This implies that the difference between the SU-achieved throughputs under the non-intrusive and intrusive spectrum sharing modes for each round of spectrum-access becomes smaller.

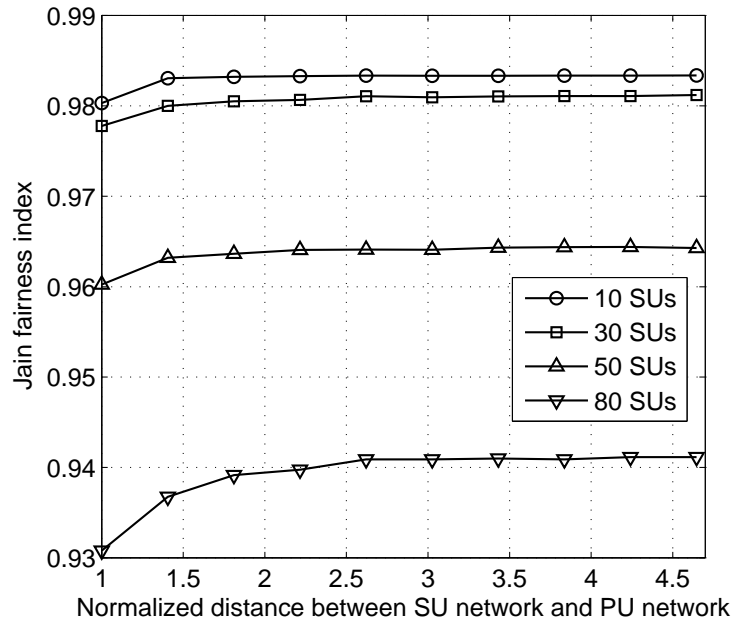


Fig. 35. The Jain fairness index vs. the distance between the secondary network and primary network. The channel utilization of PUs is 0.17 and the PUs' traffic follows lognormal distribution.

Therefore, when the distance between the secondary network and primary network gets larger, regardless of the higher or lower probabilities for SUs to use the intrusive or non-intrusive spectrum sharing modes, the statistically-averaged throughputs for all SUs intend to converge to the equal-share fairness. Thus, the larger the distance between the secondary and primary networks, the larger the Jain fairness index. Fig. 35 also shows that the more the SUs in the secondary network, the lower the Jain fairness index. It is expected because of the following reasons. With limited wireless resources, when the number of SUs becomes larger, the probability for each SU to actually use the spectrum decreases for each round of spectrum-access opportunity, resulting in the lower Jain fairness index.

In the rest of this section, we evaluate and compare our proposed scheme with the other schemes in terms of the normalized aggregate throughput of all SUs and

interference index (to be defined in the following), when the PUs' activities follow the different distributions. The comparison schemes include the transmission scheme in the ideal case, interference-confined adaptive transmission scheme, and the fixed transmission scheme. In particular, the ideal case represents the “omniscient” transmission scheme under which the SUs have the full knowledge of the PUs' activities. That is, in the ideal case, the SUs are assumed to know exactly when the PBS starts and stops broadcasting packets to the PUs. Thus, the throughput of the ideal case is the upper-bound throughput that the secondary network can achieve. Furthermore, in the ideal case, the SUs do not cause any interference to the primary network.

The interference-confined adaptive transmission scheme is an interweave-based spectrum sharing scheme which is modified based on the optimal spectrum sensing framework proposed in [102], under which the SUs can access the primary channel only when the PBS is sensed idle. The original scheme which was designed for the exponential PUs traffic case only. To fairly compare the scheme in [102] with our proposed scheme, we modify the scheme in [102] so that it can adaptively adjust the transmission duration while limiting the interference caused by the SUs to a given threshold for different PUs activity patterns.

The fixed transmission scheme combines the intrusive and non-intrusive spectrum sharing modes. However, unlike our proposed scheme which takes advantage of the PUs' activity pattern, the fixed transmission scheme makes the decisions only based on the channel sensing outcomes. Particularly, under the fixed transmission scheme, the SUs constantly sense the channel. If the channel is sensed idle, the SUs transmit packets to the SBS with a fixed transmission duration. If the channel is sensed busy, the SUs adopt the non-intrusive spectrum sharing mode to transmit packets. The difference between our proposed scheme and the fixed transmission scheme is that the fixed transmission scheme does not need the mandatory sensing and the fixed

transmission duration depends only on a pre-defined parameter. It is clear that for the fixed transmission scheme, the larger transmission duration may lead to a higher throughput, but more severe interference imposed onto the PUs.

In the simulations, besides the normalized aggregate throughput, we also use the interference index to evaluate the performance of our proposed schemes. We define the interference index as the ratio of the amount of time that the SUs operate in the intrusive spectrum sharing mode when PUs are active to the total simulation duration. The larger the interference index, the more interference caused by the SUs. In the simulations, we consider the interference occurring only when the noise level of the PU receivers is above the acceptable level due to the interference caused by the SUs that operate under the intrusive spectrum sharing mode.

First, we assume the primary network's activity pattern follows the *lognormal* distribution. The average ON state of the primary network is 0.2 s, while the average OFF state of the primary network varies between 0.2 s and 2.8 s. Fig. 36 shows the normalized aggregate throughput achieved by our proposed scheme, the fixed transmission scheme with $\tau_t = 0.01$ s, the fixed transmission scheme with $\tau_t = 0.005$ s, the interference confined adaptive transmission scheme with interference level of 10^{-3} , and the transmission scheme for the ideal case. As shown in Fig. 36, when the duration of OFF state increases, the normalized throughput of all schemes increase. In Fig. 36, our proposed scheme is the scheme that achieves the closest throughput to the ideal case's throughput among all the schemes. The throughput difference between our proposed scheme and the interference-confined adaptive transmission scheme decreases as the average duration of OFF state increase. This is because our proposed scheme can get more spectrum opportunities using the non-intrusive spectrum sharing mode when the licensed channel is in ON state.

Figure 37 shows the interference index for the different schemes. From Fig. 37,

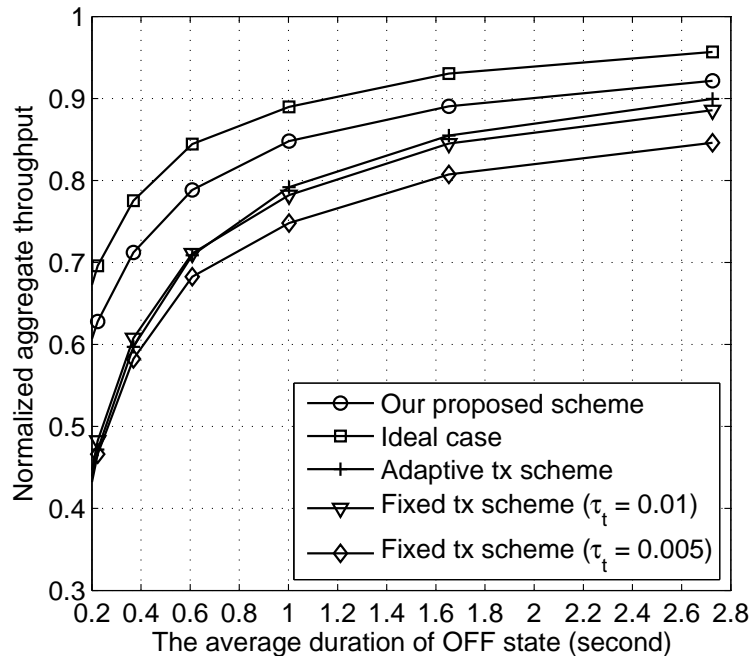


Fig. 36. The normalized aggregate throughput vs. the average duration of OFF state when the PUs' activity follows the lognormal distribution.

we can observe that for the fixed transmission schemes, the larger the fixed transmission duration τ_t , the larger the interference index. Our proposed scheme achieve the lowest interference index for any given channel utilization of PUs. Also, the interference index of the fixed transmission scheme increases more quickly than that of our proposed scheme when the average duration of ON state decreases. Based on Figs. 36 and 37, our proposed scheme significantly outperforms the fixed transmission scheme and the interference-confined adaptive transmission scheme when the PUs' activity follows the lognormal distribution.

Second, we focus on the case where the PUs' activity follows the *pareto* distribution. The average ON state of the primary network is 0.45 s, while the average OFF state of the primary network changes between 0.025 s and 6.1 s. Fig. 38 shows the normalized aggregate throughput of our proposed scheme, the fixed transmission

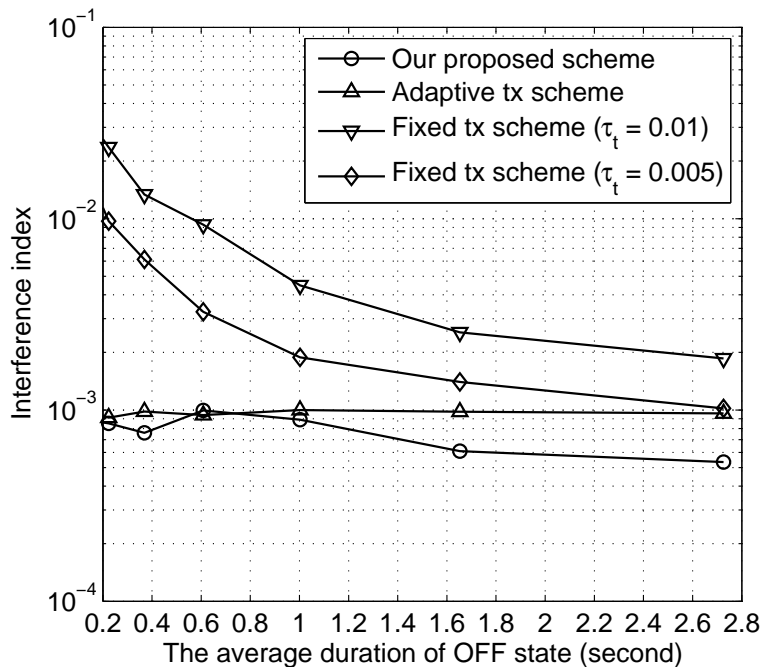


Fig. 37. The interference index vs. average duration of OFF state when the PUs' activity follows the lognormal distribution.

scheme with different τ_t 's, the interference-confined adaptive transmission scheme with interference level of 10^{-3} , and the ideal transmission scheme. The throughput of all schemes decreases as the channel utilization of PUs increases. This is because as the channel utilization of PUs increases, there is less room for the SUs to operate in the intrusive spectrum sharing mode which yields a higher throughput than the non-intrusive spectrum sharing mode. When the fixed transmission scheme adopts $\tau_t = 0.01$ s, the throughput of the fixed transmission scheme is close to that of our proposed scheme. However, the interference caused by the fixed transmission scheme is much higher than our proposed scheme. Also, the throughput of our proposed scheme yields a much higher throughput than the interference-confined adaptive transmission scheme. Figs. 38 and 39 show that when the PUs' activity follows the pareto distribution, our proposed scheme can achieve better throughput and lower interference

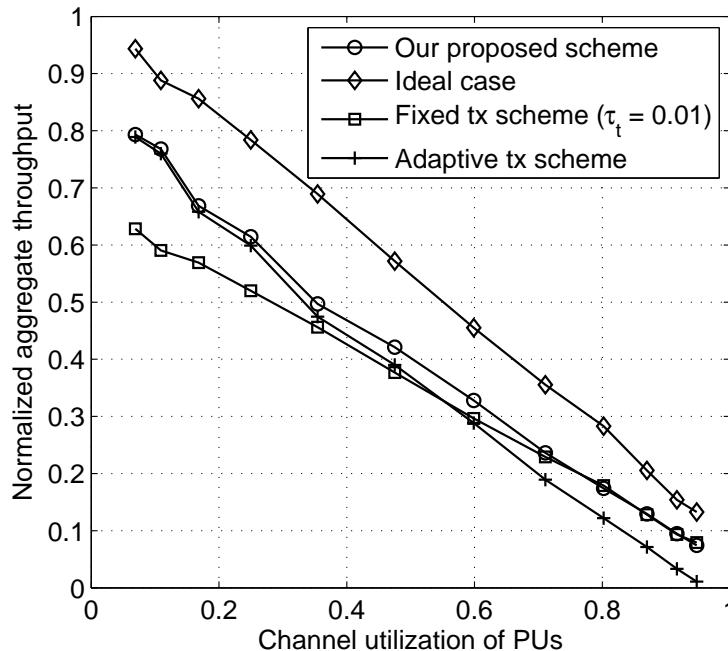


Fig. 38. The normalized aggregate throughput vs. channel utilization of PUs when the PUs' activity follows the pareto distribution.

index than the fixed transmission scheme as well as the interference-confined adaptive transmission scheme.

Third, we evaluate our proposed scheme when the PUs' activity follows the *gamma* distribution. The average ON state of the primary network is 0.12 s, while the average OFF state of the primary network changes between 0.0044 s and 1.1 s. Figs. 40 and 41 plot the normalized aggregate throughput and interference index, respectively, against the channel utilization of PUs. The interference-confined adaptive transmission scheme with interference level of 10^{-2} achieves the lower throughput than our proposed scheme. Moreover, the interference-confined adaptive transmission scheme decreases dramatically as the channel utilization of increases because it cannot utilize the spectrum opportunities when the primary network is active. For the fixed transmission scheme, larger τ_t leads to a higher throughput. As shown in

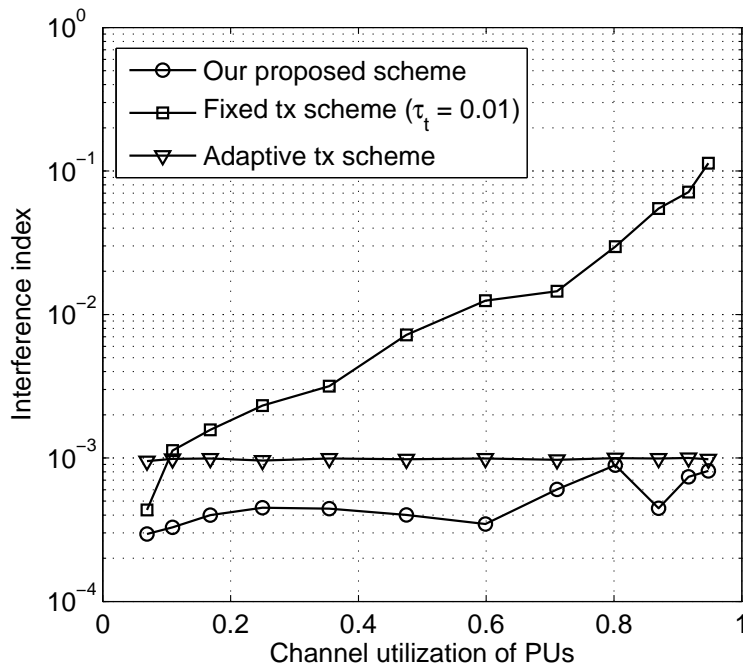


Fig. 39. The interference index vs. channel utilization of PUs when the PUs' activity follows the pareto distribution.

Fig. 40, the throughput of the fixed transmission scheme with $\tau_t = 0.01$ is larger than that of the fixed transmission scheme with $\tau_t = 0.001$. When the channel utilization of PUs is less than 0.33, our proposed scheme achieves the higher throughput than the fixed transmission scheme with $\tau_t = 0.01$. Meanwhile, when the channel utilization of PUs is higher than 0.33, our proposed scheme achieves lower throughput as compared to the fixed transmission scheme with $\tau_t = 0.01$. However, we can observe in Fig. 41 that the interference index of our proposed scheme is much lower than that of the fixed transmission scheme with $\tau_t = 0.01$.

It is worth noticing that the throughputs of the fixed transmission scheme and our proposed scheme converge together as the channel utilization of PUs increases when the PUs' activity follows the gamma distribution. The reason for this is twofold. On one hand, when the channel utilization of PUs is small, the optimal τ_t^* changes

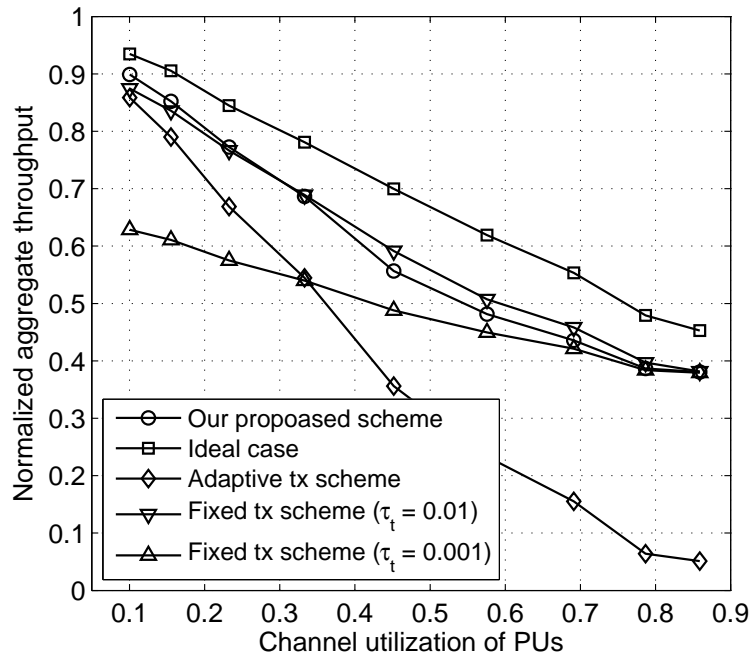


Fig. 40. The normalized aggregate throughput vs. channel utilization of PUs when the PUs' activity follows the gamma distribution.

in a large-scale manner because the range of τ_f is stochastically wide. The fixed transmission scheme does not perform well because of the fixed transmission duration. On the other hand, when the channel utilization of PUs is large, the optimal τ_t^* changes slowly with the duration of the elapsed OFF period τ_f , which implies that for a given D_{th} , our proposed scheme may virtually choose a constant τ_t due to τ_f falling into a small range. As a result, our proposed scheme performs similarly as the fixed transmission scheme.

Thus, we further evaluate our proposed scheme as follows. For a given channel utilization of PUs, we adjust D_{th} for our proposed scheme to make our proposed scheme and the fixed transmission scheme to achieve the same interference index. Then, given the same interference index, we compare the normalized aggregate throughput of our proposed scheme with that of the fixed transmission scheme

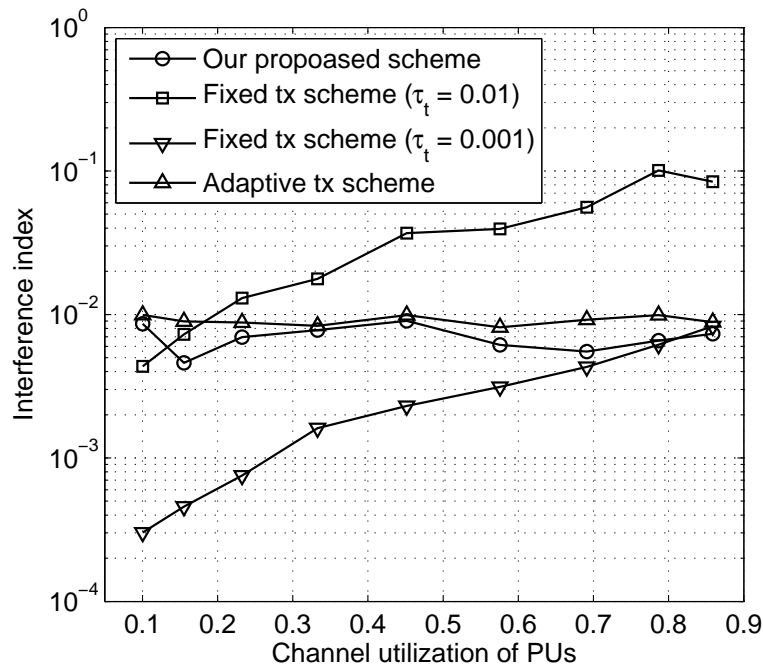


Fig. 41. The interference index vs. channel utilization of PUs when the PUs' activity follows the gamma distribution.

for $\tau_t = 0.01$ and $\tau_t = 0.001$, respectively, which is shown in Fig. 42. When the fixed transmission scheme selects $\tau_t = 0.001$, the improvement of our proposed scheme over the fixed transmission scheme is significant. This is because the fixed transmission scheme with smaller τ_t results in larger sensing overhead. In addition, when the channel utilization of PUs is small, we can see that given the same interference index, the throughput improvement of our proposed scheme over the fixed transmission scheme is noticeable. When the channel utilization of PUs keeps on increasing, the throughput of our proposed scheme converges to the throughput of the fixed transmission scheme.

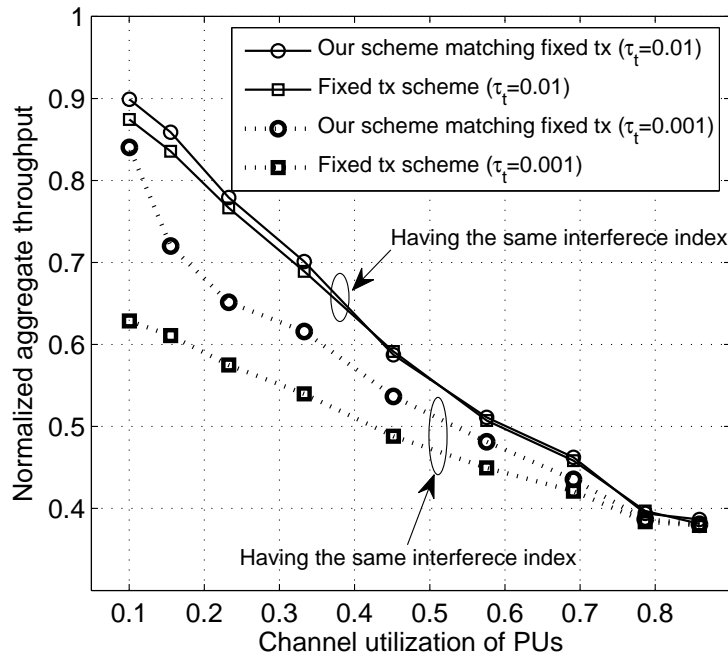


Fig. 42. Given the same interference index, the normalized aggregate throughput comparison between our proposed scheme and the fixed transmission scheme when the PUs' activity follows the gamma distribution. Note that in the above figure, the plots with the same line style represent that the corresponding schemes have the same interference index.

E. Summary

We proposed the opportunistic spectrum sharing schemes in the CDMA-based uplink MAC over the cognitive radio networks to achieve the tradeoff between the interference imposed onto the PUs and overall spectrum utilization. In particular, we formulated the power control optimization problems for the intrusive and non-intrusive spectrum sharing modes. We designed the selection rules of intrusive and non-intrusive spectrum sharing modes. Under our proposed schemes, the SUs can dynamically determine to choose between the intrusive spectrum sharing mode and non-intrusive spectrum sharing mode based on the channel utilization, the number

of active SUs, and the interference constraints. Our proposed schemes take into consideration the joint channel sensing and data transmission, and the power and rate allocations. We conducted the extensive simulations with different types of PUs' activities. Comparing with the other schemes, the simulation results show that our proposed scheme can optimally trade off the spectrum utilization with the interference caused by SUs to significantly increase the aggregate throughput of all the SUs in the cognitive radio network.

CHAPTER VI

SECONDARY-USER-FRIENDLY TDMA-BASED MAC FOR PRIMARY USERS
NETWORKS

A. Introduction

Several cognitive MAC protocols for synchronous cognitive radio networks have been proposed to take advantage of the vacant channels that are not used by the PUs in the context of the time division multiple access (TDMA)-based wireless networks. In Chapter II, we proposed the random and negotiation-based channel sensing policies for SUs to efficiently identify and utilize the vacant channels that are unused by PUs. In Chapter III, we developed a channel hopping-based cognitive MAC protocol which enables the SUs to conduct channel negotiations at multiple rendezvous. The authors of [103] proposed a cognitive MAC protocol to improve the channel utilization for the TDMA-based cellular systems. The authors of [13] developed a cognitive MAC protocol based on the POMDP framework. They further improved the POMDP-based cognitive MAC protocol by considering the presence of sensing errors in [104]. All the above cognitive MAC protocols share one common feature: they are designed to work on top of the TDMA-based primary networks. In particular, the licensed channels are slotted in time and each PU is assigned with a time slot periodically. The SUs, which are synchronized with the PUs, scan the licensed channels at the beginning of a time slot. If the time slot is idle, then it can be utilized by the SUs. Otherwise, the time slot is occupied by PUs and not available for the SUs.

©2009 IEEE. Part of this chapter is reprinted with permission from “Secondary user friendly TDMA scheduling for primary users in cognitive radio networks” by H. Su and X. Zhang, published in *Proc. IEEE Global Telecommunications Conference (GLOBECOM)*, pp. 1-6, Dec. 2009.

With the traditional TDMA scheme, the PU transmits the packets (if any) once its assigned time slots arrive. Under the wireless fading channel environment, the number of packets that can be sent in a time slot depends on the number of buffered packets and the channel condition. It can be expected that in some time slots, the number of sent packets is small because either the number of buffered packets is small or the channel condition is poor. In this sense, such time slots are not utilized efficiently and the wireless resource is wasted. The wasted wireless resource can be utilized by the SUs if we carefully design the TDMA scheduling scheme for the primary network.

In this chapter, we therefore develop a cross-layer design based packet scheduling scheme by taking into account the joint effect of queue management at the data link layer and wireless fading channel at the physical layer. Our proposed scheme, which is set up to operate friendly towards the SUs in terms of vacant-channel probability, can be implemented with just slight modification on the traditional TDMA scheduling algorithm. We construct a finite state Markov chain (FSMC) based queuing model to quantitatively analyze the performance metrics of our proposed scheme, in terms of idle probability of time slots, throughput, packet drop rate, average packet delay, head-of-line (HOL) delay. Based on the analytical model, we identify the tradeoff among the performance metrics and determine when and where the cost for favoring the SUs is worthy. The analytical results show that our proposed scheme can create more vacant-channel opportunities for SUs, at the expense of very slight increasing packet delay, as compared with the traditional wireless TDMA scheduling algorithm, when the PU's traffic load is not heavy.

The rest of this chapter is organized as follows. Section B presents the related work. Section C describes the system model. Section D proposes the queue-driven secondary-user-friendly TDMA scheduling scheme. Section E develops the analytical

model to analyze our proposed scheme. Section F evaluates our scheme based on the analytical model and simulation experiments. The chapter concludes with Section G.

B. Related Work

Scheduling schemes have been extensively studied in the framework of cellular networks [105–108]. In [105], scheduling algorithms were developed to exploit channel variation across users and allow the user with the best channel state to transmit. The authors of [106] developed the proportional fair scheduling to aim at maximizing long-term average throughput, while maintaining longterm fairness among users. In [107], the modified largest weighted delay first scheduling algorithm was proposed to provide different types of quality of service (QoS). In [108], the authors analyzed the traditional TDMA scheduling scheme in the environment of the wireless fading channel given a fixed packet error rate. Most of the prior work on scheduling have focused on either maximizing the system throughput or achieving fairness among multiple users. In this chapter, however, we focus on the secondary-user-friendly TDMA scheduling scheme for the primary network in the context of cognitive radio networks. To the best of our knowledge, this is the first chapter to explore whether it is worthy for the primary network to operate friendly towards the SUs while still satisfying the PUs' own QoS requirements.

The approaches that implement the cognitive radio networks can be broadly categorized into the following three types in terms of the relationship between the primary and secondary signals: overlay, underlay, and interweave [25]. For the overlay approach [109], the SUs may use part of their energy to assist the communications of PUs and the rest energy to transmit their own signal. In the underlay approach (e.g., [32]), the SUs transmit the spread wideband signals in a low power level such

that the interference caused by the SUs is below the acceptable noise floor in the perspective of the PUs. In the interweave approach (e.g., [13,14,17,103,104]), the SUs opportunistically utilize the unused licensed channels after sensing vacancy of PUs. The interweave approach does not need secondary users to have the priori knowledge of the primary signals. Since the key of our proposed secondary-user-friendly scheme is to increase the vacant-channel probability, our proposed scheme can benefit every type of the cognitive radio networks.

C. The System Models

Figure 43 shows the cognitive radio network model considered in the chapter. The cognitive radio network consists of two types of networks, the primary network and the secondary network. The primary network and the secondary network are independent with each other. In the primary network, the PUs which are licensed to use the wireless spectrum have the highest priority to utilize the wireless channel. The PUs don't conceive the existence of the secondary network. The PUs communicate with the base stations with a single-transmit and a single-receive antenna. The PUs share the wireless resource in a time division manner, i.e., the uplink/downlink is on the basis of TDMA scheduling. In particular, the time axis is divided into periodical frame periods, each of which consists of a constant number of time slots each with a length of T_s time units. In every frame period, each time slot is owned by a distinct PU. According to the scheduling scheme and channel condition, the PUs decide to whether or not use the channel during different frame periods.

On the other hand, the SUs, each of which is equipped with a cognitive radio, are synchronized with the PUs. In other words, the SUs know when every time slot of the primary network starts. From the perspective of the SUs, there may be vacant

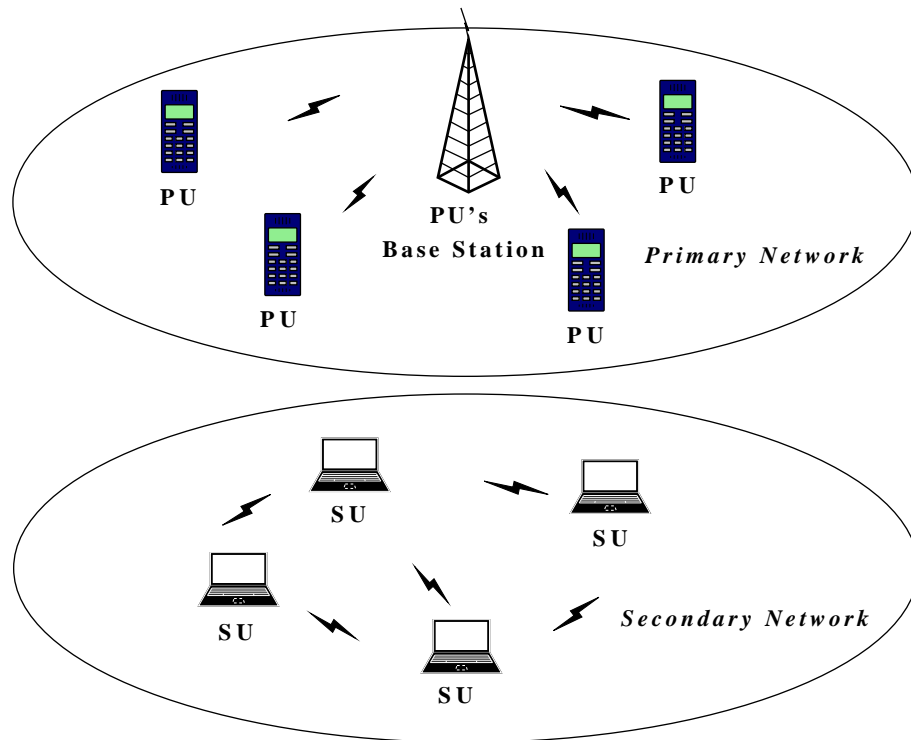


Fig. 43. The network model. PU and SU denotes PUs and SUs, respectively. The PUs communicate with the base station in a TDMA way. The SUs equipped with the cognitive radio, which are synchronized with the primary users, sense and utilize the vacant channels.

time slots that are not used by the PUs. By using the built-in cognitive radio, the SUs can periodically scan and identify the vacant time slots in the spectrum. Based on the scanned results, the SUs dynamically tune their transceivers to the identified spare channel spectrum to communicate among themselves during those vacant time slots.

We focus on the uplink communications of the PUs in this chapter. However, our scheme and the analytical model are also applicable for the downlink communications. As shown in Fig. 44, a finite-length first-in-first-out (FIFO) queue/buffer is employed at the PUs. If the buffer is full, the new arriving packets will be dropped. Suppose that each packet has a fixed number of bytes. The packets queued in the buffer

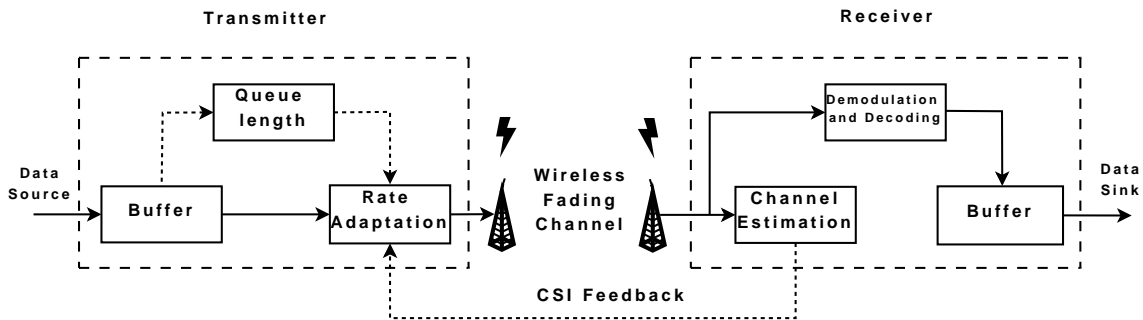


Fig. 44. Queue-driven secondary-user-friendly TDMA scheduling model.

are processed at the adaptive modulation module, and then transmitted through the antenna. The channel estimation module of the receiver side (base station) provides the channel state information (CSI) to the PUs via feedback channel. The CSI and the queue length of the buffer together control the rate adaptation module to decide the data rate on which the packets are transmitted.

Suppose that the wireless link between the PUs and the base station is characterized by a slow flat fading channel. The channel state remains unchanged during the same time slot, but varies from time slot to time slot. The channel state can be characterized by the received signal-to-noise ratio (SNR), denoted by γ . Without loss of generality, we model the wireless channel state by using the general Nakagami- m model [110], with average received SNR $\bar{\gamma} = E[\gamma]$. The probability density function of the received SNR (γ) can be given by

$$p_{\gamma}(\gamma) = \frac{1}{\gamma\Gamma(m)} \left(\frac{m\gamma}{\bar{\gamma}} \right)^m e^{-\frac{m\gamma}{\bar{\gamma}}}, \quad (6.1)$$

where m , ($m \geq 1/2$) is the Nakagami fading parameter and $\Gamma(x) = \int_0^{\infty} t^{x-1} e^{-t} dt$ is the Gamma function. The Nakagami- m model can embrace variant types of wireless fading channels. For example, Rayleigh channel is a special case of Nakagami- m when $m = 1$. Furthermore, the Rician fading channels can be approximated by

the Nakagami- m model by an one-to-one mapping between the Nakagami fading parameter m and the Rician factor [110].

D. Our Proposed Secondary-User-Friendly Scheme

In the traditional TDMA scheme, a given PU transmits the buffered packets as many as the channel can accommodate during each time slot that is assigned to the PU. The number of packets that can be sent depends on i) the number of buffered packets (i.e., queue size) and ii) the number of packets the channel can accommodate. Thus, in some time slots, the number of sent packets is small because either the queue size is small or the channel condition is poor. In this way, such time slots are not utilized efficiently, and thus the wireless resource is wasted. The wasted wireless resource can be utilized by the SUs with the help of the cognitive radio.

Motivated by the above observations, we proposed the queue-driven secondary-user-friendly TDMA scheduling scheme, which takes into account the joint effect of the wireless-channel qualities at the physical layer and queuing characteristics at the data link layer. The key idea of our proposed scheme is to make each PU to efficiently utilize its owned time slots when the PU occupies them. Particularly, in our proposed scheme, the PU may hold the packets until there are sufficient packets available in the buffer and the channel is in good state. In other words, any given PU transmits the buffered packets to the base station only if the buffer size of the PU is large enough and the channel between the PU and the base station is good. In this way, the number of idle time slots may increase, which is welcome by the SUs. On the other hand, however, holding more packets in the buffer introduces higher packet delay and packet drop rate for the PUs, which clearly imposes a tradeoff between the idle probability of time slots and the delay QoS requirements.

We introduce three parameters, θ_A , θ_B , and θ_C , to achieve the desirable tradeoff between the idle probability of time slots and the packet delay as well as the packet drop rate. All the parameters, θ_A , θ_B , and θ_C are integers, and $\theta_C > \max\{\theta_A, \theta_B\}$. In our proposed scheme, when the packet size is no larger than θ_C , the PU avoids transmitting packets if the estimated number of packets that can be transmitted is less than θ_A or the queue size is smaller than θ_B . Note that the traditional TDMA scheme is a special case of our proposed scheme when $\theta_A = \theta_B = 1$ and it provision the most stringent delay QoS-requirement for the PUs. The objective of θ_C is to make our proposed scheme to work as the traditional TDMA scheme when the buffer size is high. **Algorithm 1** shows our proposed scheme. As we can predict, the larger the values of θ_A and θ_B are, the higher the packet delay, packet drop rate, and idle probability of time slots are. In Sections E and F, we will detail how to balance the tradeoff between idle probability of time slots and packet delay by tuning up these parameters through analytical models and simulations.

Algorithm 1 Queue-driven secondary-user-friendly TDMA scheduling

For each PU in its assigned time slot of the t -th frame period, $t = 1, 2, \dots$

- 1: get the CSI information through the feedback channel
 - 2: $n :=$ the number of packets in the buffer
 - 3: $m :=$ the estimated number of packets it can transmit based on the CSI
 - 4: **if** $n \geq \theta_C$ or $(m \geq \theta_A$ and $n \geq \theta_B)$ **then**
 - 5: transmit the buffered packets to the base station
 - 6: **else**
 - 7: hold packets in the buffer
 - 8: **end if**
-

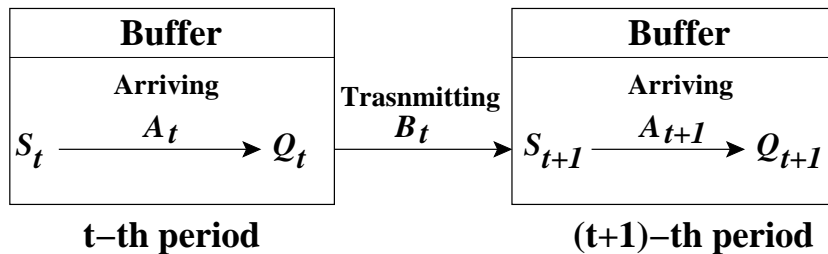


Fig. 45. Diagram of the evolution of the queue states.

E. The Analytical Model

In this section, we develop a mathematical model to analyze our proposed scheme's performance, in terms of the idle probability of time slots, packet drop rate, throughput, head of line delay, and average packet delay. We assume that the CSI is fed back to the transmitter without error and latency. It can be implemented by using training-based channel estimation at the receiver side to obtain the perfect CSI and then employing coded and fast feedback channels to inform the transmitter of the CSI.

Let t , with $t = 0, 1, 2, \dots$, index the frame periods, each of which has a length of T . Denote by S_t and Q_t the queue lengths of the buffer at the beginning and the end of the t -th frame period, respectively. Let K be the buffer capacity in terms of packets. It is clear that the evolution of queue states can be characterized by Q_t with $0 \leq Q_t \leq K$, as shown in Fig. 45.

Let A_t be the number of packets arrival during t -th frame period. The packet arrival process $\{A_t\}$ is stationary and independent of the queue states and the channel states. Also, if we denote by λ the packet arrival rate, then $E[A_t] = \lambda T$. In this chapter, we assume that the packet arrival process A_t is a Poisson process with a packet arrival rate of λ . Then, we have the probability mass function (pmf) of A_t as

follows:

$$\Pr\{A_t = a\} = \begin{cases} \frac{(\lambda T)^a e^{-\lambda T}}{a!}, & a \geq 0 \\ 0, & a < 0. \end{cases} \quad (6.2)$$

Denote by B_t the random variable for the number of transmitted packets at the t -th frame period. It is clear that B_t depends on the received SNR γ during the assigned time slot of the frame period. According to the Shannon capacity, given γ , the number of transmitted packets can be written as

$$B_t = \left\lfloor \frac{WT_s \log_2(1 + \gamma)}{\ell} \right\rfloor \quad (6.3)$$

where T_s is the length of a time slot, W is the channel bandwidth, and ℓ is the constant packet size. Note that γ follows Nakagami- m , distribution. We obtain the pmf of B_t by

$$\begin{aligned} \Pr\{B_t = b\} &= \int_{\kappa(b)}^{\kappa(b+1)} p_\gamma(\gamma) d\gamma \\ &= \frac{1}{\Gamma(m)} \left[\Gamma\left(m, \frac{m\kappa(b)}{\bar{\gamma}}\right) - \Gamma\left(m, \frac{m\kappa(b+1)}{\bar{\gamma}}\right) \right] \end{aligned} \quad (6.4)$$

where $b = 0, 1, 2, \dots$, $\kappa(x) = 2^{\frac{x\ell}{WT_s}} - 1$, and $\Gamma(a, z)$ is the upper incomplete Gamma function which is defined as:

$$\Gamma(a, z) = \int_z^\infty t^{a-1} e^{-t} dt. \quad (6.5)$$

Define S_{t+1} as the number packets in the buffer at the beginning of the $(t + 1)$ -th frame period. According to our proposed TDMA scheduling scheme, S_{t+1} is dependent of Q_t and B_t . In particular, we derive S_{t+1} as follows:

$$S_{t+1} = \max\{0, Q_t - \delta_t B_t\} \quad (6.6)$$

where

$$\delta_t = \begin{cases} 0, & (Q_t < \theta_B) \vee ((B_t < \theta_A) \wedge (Q_t < \theta_C)) \\ 1, & \text{otherwise} \end{cases} \quad (6.7)$$

with $1 \leq \theta_A, \theta_B, \theta_C \leq K$ and $\theta_C > \max\{\theta_A, \theta_B\}$. θ_A , θ_B and θ_C are predefined parameters. In fact, δ_t indicates whether packets will be transmitted or not based on the current channel and queue states.

Given that the buffer already has r packets at the end of t -th frame period, since the conditional probability that there are s packets in the buffer at the beginning of the $(t+1)$ -th frame period depends on the number of packets transmitted at the t -th frame period, we have

$$\Pr\{S_{t+1} = s | Q_t = r\} = \begin{cases} \Pr\{B_t = r - s\}, & \{[(\theta_B \leq r < \theta_C) \wedge (r - s \geq \theta_A)] \\ & \vee (r \geq \theta_C)\} \wedge (s > 0) \\ \sum_{b=r}^{\infty} \Pr\{B_t = b\}, & \{[(\theta_B \leq r < \theta_C) \wedge (r - s \geq \theta_A)] \\ & \vee (r \geq \theta_C)\} \wedge (s = 0) \\ \Pr\{B_t < \theta_A\}, & \max\{\theta_A, \theta_B\} \leq r = s < \theta_C \\ 1, & r = s < \max\{\theta_A, \theta_B\} \\ 0, & \text{otherwise.} \end{cases} \quad (6.8)$$

The queue length of buffer at the $(t+1)$ -th frame period is $Q_{t+1} = \max\{K, S_{t+1} + A_{t+1}\}$. Then, given $S_{t+1} = s$, the conditional pmf of Q_{t+1} can be expressed as follows:

$$\Pr\{Q_{t+1} = q | S_{t+1} = s\} = \begin{cases} \Pr\{A_{t+1} = q - s\}, & (s \leq q) \wedge (q < K) \\ \sum_{a=q-s}^{\infty} \Pr\{A_{t+1} = a\}, & (s < q) \wedge (q = K) \\ 1, & s = q = K \\ 0, & \text{otherwise.} \end{cases} \quad (6.9)$$

For simplicity of presentation, we define the following equations:

$$\begin{cases} \alpha_{q,s} \triangleq \Pr\{Q_{t+1} = q | S_{t+1} = s\} \\ \beta_{s,r} \triangleq \Pr\{S_{t+1} = s | Q_t = r\}. \end{cases} \quad (6.10)$$

Then, we can obtain the transition probability, denoted by $P_{q,r}$, that there are q packets in the buffer given that the queue size is r at the previous frame period as follows

$$\begin{aligned} P_{q,r} &\triangleq \Pr\{Q_{t+1} = q | Q_t = r\} \\ &= \sum_{s=0}^K \Pr\{Q_{t+1} = q | S_{t+1} = s, Q_t = r\} \\ &\quad \times \Pr\{S_{t+1} = s | Q_t = r\} \\ &\stackrel{(a)}{=} \sum_{s=0}^K \Pr\{Q_{t+1} = q | S_{t+1} = s\} \Pr\{S_{t+1} = s | Q_t = r\} \\ &= \sum_{s=0}^K \alpha_{q,s} \beta_{s,r} \end{aligned} \quad (6.11)$$

where the equation of (a) holds because the number of packets in the buffer at the end of $(t+1)$ -th frame period depends only on the number of packets at the beginning of $(t+1)$ -th frame period and the number of arrived packets during $(t+1)$ -th frame period. Note that $\{Q_t\}$ can be modeled as a finite state Markov chain (FSMC). We then construct the probability transition matrix $\mathbf{P} = \{P_{q,r}\}_{(K+1) \times (K+1)}$. It is clear that the stationary distribution of the FSMC $\{Q_t\}$ exists and unique. Denote by π the stationary pmf of the number of packets in the buffer at the end of a frame period, i.e.,

$$\pi(n) = \lim_{t \rightarrow \infty} \Pr\{Q_t = n\} \quad (6.12)$$

where $0 \leq n \leq K$. For the convenience of presentation, we define $\pi_n \triangleq \pi(n)$.

The stationary pmf π satisfies the following equations:

$$\begin{cases} \sum_{n=0}^K \pi_n = 1 \\ \mathbf{\Pi} = \mathbf{P}\mathbf{\Pi} \end{cases} \quad (6.13)$$

where $\mathbf{\Pi}$ is the column vector of π and is given by

$$\mathbf{\Pi} \triangleq [\pi_0, \pi_1, \dots, \pi_K]^T. \quad (6.14)$$

After obtaining $\{\pi_n\}$, we therefore use Eq. (6.8) to obtain the stationary pmf, denoted by σ , of the number of packets at the beginning of a frame period, i.e.,

$$\sigma(n) = \lim_{t \rightarrow \infty} \Pr\{S_t = n\} = \lim_{t \rightarrow \infty} \sum_{r=0}^K \Pr\{S_{t+1} = n | Q_t = r\} \pi_r = \sum_{r=0}^K \beta_{n,r} \pi_r. \quad (6.15)$$

Let also $\sigma_n \triangleq \sigma(n)$, which will be used in the followings.

1) Packet Drop Rate

If we denote by L_t the number of dropped packets due to the buffer overflow during the t -th frame period, then we obtain

$$L_t = \max\{0, A_t - (K - S_t)\}. \quad (6.16)$$

The pmf of L_t can be expressed as follows:

$$\Pr\{L_t = n\} = \begin{cases} \sum_{s=0}^K \sum_{m=0}^{K-s} \Pr\{A_t = m\} \Pr\{S_t = s\}, n = 0 \\ \sum_{s=0}^K \Pr\{A_t = n + K - s\} \Pr\{S_t = s\}, n > 0. \end{cases} \quad (6.17)$$

The packet dropping rate, denoted by ω , in the steady state is equal to the ratio of the average number of drop packets to the average number of arrival packets in a

frame period. Thus, we derive ω as follows:

$$\begin{aligned}\omega &= \lim_{t \rightarrow \infty} \frac{E[L_t]}{E[A_t]} \\ &= \frac{\sum_{n=1}^{\infty} \sum_{s=0}^K n \sigma_s \Pr\{A_t = n + K - s\}}{\lambda T}.\end{aligned}\quad (6.18)$$

2) The Idle Probability of Time Slots

Then, we calculate the idle probability, denoted by ϕ , that a time slot is not used by the PU in the steady state. The idle probability is equivalent to the probability that the number of packets in the buffer at the end of the current frame period is equal to that at the beginning of the next frame period, i.e.,

$$\phi = \sum_{n=0}^K \Pr\{S_{t+1} = n, Q_t = n\} = \sum_{n=0}^K \beta_{n,n} \pi_n \quad (6.19)$$

where $\beta_{n,n}$ is given by Eq. (6.10). It is worth noting that the higher the idle probability of time slots, the more opportunities for the SUs utilize the vacant channel. That is, the vacant-channel probability is proportional to the idle probability of time slots.

3) The Head-of-Line (HOL) Delay

To study the packet waiting time in the buffer in the worst case, we introduce the HOL delay, denoted by D , which is defined as the duration in terms of the frame period from the time when a packet arrives at the head of the buffer to the time when the packet leaves the buffer in the steady state. We first derive the conditional probability that given $Q_t = n$, $S_{t+1} = Q_t$ and $Q_{t+1} = m$ in the steady state as follows:

$$\begin{aligned}\Pr\{Q_{t+1} = m, S_{t+1} = n | Q_t = n\} \\ &= \Pr\{Q_{t+1} = m | Q_t = n, S_{t+1} = n\} \Pr\{S_{t+1} = n | Q_t = n\} \\ &= \Pr\{Q_{t+1} = m | S_{t+1} = n\} \Pr\{S_{t+1} = n | Q_t = n\} \\ &= \alpha_{m,n} \beta_{n,n}.\end{aligned}\quad (6.20)$$

Given $Q_t = n$, the conditional probability that at least one packet is transmitted at the t -th frame period and there are m packets at the end of the $(t+1)$ -th frame period is given by

$$\begin{aligned}
\Pr\{Q_{t+1} = m, S_{t+1} < n | Q_t = n\} &= \sum_{i=0}^{n-1} \Pr\{Q_{t+1} = m, S_{t+1} = i | Q_t = n\} \\
&= \sum_{i=0}^{n-1} \Pr\{Q_{t+1} = m | S_{t+1} = i\} \Pr\{S_{t+1} = i | Q_t = n\} \\
&= \sum_{i=0}^{n-1} \alpha_{m,i} \beta_{i,n}. \tag{6.21}
\end{aligned}$$

The probability that the HOL delay (D) is equal to d frame periods in the steady state is equivalent to the probability that no packet is transmitted for exact d consecutive times. If $d = 0$, we have

$$\begin{aligned}
\Pr\{D = 0\} &= \Pr\{Q_t = 0 \vee (Q_t > 0 \wedge Q_t \neq S_{t+1})\} \\
&= \pi_0 + \sum_{n=1}^K \sum_{i=0}^{n-1} \pi_n \beta_{i,n}. \tag{6.22}
\end{aligned}$$

On the other hand, We derive the probability that the HOL delay is d frame periods

in the steady state when $d > 0$ as follows:

$$\begin{aligned}
\Pr\{D = d\} &= \Pr\{(Q_t = S_{t+1}) \wedge (Q_{t+1} = S_{t+2}) \wedge (Q_{t+2} = Q_{t+3}) \\
&\quad \cdots \wedge (Q_{t+d-1} = S_{t+d}) \wedge (Q_{t+d} \neq S_{t+d+1})\} \\
&= \sum_{q_0, q_1, q_2, \dots, q_d=1}^K \Pr\{Q_t = q_0, S_{t+1} = q_0, Q_{t+1} = q_1, S_{t+2} = q_1, Q_{t+2} = q_2, \dots, \\
&\quad Q_{t+d-1} = q_{d-1}, S_{t+d} = q_{d-1}, Q_{t+d} = q_d, S_{t+d+1} < q_d\} \\
&= \sum_{q_0, q_1, q_2, \dots, q_d=1}^K \pi_{q_0} \Pr\{Q_{t+1} = q_1, S_{t+1} = q_0 | Q_t = q_0\} \\
&\quad \times \Pr\{Q_{t+2} = q_2, S_{t+2} = q_1 | Q_{t+1} = q_1\} \times \cdots \\
&\quad \times \Pr\{Q_{t+d} = q_d, S_{t+d} = q_{d-1} | Q_{t+d-1} = q_{d-1}\} \\
&\quad \times \Pr\{S_{t+d+1} < q_d | Q_{t+d} = q_d\} \\
&= \sum_{q_0, q_1, q_2, \dots, q_d=1}^K \pi_{q_0} (\alpha_{q_1, q_0} \beta_{q_0, q_0}) \cdots (\alpha_{q_d, q_{d-1}} \beta_{q_{d-1}, q_{d-1}}) \left(\sum_{i=0}^{q_d-1} \beta_{i, q_d} \right) \\
&= \sum_{q_0, q_1, q_2, \dots, q_d=1}^K \pi_{q_0} \left(\sum_{i=0}^{q_d-1} \beta_{i, q_d} \right) \prod_{j=0}^{d-1} \alpha_{q_{j+1}, q_j} \beta_{q_j, q_j}. \tag{6.23}
\end{aligned}$$

Hence, combining Eqs. (6.22) and (6.23) together, we obtain the pmf of the HOL delay as follows:

$$\Pr\{D = d\} = \begin{cases} \sum_{q_0, q_1, \dots, q_d=1}^K \pi_{q_0} \left(\sum_{i=0}^{q_d-1} \beta_{i, q_d} \right) \prod_{j=0}^{d-1} \alpha_{q_{j+1}, q_j} \beta_{q_j, q_j}, & d > 0 \\ \pi_0 + \sum_{n=1}^K \sum_{i=0}^{n-1} \pi_n \beta_{i, n}, & d = 0 \end{cases} \tag{6.24}$$

where d is a nonnegative integer.

4) The Throughput

Since the packet that successfully enters the buffer can be eventually sent to the base station, the throughput, denoted by η , can be obtained by

$$\eta = \lambda \ell (1 - \omega) \tag{6.25}$$

where ℓ is the packet length.

5) The Average Packet Delay

It is a well-known fact that in models where the arrivals follow a Poisson process, the queue state as seen by an arriving packet is the same as for an outside observer (random epoch). Denote by N_t^τ the number of packets at the $tT + \tau$ epoch where $0 \leq \tau \leq T$. Given there are s packets at the beginning of the t -th frame period, the probability that $N_t^\tau = n$ is equal to the probability that there are $(n - s)$ packets arriving during τ . Then, we obtain

$$\Pr\{N_t^\tau = n | S_t = s\} = \begin{cases} \frac{(\lambda\tau)^{n-s} e^{-(\lambda\tau)}}{(n-s)!}, & s \leq n < K \\ \sum_{j=K-s}^{\infty} \frac{(\lambda\tau)^j e^{-(\lambda\tau)}}{j!}, & n = K. \end{cases} \quad (6.26)$$

Let N^τ be the number of packets at the $tT + \tau$ epoch in the steady state. Then, we derive the probability, denoted by ν_n , that there are n packets in the queue at any random epoch as follows:

$$\begin{aligned} \nu_n &= \frac{1}{T} \int_0^T \Pr\{N^\tau = n\} d\tau \\ &= \sum_{s=0}^K \frac{\sigma_s}{T} \int_0^T \Pr\{N_t^\tau = n | S_t = s\} d\tau \\ &= \begin{cases} \sum_{s=0}^K \frac{\sigma_s}{\lambda T} \left(1 - \frac{\Gamma(n-s+1, \lambda T)}{(n-s)!}\right), & 0 < n < K \\ \sum_{s=0}^K \sum_{j=K-s}^{\infty} \frac{\sigma_s}{\lambda T} \left(1 - \frac{\Gamma(j+1, \lambda T)}{j!}\right), & n = K. \end{cases} \end{aligned} \quad (6.27)$$

Thus, we obtain the average packet length, denoted by \bar{N} , at any random epoch as follows:

$$\bar{N} = \sum_{n=0}^K n \nu_n. \quad (6.28)$$

Applying the Little's Formula, we have

$$\bar{W}_q = \frac{\bar{N}}{\lambda(1 - \omega)}. \quad (6.29)$$

F. Performance Evaluations

1. Numerical Results

The parameters used to evaluate our proposed TDMA scheduling scheme are set as follows: $W = 1$ Mbps, $T = 18.9$ ms, $T_s = 1.89$ ms, $\ell = 200$ bytes, $K = 30$. To satisfy different QoS requirements in terms of packet drop rate, average packet delay, and HOL delay in different situations, we adopt different combinations of θ_A , θ_B , and θ_C . Clearly, when θ_A , θ_B , and θ_C become larger, the proposed scheme achieves poorer QoS performance for the PUs, but provides higher idle probability of time slots for the SUs. After conducting extensive numerical evaluations, we find a set of triplets $(\theta_A, \theta_B, \theta_C)$, each of which represents a typical application case with different QoS requirements. In particular, the triplet $(\theta_A, \theta_B, \theta_C)$ is set to be $(1, 1, 2)$, $(2, 2, 5)$, $(2, 3, 5)$, $(3, 4, 25)$, and $(6, 10, 20)$, respectively, for different application cases in the order of low to high QoS requirements. Note that when $(\theta_A, \theta_B, \theta_C) = (1, 1, 2)$, it corresponds to the traditional TDMA scheduling scheme.

Figures 46(a), (b), (c), and (d) shows the performance metrics of our proposed scheme when different triplets $(\theta_A, \theta_B, \theta_C)$ are adopted. The average SNR ($\bar{\gamma}$) changes from 5 to 25 dB. The packet arrival rate is set to be 53 packets per second. As shown in Figs 46(a), (b), (c), and (d), by tuning up the different settings of θ_A , θ_B , and θ_C , the proposed scheme can achieve different tradeoffs among the idle probability of time slots, average packet delay, and packet drop rate. We observe that with appropriate settings of $(\theta_A, \theta_B, \theta_C)$, the proposed TDMA scheme can achieve higher

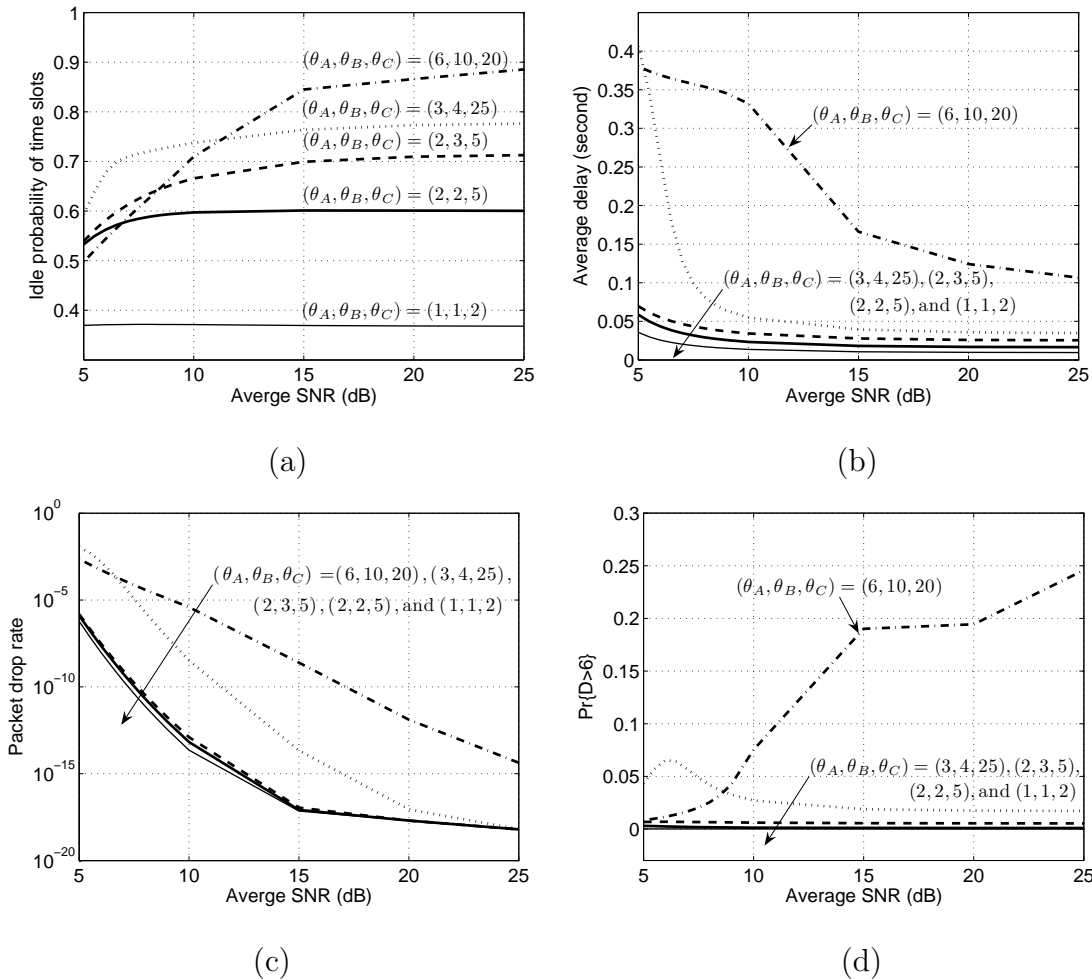


Fig. 46. The performance metrics of the proposed scheme against average SNR with different combinations of θ_A , θ_B , and θ_C . The packet arrival rate (λ) is set to be 53 packets per second and the Nakagami fading parameter (m) is 1. (a) The idle probability of time slots. (b) The average queuing delay. (c) The packet drop rate. (d) The probability that the HOL delay is larger than 6 frame periods. In each sub-figure, the plots with thin solid line, thickly solid line, thickly dashed line, thickly dotted line, and thickly dashed-dotted line denote our scheme with triplets $(1, 1, 2)$, $(2, 2, 5)$, $(2, 3, 5)$, $(3, 4, 25)$, and $(6, 10, 20)$, respectively.

idle probability of time slots at the cost of little increase of average packet delay, as compared with the traditional TDMA scheme. Note that higher idle probability of time slots means more opportunities for the secondary users to utilize the channel. For example, when average SNR is 15 dB, the idle probability of time slots of our proposed scheme with $(\theta_A, \theta_B, \theta_C) = (2, 2, 5)$ is 65% higher than that of traditional TDMA scheme, while the differences of the average packet delays and the packet drop rates between these two schemes are almost unnoticeable. We can further increase the idle probability of time slots if the triplet $(\theta_A, \theta_B, \theta_C)$ is set to be $(3, 4, 25)$, the idle probability of time slots is 103% higher than that of traditional TDMA scheme, while the average packet delay also increases by 0.02 second as compared with the tradition TDMA scheme.

As shown in Fig. 46(a), the idle probability of time slots achieved by the traditional TDMA scheme remains constant regardless of the average SNR. This is because under the traditional TDMA scheme, each PU occupies the assigned time slots as long as the buffer is non-empty. In this way, the idle probability of time slots depends only on the packet arrival rate. In Fig. 46(c), as the average SNR increases, the packet drop rate decreases monotonically. As shown in Figs. 46(b) and (d), as the average SNR increases, the HOL delay of the scheme with $(6, 10, 20)$ gets larger while the average delay decreasing. This is because that with higher average SNR, the PUs can transmit more packets at a time slot, resulting in the higher probability that the HOL packets need to wait longer for additional $(\theta_A - 1)$ packets. Thus, in the high average SNR case, although our proposed scheme with large θ_A and θ_B can achieve high idle probability of time slots and low average packet delay and packet drop rate, the HOL delay increases significantly, which is not acceptable for certain applications.

Then, we evaluate the impact of traffic load on the performance of the proposed scheme when Nakagami fading parameter is set to be 1 and 2, respectively. The

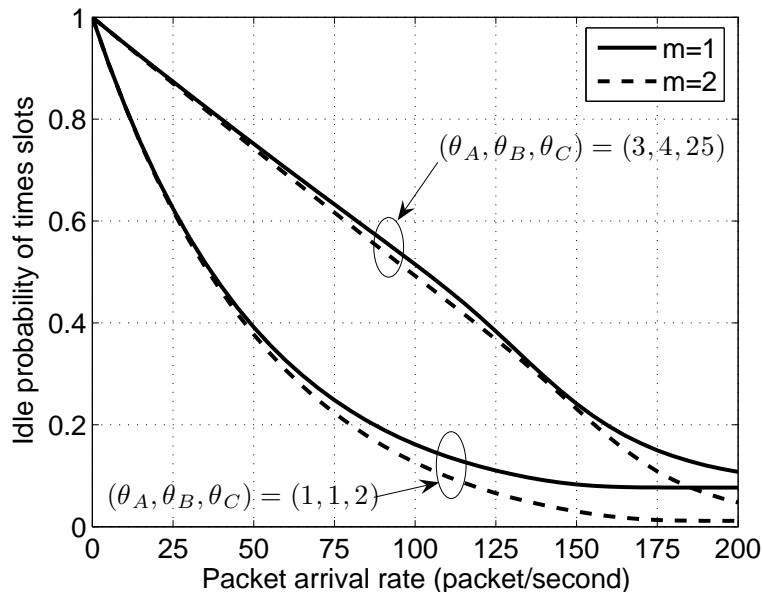


Fig. 47. The idle probability of time slots against the packet arrival rate. The average SNR ($\bar{\gamma}$) is 10 dB.

triplet is set to be $(1, 1, 2)$ and $(3, 4, 25)$, respectively. Figs. 47 through 49 show the idle probability of time slots, the average packet delay, the packet drop rate, the throughput, and the probability that the HOL delay is larger than 3 and 6 frame periods, respectively. As expected, our proposed scheme with the same triplet achieves better performance when the value of m changes from 1 to 2. This is because $m = 1$ corresponds to Rayleigh fading channel, which is the worst fading scenario. Fig. 47 illustrates that the idle probability of time slots decreases as the packet arrival rate increases. As shown in Fig. 47, by achieving the higher idle probability of time slots, our proposed scheme with $(3, 4, 25)$ can create more spectrum opportunities for SUs than the traditional TDMA scheduling algorithm.

As shown in Figs. 48 and 49, the HOL delay in the traditional TDMA scheduling algorithm is close to 0 because $\theta_A = \theta_B = 1$. When the traffic load is light, the HOL delay is significantly high for setup of $(3, 4, 25)$ because the HOL packets in the

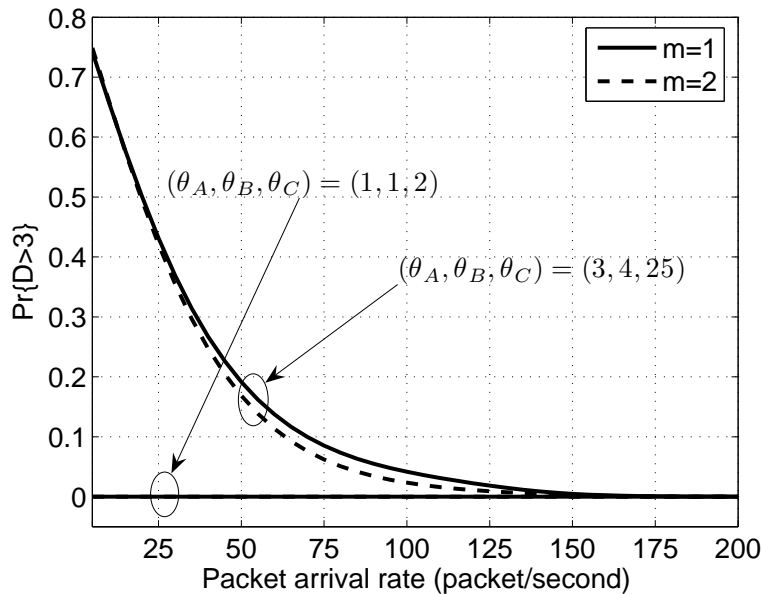


Fig. 48. The probability that the HOL delay is larger than 3 frame periods when the packet arrival rate varies and the average SNR ($\bar{\gamma}$) is 10 dB.

buffer have to wait a long time for the additional packets to satisfy the transmission condition that queue size is larger than 3.

As shown in Fig. 50, the average packet delay of our proposed scheme with $(3, 4, 25)$ decreases when the packet arrival rate increases from 2 to 60 packet/second, and then increases as the packet arrival rate increases from 62 to 158 packet/second, but finally decreases as the packet arrival rate further increases. That is because the following reasons. First, when the packet arrival rate increases from 2 to 60 packet/second, higher packet arrival rate means that the packets in the buffer can accumulate in higher speed to satisfy the transmission condition that the queue size is larger than θ_B . Second, as the packet arrival rate changes from 62 to 158, the average packet delay increases because the system load gets heavier. Finally, when the packet arrival rate keep increasing, as shown in Fig. 48, 49, and 51, the packet drop rate increases sharply and the HOL delay decreases, resulting in that in average

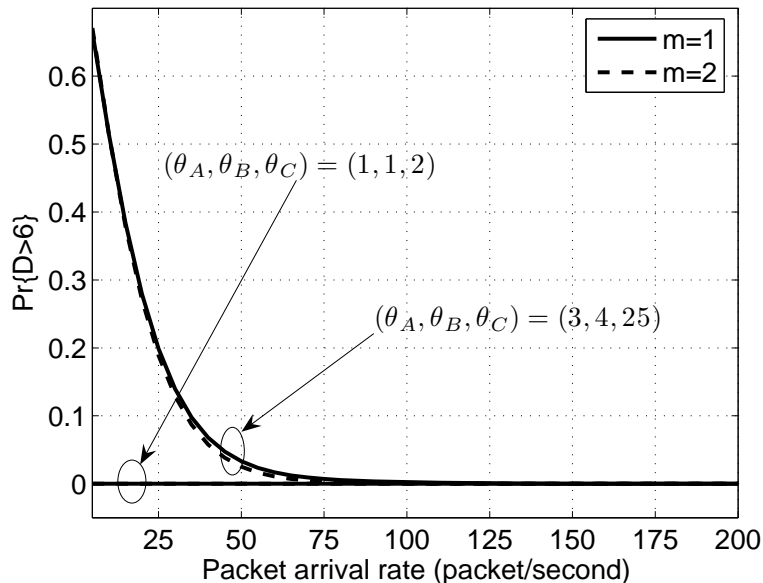


Fig. 49. The probability that the HOL delay is larger than 6 frame periods when the packet arrival rate varies and the average SNR ($\bar{\gamma}$) is 10 dB.

the packets wait for less time in the queue.

Thus, when the traffic load is light, it is not worth employing high θ_A or θ_B for our proposed scheme because it increases little idle probability of time slots but at a cost of significant increase of average packet delay. On the other hand, when the traffic load gets heavier, our proposed scheme can achieve high idle probability of time slots at the expense of unnoticeable increase of average packet delay and packet drop rate.

2. Case Study

We consider a licensed spectrum band consisting of 5 uplink channels each with 1 Mbps bandwidth. Each uplink channel accommodates 10 PUs. All the PUs have the same packet arrival rate of 75 packet/second. The length of a frame period is 18.9 ms. Each frame comprises 10 time slots each spanning 1.89 ms and corresponding to

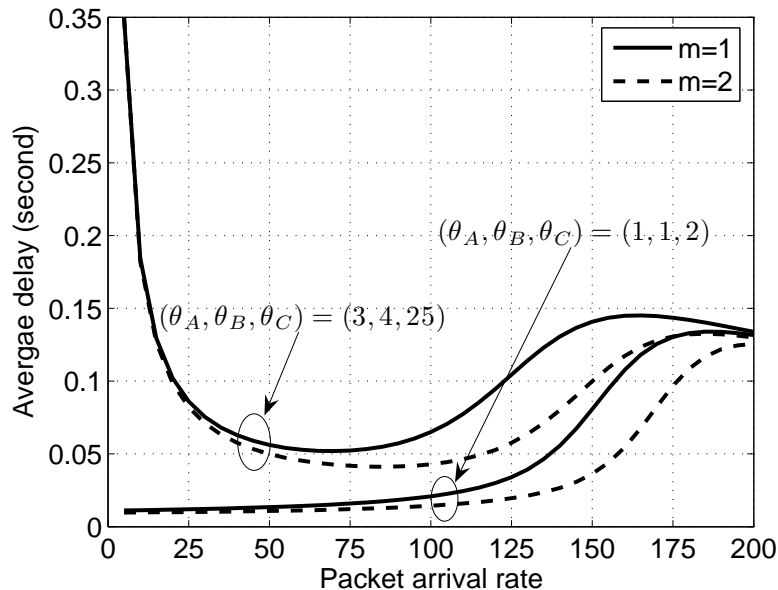


Fig. 50. The average packet delay against the packet arrival rate. The average SNR ($\bar{\gamma}$) is 10 dB.

a PUs in that channel. Meanwhile, there are 20 SUs composing a secondary ad hoc network which overlays on the primary networks. The SUs adopt the cognitive MAC protocol with the negotiation-based channel sensing policy [14]. In particular, under the cognitive MAC protocol, each SU, which is synchronized with the PUs, consists of a control transceiver working on the dedicated control channel and a SDR-based transceiver that can be dynamically tuned to any one of the licensed channels to sense for the spare spectrum, and then to receive/transmit the SUs' packets. The SUs cooperatively identify the vacant licensed channels at the beginning of each time slot. After the cooperative channel sensing, the SUs utilize all of the vacant channels. The system utilization of the SUs is set to be 0.1.

We develop a customized discrete event-driven simulator to study the performance of our proposed scheme with different triplets $(\theta_A, \theta_B, \theta_C)$. Suppose the average SNR is 15 dB. Table V shows the improvements for the SUs and the costs

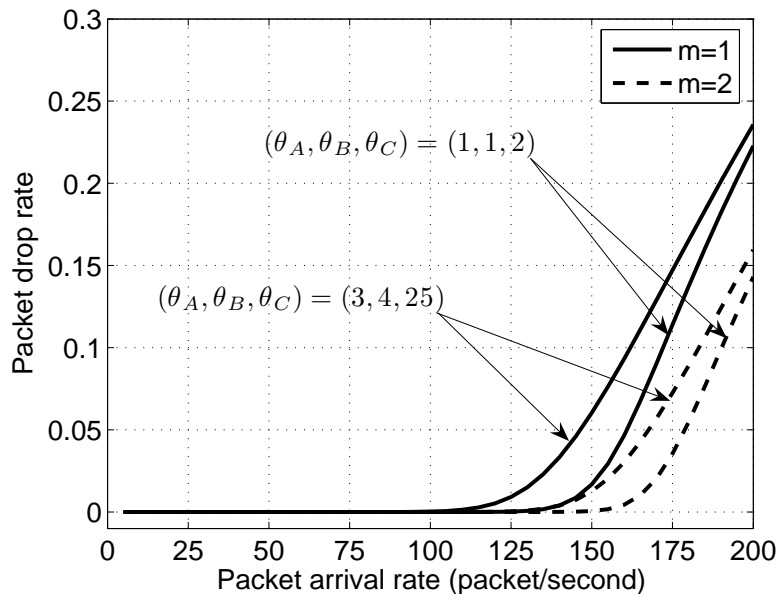


Fig. 51. The packet drop rate against the packet arrival rate. The average SNR ($\bar{\gamma}$) is 10 dB.

of the PUs when different triplets $(\theta_A, \theta_B, \theta_C)$ are employed. As shown in Table V, the analytical results of the average delay of PUs agree well with the simulations results. As compared with the traditional TDMA scheduling, our proposed scheme with $(\theta_A, \theta_B, \theta_C) = (1, 2, 2)$ enables the aggregate throughput of SUs to increase 82.2% and the average packet delay of SUs to decrease 186.0% at the cost of average packet delay increasing 4.38 ms. Also, the aggregate throughput of the PUs remains the same regardless of $(\theta_A, \theta_B, \theta_C)$.

If the PUs are allowed for a loose QoS requirement, we can set the larger θ_A , θ_B , and θ_C to further increase the aggregate throughput and decrease average packet delay of SUs. For example, when $(\theta_A, \theta_B, \theta_C) = (3, 4, 20)$, the average packet delay of the SUs can decrease 474.7% as compared with the traditional TDMA scheme. Given the QoS-requirements of the PUs, we can carefully devise $(\theta_A, \theta_B, \theta_C)$ in our proposed scheme to make the primary network to operate friendly towards the SUs, resulting

Table V. Case study of our proposed secondary-user-friendly scheme when $\bar{\gamma} = 15$ dB.

	$(\theta_A, \theta_B, \theta_C)$		
	(1,1,2)	(1,2,2)	(3,4,20)
Aggregate throughput of SU (simulation)	124 Kbps	226 Kbps	327 Kbps
Average delay of SU (simulation)	56.72 ms	19.83 ms	9.87ms
Throughput of PU (simulation)	120 Kbps	120 Kbps	120 Kbps
Throughput of PU (analytical)	120 Kbps	120 Kbps	120 Kbps
Average delay of PU (simulation)	11.12 ms	15.50 ms	32.03 ms
Average delay of PU (analytical)	11.02 ms	15.45 ms	31.46 ms

in the win-win outcome.

G. Summary

Motivated by the insufficient utilization of the wireless spectrum, we developed a secondary-user-friendliness driven TDMA scheduling scheme for the primary networks, which takes advantage of the property of wireless fading channel and cross-layer design technique. Our proposed scheme can be implemented with only slight modification on top of the traditional TDMA scheduling algorithm. By employing different parameter triplets of $(\theta_A, \theta_B, \theta_C)$, our proposed scheme can achieve the given QoS requirements of PUs while providing high vacant channel opportunities for the SUs. We developed the queuing model to analyze the performance of our scheme, in terms of the idle probability of time slots, the average packet delay, the HOL delay, the throughput, and the packet drop rate. The analytical results show that our proposed scheme can increase the idle probability of time slots (which means more vacant channel opportunities for SUs) at the cost of little increasing packet delay and packet drop rate, as compared with the traditional wireless TDMA scheduling algorithm.

CHAPTER VII

CONCLUSIONS

By enabling the opportunistic spectrum access for SUs, the cognitive radio networks emerge as the promising solution to the paradox between the spectral underutilization and scarcity. The objective of this dissertation was to design and analyze the opportunistic MAC protocols for various types of cognitive radio networks. This chapter summarizes the achieved research contributions of this dissertation and proposes some future research directions.

A. Summary of the Dissertation

In Chapter I, we introduced and motivated the problems. In Chapter II, we proposed the cross-layer based opportunistic MAC protocols, which integrate the cooperative spectrum sensing at PHY layer and the packets scheduling at MAC layer, for the synchronous cognitive radio networks. Specifically, the MAC protocols enable the SUs to identify and utilize the vacant frequency spectrum in a way that constrains the level of interference to the PUs. In our proposed protocols, each SU is equipped with two transceivers. One transceiver is tuned to the dedicated control channel, while the other is used as a cognitive radio that can periodically sense and dynamically use the identified vacant channels. To obtain the channel status accurately, we proposed two collaborative channel spectrum-sensing policies, namely, the random sensing policy and the negotiation-based sensing policy, to help the MAC protocols detect the availability of vacant channels. Under the random sensing policy, each SU just randomly selects one of the channels for sensing. On the other hand, under the negotiation-based sensing policy, different SUs attempt to select the distinct channels to sense by overhearing the control packets over the control channel. We developed the Markov

chain model and the $M/G^Y/1$ -based queueing model to characterize the performance of our proposed multi-channel MAC protocols under the two types of channel-sensing policies for the saturation network and the non-saturation network scenarios, respectively. In the non-saturation network case, we quantitatively identified the tradeoff between the aggregate traffic throughput and the packet transmission delay, which can provide the insightful guidelines to improve the delay-QoS provisionings over cognitive radio wireless networks.

In Chapter III, we proposed a channel-hopping based cognitive radio MAC protocol for synchronized wireless networks with hardware constraints, which can enable the SUs to opportunistically utilize the unused licensed-spectrum without interfering with the PUs. In our proposed scheme, the SUs switch across the licensed channels with their distinct channel-hopping sequences. In particular, when an SU sender wants to send packets to its intended SU receiver, the SU sender changes its hopping schedule and follows the hopping sequence of the intended receiver to conduct the negotiation and then transmit data packets if the channel is not currently used by PUs. The main advantages of our proposed scheme include the followings: 1) no extra control channel is needed; 2) it overcomes the single control channel bottleneck problem; and 3) one transceiver is sufficient. We developed an Markov chain based analytical model to analyze the performance of our proposed scheme in terms of throughputs. We also identified the tradeoff between the channel utilization and the packet transmission delay.

Chapter IV proposed an efficient Cognitive Radio-Enabled Multi-channel MAC (CREAM-MAC) protocol, which integrates the sequential spectrum sensing at physical layer and the packet scheduling at MAC layer, over the wireless DSA networks. Under the proposed CREAM-MAC protocol, each SU is equipped with a cognitive radio-enabled transceiver and multiple channel sensors. Our cooperative sequential

spectrum sensing scheme improves the accuracy of spectrum sensing and further protects the PUs. The proposed CREAM-MAC enables the SUs to best utilize the unused frequency spectrum while avoiding the collisions among SUs and between SUs and PUs. We developed the Markov chain model and $M/G^Y/1$ queueing model to rigorously study our proposed CREAM-MAC protocol for both the saturation networks and the non-saturation networks. We also conducted extensive simulations to validate our developed protocol and analytical models.

In Chapter V, we considered a cognitive radio wireless network in which a set of SUs opportunistically utilize the wireless spectrum licensed to the PUs to transmit packets to the secondary base station. It is challenging to maximize the spectrum utilization while limiting the interference imposed to PUs due to SUs. To achieve the optimal tradeoff between the spectrum utilization and the interference caused by SUs, we proposed the adaptive spectrum sharing schemes for code division multiple access (CDMA) based cognitive medium access control (MAC) in the uplink communications over the cognitive radio networks. Our proposed schemes address the joint problems of channel sensing, data transmission, and power and rate allocations. Under our proposed schemes, the SUs can adaptively select between the intrusive spectrum sharing and the non-intrusive spectrum sharing operations to transmit data to secondary base station based on the channel utilization, traffic load, and interference constraints. Our proposed schemes enable the SUs to efficiently utilize the available frequency spectrum which is licensed to the PUs while stringently limiting the interference to the PUs. We also conducted extensive simulations to validate and evaluate our proposed schemes, which show the superiority of our proposed schemes as compared with the other schemes.

In Chapter VI, instead of focusing on the SUs, we concentrate on the PU networks. By exploiting the unique property of the wireless fading channel and cross-

layer design technique, we developed a packet scheduling scheme for the PUs in the context of wireless TDMA networks, which is set up to operate friendly towards the SUs in terms of vacant-channel probability. Our proposed scheme can be implemented with just slight modification on the traditional TDMA scheduling algorithm. We developed a rigorous queuing model, and then quantitatively analyze the tradeoff among multiple performance metrics to identify when and where the cost for favoring the SUs is worthy. The analytical results show that our proposed scheme can generate more vacant-channel opportunities for SUs, at the expense of little increasing packet delay for PUs, as compared with the traditional wireless TDMA scheduling algorithm. In addition, since the implementation of our proposed scheme only needs little modification on the existing TDMA scheduling algorithm, our proposed scheme is a practical and cost-effective approach to increase the wireless spectrum utilization.

B. Future Work

We summarize the relevant research topics that are of importance and deserve further investigation as follows.

1. Development of the More-Sophisticated Primary Users' Channel Usage Models

The licensed channel usage patterns of PUs were modeled as a two-state Markov chain (i.e., ON/OFF source model) in Chapters II and III, which is a common model widely used in cognitive radio networks. This model makes the analytical models tractable due to the memoryless feature of the distribution of the two-state periods. However, the more sophisticated models that can accurately catch the channel usage patterns of PUs on the licensed channels in the complicated real-world environments are needed in the future research.

To develop the more-sophisticated PUs' channel usage models, we can first conduct experimental measurement on the PUs' occupancy in the licensed channels in the real world by using the spectrum analyzer. The spectrum usage patterns of PUs can be modeled through the measured spectrum data. One of the effective approaches to analyze the PUs' spectrum usage patterns is *machine learning* based modeling technique, such as the hidden Markov models [111], neural networks [112], information fuzzy networks [113], and support machine vectors [114], etc. By collecting sufficient spectrum usage data of the PUs, we can use machine learning based models to analyze and predict the spectrum usage patterns of PUs. Then, we can modify our proposed MAC protocols in this dissertation to improve their performance in the real-world environments based on the more sophisticated channel usage models for PUs.

2. Impact of the SUs' Behaviors on Primary Users' Channel Usage Patterns

The design rule for the asynchronous cognitive radio network is that the interference caused by the SUs must be confined to a level acceptable by the PUs because the PUs licensed to the spectrum have the highest priority to access the spectrum while the SUs inevitably cause interference to the PUs in the asynchronous cognitive radio networks, as shown in Chapters IV and V. In this dissertation, we assume that PUs fixedly follow their inherent channel usage patterns and cannot be changed by the SUs' opportunistic spectrum access, which is widely accepted in the research community and is true for most of the PU networks. However, in the CSMA based PU networks, such as the IEEE 802.11 based PU networks, this assumption may not hold. With the interference from the SUs, the PUs may change the channel usage patterns when they need to sense the channel before transmission. In this sense, the SUs' activities inevitably create the casual effect on channel usage patterns and networking behaviors of the PUs even though the interference caused by the SUs

are expected to be confined to a low level. In the future research, we will take into account the impact of the SUs' behaviors on the PUs' channel usage patterns when designing the cognitive radio networks.

3. Secondary-User-Friendly MAC for Different Primary User Networks

In Chapter VI, we proposed the secondary-user-friendly MAC protocol for the wireless TDMA-based PU networks. By exploiting the unique property of the wireless fading channel and cross-layer design technique, the proposed secondary-user-friendly MAC protocol can improve the overall spectrum utilization. In the future research, we can extend the design experience to different types of PU networks, such as the contention-based PU networks and CDMA-based PU networks.

REFERENCES

- [1] M. McHenry, “NSF spectrum occupancy measurements project summary,” Shared Spectrum Company, 2005. [Online]. Available: http://www.sharedspectrum.com/inc/content/measurements/nsf/NSF_Project_Summary.pdf
- [2] M. McHenry, P. Tenhula, D. McCloskey, D. Roberson, and C. Hood, “Chicago spectrum occupancy measurements & analysis and a long-term studies proposal,” in *Proc. of the First International Workshop on Technology and Policy for Accessing Spectrum (TAPAS)*, Boston, Massachusetts, 2006.
- [3] FCC Spectrum Policy Task Force, “Spectrum policy task force report,” ET Docket No. 02-135, 2002. [Online]. Available: http://hraunfoss.fcc.gov/edocs_public/attachmatch/DOC-228542A1.pdf
- [4] FCC Spectrum Policy Task Force, “Establishment of an interference temperature metric to quantify and manage interference and to expand available unlicensed operation in certain fixed, mobile and satellite frequency band,” ET Docket No. 03-237, 2003. [Online]. Available: http://hraunfoss.fcc.gov/edocs_public/attachmatch/FCC-03-289A1.pdf
- [5] J. Mitola III, “Cognitive radio: an integrated agent architecture for software defined radio,” Ph.D. Thesis, Royal Institute of Technology, Stockholm, Sweden, 2000.
- [6] S. Haykin, “Cognitive radio: brain-empowered wireless communications,” *IEEE Journal on Selected Areas in Communications*, vol. 23, no. 2, February 2005, pp. 201–220.

- [7] I. Akyildiz, W. Lee, M. Vuran, and S. Mohanty, “NeXt generation/dynamic spectrum access/cognitive radio wireless networks: a survey,” *Elsevier Computer Networks*, vol. 50, September 2006, pp. 2127–2159.
- [8] N. Devroye, P. Mitran, and V. Tarokh, “Limits on communications in a cognitive radio channel,” *IEEE Communications Magazine*, vol. 44, no. 6, June 2006, pp. 44–49.
- [9] A. Jovicic and P. Viswanath, “Cognitive radio: an information-theoretic perspective,” *IEEE Transactions on Information Theory*, vol. 55, no. 9, September 2009, pp. 3945–3958.
- [10] F. K. Jondral, “Software-defined radio: basics and evolution to cognitive radio,” *EURASIP Journal on Wireless Communications and Networking*, vol. 2005, no. 3, 2005, pp. 275–283.
- [11] J. Mitola III and G.Q. Maguire, “Cognitive radio: making software radios more personal,” *IEEE Personal Communications*, vol. 6, no. 4, August 1999, pp. 13–18.
- [12] Q. Zhao, L. Tong, and A. Swami, “Decentralized cognitive MAC for dynamic spectrum access,” in *Proc. of the First IEEE International Symposium New Frontiers in Dynamic Spectrum Access Networks (DySPAN)*, November 2005, pp. 224–232.
- [13] Q. Zhao, L. Tong, A. Swami, and Y. Chen, “Decentralized cognitive MAC for opportunistic spectrum access in ad hoc networks: a POMDP framework,” *IEEE Journal on Selected Areas in Communications*, vol. 25, no. 3, April 2007, pp. 589–600,.

- [14] H. Su and X. Zhang, "Cross-layer based opportunistic MAC protocols for QoS provisionings over cognitive radio wireless networks," *IEEE Journal on Selected Areas in Communications*, vol. 26, no. 1, January 2008, pp. 118–129.
- [15] H. Su and X. Zhang, "Opportunistic MAC protocols for cognitive radio based wireless networks," in *Proc. of the 41st Annual Conference on Information Sciences and Systems (CISS)*, March 2007, pp. 363–368.
- [16] H. Su and X. Zhang, "Cognitive radio based multi-channel mac protocols for wireless ad hoc networks," in *Proc. of the IEEE Global Telecommunications Conference (GLOBECOM)*, November 2007, pp. 4857–4861.
- [17] H. Su and X. Zhang, "Channel-hopping based single transceiver MAC for cognitive radio networks," in *Proc. of the 42nd Annual Conference on Information Sciences and Systems (CISS)*, March 2008, pp. 197–202.
- [18] Y. Yuan, P. Bahl, R. Chandra, P. A. Chou, J. I. Ferrell, T. Moscibroda, S. Narlanka, and Y. Wu, "KNOWS: cognitive radio networks over white spaces," in *Proc. of the 2nd IEEE International Symposium on New Frontiers in Dynamic Spectrum Access Networks (DySPAN)*, April 2007, pp. 416–427.
- [19] S. Huang, X. Liu, and Z. Ding, "Optimal transmission strategies for dynamic spectrum access in cognitive radio networks," *IEEE Transactions on Mobile Computing*, vol. 8, no. 12, December 2009, pp. 1636–1648.
- [20] H. Su and X. Zhang, "CREAM-MAC: an efficient cognitive radio-enabled multi-channel MAC protocol for wireless networks," in *Proc. of the International Symposium on a World of Wireless, Mobile and Multimedia Networks (WoWMoM)*, June 2008, pp. 1–8.

- [21] X. Zhang and H. Su, "CREAM-MAC: cognitive radio-enabled multi-channel MAC protocol over dynamic spectrum access networks," *IEEE Journal of Selected Topics in Signal Processing*, Accepted to appear 2011.
- [22] H. Su and X. Zhang, "Adaptive uplink MAC for CDMA-based cognitive radio networks," in *Proc. of the IEEE MILCOM*, October 2009.
- [23] X. Zhang and H. Su, "Opportunistic spectrum sharing schemes for CDMA-based uplink MAC in cognitive radio networks," *IEEE Journal on Selected Areas in Communications*, Accepted to appear 2011.
- [24] H. Su and X. Zhang, "Interference-confined adaptive transmission scheme for cognitive radio networks," in *Proc. of the IEEE International Conference on Communications (ICC)*, May 2010, pp. 1–5.
- [25] B. Fette, "SDR technology implementation for the cognitive radio," in *Cognitive Radio Workshop, FCC*, 2003. [Online]. Available: <http://www.fcc.gov/oet/cognitiveradio/>
- [26] A. Goldsmith, S. A. Jafar, I. Maric, and S. Srinivasa, "Breaking spectrum gridlock with cognitive radios: an information theoretic perspective," *Proceedings of the IEEE*, vol. 97, no. 5, May 2009, pp. 894–914.
- [27] S. Sridharan and S. Vishwanath, "On the capacity of a class of MIMO cognitive radios," *IEEE Journal of Selected Topics in Signal Processing*, vol. 2, no. 1, February 2008, pp. 103–117.
- [28] I. Maric, A. Goldsmith, G. Kramer, and S. Shamai, "On the capacity of interference channels with a partially-cognitive transmitter," in *Proc. of the IEEE International Symposium Information Theory (ISIT)*, June 2007, pp. 2156–2160.

- [29] P. Grover and A. Sahai, “On the need for knowledge of the phase in exploiting known primary transmissions,” in *Proc. of the Second IEEE International Symposium on New Frontiers in Dynamic Spectrum Access Networks (DySPAN)*, April 2007, pp. 462–471.
- [30] A. Nosratinia, T. E. Hunter, and A. Hedayat, “Cooperative communication in wireless networks,” *IEEE Communications Magazine*, vol. 42, no. 10, October 2004, pp. 74–80.
- [31] A. Bletsas, H. Shin, and M. Z. Win, “Cooperative communications with outage-optimal opportunistic relaying,” *IEEE Transactions on Wireless Communications*, vol. 6, no. 9, September 2007, pp. 3450–3460.
- [32] D. Cabric, S. M. Mishra, and R. W. Brodersen, “Implementation issues in spectrum sensing for cognitive radios,” in *Proc. of the Thirty-Eighth Asilomar Conference on Signals, Systems and Computers*, vol. 1, November 2004, pp. 772–776.
- [33] A. Ghasemi and E. S. Sousa, “Spectrum sensing in cognitive radio networks: requirements, challenges and design trade-offs,” *IEEE Communications Magazine*, vol. 46, no. 4, April 2008, pp. 32–39.
- [34] K. R. Chowdhury and T. Melodia, “Platforms and testbeds for experimental evaluation of cognitive ad hoc networks,” *IEEE Communications Magazine*, vol. 48, no. 9, September 2010, pp. 96–104.
- [35] I. Akyildiz, W. Lee, and K. Chowdhury, “CRAHNs: cognitive radio ad hoc networks,” *Ad Hoc Networks*, vol. 7, no. 5, 2009, pp. 810–836.

- [36] T. Vamsi Krishna and A. Das, "A survey on MAC protocols in OSA networks," *Computer Networks*, vol. 53, no. 9, 2009, pp. 1377–1394.
- [37] C. Cormio and K. R. Chowdhury, "A survey on MAC protocols for cognitive radio networks," *Ad Hoc Networks*, vol. 7, no. 7, 2009, pp. 1315 – 1329. [Online]. Available: <http://www.sciencedirect.com/science/article/B7576-4VHSDJ5-1/2/639ebccfcfd56e0380a799af8b6f55d>
- [38] A. Elezabi, M. Kashef, M. Abdallah, and M. M. Khairy, "Cognitive interference-minimizing code assignment for underlay CDMA networks in asynchronous multipath fading channels," in *Proc. of the International Conference on Wireless Communications and Mobile Computing (IWCMC)*, June 2009, pp. 1279–1283.
- [39] B. Wang and D. Zhao, "Performance analysis in CDMA-based cognitive wireless networks with spectrum underlay," in *Proc. of the IEEE Global Communications Conference (GLOBECOM)*, November 2008.
- [40] A. T. Hoang and Y.-C. Liang, "A two-phase channel and power allocation scheme for cognitive radio networks," in *Proc. of the IEEE 17th International Symposium on Personal, Indoor and Mobile Radio Communications (PIMRC)*, September 2006.
- [41] L. Zhang, Y.-C. Liang, and Y. Xin, "Joint beamforming and power allocation for multiple access channels in cognitive radio networks," *IEEE Journal on Selected Areas in Communications*, vol. 26, no. 1, January 2008, pp. 38–51.
- [42] Q. Qu, L. B. Milstein, and D. R. Vaman, "Cognitive radio based multi-user resource allocation in mobile ad hoc networks using multi-carrier cdma modulation," *IEEE Journal on Selected Areas in Communications*, vol. 26, no. 1, January 2008, pp. 70–82.

- [43] D. Kim, L. Le, and E. Hossain, "Joint rate and power allocation for cognitive radios in dynamic spectrum access environment," *IEEE Transactions on Wireless Communications*, vol. 7, no. 12, December 2008, pp. 5517–5527.
- [44] A. Mishra, "A multi-channel MAC for opportunistic spectrum sharing in cognitive networks," in *Proc. of the Military Communications Conference (MILCOM)*, 23–25 October 2006, pp. 1–6.
- [45] C. Cordeiro and K. Challapali, "C-MAC: a cognitive MAC protocol for multi-channel wireless networks," in *Proc. of the 2nd IEEE International Symposium on New Frontiers in Dynamic Spectrum Access Networks (DySPAN)*, April 2007, pp. 147–157.
- [46] N. Nie and C. Comaniciu, "Adaptive channel allocation spectrum etiquette for cognitive radio networks," *Mobile Networks and Applications*, vol. 11, no. 6, 2006, pp. 779–797.
- [47] Y.-C. Liang, Y. Zeng, E. Peh, and A. T. Hoang, "Sensing-throughput tradeoff for cognitive radio networks," in *Proc. of the IEEE International Conference Communications (ICC)*, June 2007, pp. 5330–5335.
- [48] Y.-C. Liang, Y. Zeng, E. C. Y. Peh, and A. T. Hoang, "Sensing-throughput tradeoff for cognitive radio networks," *IEEE Transactions on Wireless Communications*, vol. 7, no. 4, April 2008, pp. 1326–1337.
- [49] M. Maskery, V. Krishnamurthy, and Q. Zhao, "Decentralized dynamic spectrum access for cognitive radios: cooperative design of a non-cooperative game," *IEEE Transactions on Communications*, vol. 57, no. 2, February 2009, pp. 459–469.

- [50] K. Liu, Q. Zhao, and B. Krishnamachari, “Dynamic multichannel access with imperfect channel state detection,” *IEEE Transactions on Signal Processing*, vol. 58, no. 5, May 2010, pp. 2795–2808.
- [51] L. Ma, X. Han, and C.-C. Shen, “Dynamic open spectrum sharing mac protocol for wireless ad hoc networks,” in *Proc. of the First IEEE International Symposium on New Frontiers in Dynamic Spectrum Access Networks (DySPAN)*, November 2005, pp. 203–213.
- [52] Y. Xing, C. N. Mathur, M. A. Haleem, R. Chandramouli, and K. P. Subbalakshmi, “Dynamic spectrum access with QoS and interference temperature constraints,” *IEEE Transactions on Mobile Computing*, vol. 6, no. 4, April 2007, pp. 423–433.
- [53] D. Niyato and E. Hossain, “A game-theoretic approach to competitive spectrum sharing in cognitive radio networks,” in *Proc. of the IEEE Wireless Communications and Networking Conference (WCNC)*, March 2007, pp. 16–20.
- [54] A. Chia-Chun Hsu, D. S. L. Weit, and C.-C. J. Kuo, “A cognitive mac protocol using statistical channel allocation for wireless ad-hoc networks,” in *Proc. of the IEEE Wireless Communications and Networking Conference (WCNC)*, March 2007, pp. 105–110.
- [55] C.-T. Chou, N. Sai Shankar, H. Kim, and K. G. Shin, “What and how much to gain by spectrum agility?” *IEEE Journal on Selected Areas in Communications*, vol. 25, no. 3, April 2007, pp. 576–588.
- [56] S. Huang, X. Liu, and Z. Ding, “Opportunistic spectrum access in cognitive radio networks,” in *Proc. of the IEEE INFOCOM*, April 2008, pp. 1427–1435.

- [57] S. Huang, X. Liu, and Z. Ding, "Optimal sensing-transmission structure for dynamic spectrum access," in *Proc. of the IEEE INFOCOM*, April 2009, pp. 2295–2303.
- [58] S. Geirhofer, L. Tong, and B. M. Sadler, "Cognitive medium access: constraining interference based on experimental models," *IEEE Journal on Selected Areas in Communications*, vol. 26, no. 1, January 2008, pp. 95–105.
- [59] Q. Zhao and A. Swami, "A survey of dynamic spectrum access: signal processing and networking perspectives," in *Proc. of the IEEE International Conference on Acoustics, Speech and Signal Processing (ICASSP)*, vol. 4, April 2007.
- [60] T. Yucek and H. Arslan, "A survey of spectrum sensing algorithms for cognitive radio applications," *IEEE Communications Surveys & Tutorials*, vol. 11, no. 1, 2009, pp. 116–130.
- [61] D. Cabric, A. Tkachenko, and R. W. Brodersen, "Spectrum sensing measurements of pilot, energy, and collaborative detection," in *Proc. of the IEEE Military Communications Conference (MILCOM)*, October 2006, pp. 1–7.
- [62] N. Nie and C. Comaniciu, "Adaptive channel allocation spectrum etiquette for cognitive radio networks," in *Proc. of the First IEEE International Symposium on New Frontiers in Dynamic Spectrum Access Networks (DySPAN)*, November 2005, pp. 269–278.
- [63] D. Duan, L. Yang, and J. C. Principe, "Cooperative diversity of spectrum sensing for cognitive radio systems," *IEEE Transactions on Signal Processing*, vol. 58, no. 6, June 2010, pp. 3218–3227.
- [64] Q. Zhao, W. Ren, and A. Swami, "Spectrum opportunity detection: how good is

- listen-before-talk?” in *Proc. of the Forty-First Asilomar Conference on Signals, Systems and Computers (ACSSC)*, November 2007, pp. 767–771.
- [65] Y. Hur, J. Park, W. Woo, J. S. Lee, K. Lim, C.-H. Lee, H. S. Kim, and J. Laskar, “A cognitive radio (CR) system employing a dual-stage spectrum sensing technique : a multi-resolution spectrum sensing (MRSS) and a temporal signature detection (TSD) technique,” in *Proc. of the IEEE Global Telecommunications Conference (GLOBECOM)*, November 2006, pp. 1–5.
- [66] A. Fehske, J. Gaeddert, and J. H. Reed, “A new approach to signal classification using spectral correlation and neural networks,” in *Proc. of the First IEEE International Symposium on New Frontiers in Dynamic Spectrum Access Networks (DySPAN)*, November 2005, pp. 144–150.
- [67] Y. Zeng and Y.-C. Liang, “Spectrum-sensing algorithms for cognitive radio based on statistical covariances,” *IEEE Transactions on Vehicular Technology*, vol. 58, no. 4, May 2009, pp. 1804–1815.
- [68] Y. Zeng and Y.-C. Liang, “Covariance based signal detections for cognitive radio,” in *Proc. of the 2nd IEEE International Symposium on New Frontiers in Dynamic Spectrum Access Networks (DySPAN)*, April 2007, pp. 202–207.
- [69] H. Su and X. Zhang, “Power-efficient periodic spectrum sensing for cognitive MAC in dynamic spectrum access networks,” in *Proc. of the IEEE Wireless Communications and Networking Conference (WCNC)*, April 2010, pp. 1–6.
- [70] N. B. Chang and M. Liu, “Optimal competitive algorithms for opportunistic spectrum access,” *IEEE Journal on Selected Areas in Communications*, vol. 26, no. 7, September 2008, pp. 1183–1192.

- [71] H. Kim and K. G. Shin, “In-band spectrum sensing in cognitive radio networks: energy detection or feature detection?” *in Proc. of the ACM MobiCom*, September 2008, pp. 14–25.
- [72] A. T. Hoang and Y.-C. Liang, “Adaptive scheduling of spectrum sensing periods in cognitive radio networks,” *in Proc. of the IEEE Global Telecommunications Conference (GLOBECOM)*, November 2007, pp. 3128–3132.
- [73] G. Ganesan, Y. Li, B. Bing, and S. Li, “Spatiotemporal sensing in cognitive radio networks,” *IEEE Journal on Selected Areas in Communications*, vol. 26, no. 1, January 2008, pp. 5–12.
- [74] S. M. Mishra, A. Sahai, and R. W. Brodersen, “Cooperative sensing among cognitive radios,” *in Proc. of the IEEE International Conference on Communications (ICC)*, vol. 4, June 2006, pp. 1658–1663.
- [75] G. Ganesan and Y. Li, “Cooperative spectrum sensing in cognitive radio, part I: two user networks,” *IEEE Transactions on Wireless Communications*, vol. 6, no. 6, June 2007, pp. 2204–2213.
- [76] Q. Zhao, B. Krishnamachari, and K. Liu, “On myopic sensing for multi-channel opportunistic access: structure, optimality, and performance,” *IEEE Transactions on Wireless Communications*, vol. 7, no. 12, December 2008, pp. 5431–5440.
- [77] E. Peh and Y. Liang, “Optimization for cooperative sensing in cognitive radio networks,” *in Proc. of the IEEE Wireless Communications and Networking Conference (WCNC)*, March 2007, pp. 27–32.
- [78] Z. Quan, S. Cui, and A. H. Sayed, “Optimal linear cooperation for spectrum

- sensing in cognitive radio networks,” *IEEE Journal of Selected Topics in Signal Processing*, vol. 2, no. 1, February 2008, pp. 28–40.
- [79] Z. Quan, W.-K. Ma, S. Cui, and A. H. Sayed, “Optimal linear fusion for distributed detection via semidefinite programming,” *IEEE Transactions on Signal Processing*, vol. 58, no. 4, April 2010, pp. 2431–2436.
- [80] X. Zheng, J. Wang, Q. Wu, and J. Chen, “Cooperative spectrum sensing algorithm based on dempster-shafer theory,” in *Proc. of the 11th IEEE Singapore International Conference Communication Systems (ICCS)*, November 2008, pp. 218–221.
- [81] H. Su and X. Zhang, “Secondary user friendly TDMA scheduling for primary users in cognitive radio networks,” in *Proc. IEEE Global Telecommunications Conference (GLOBECOM)*, December 2009, pp. 1–6.
- [82] IEEE 802.11 Working Group, “IEEE Standard 802.11 - 1999, Wireless LAN Medium Access Control (MAC) and Physical Layer (PHY) Specifications”, *IEEE Standards*, November 1999.
- [83] L. Kleinrock and F. Tobagi, “Packet switching in radio channels: part I—carrier sense multiple-access modes and their throughput-delay characteristics,” *IEEE Transactions on Communications*, vol. 23, no. 12, December 1975, pp. 1400–1416.
- [84] C. Cordeiro, K. Challapali, D. Birru, and S. Shankar, “IEEE 802.22: An introduction to the first wireless standard based on cognitive radios,” *Journal of Communications*, vol. 1, no. 1, 2006, pp. 38–47.
- [85] H. Chhaya and S. Gupta, “Performance modeling of asynchronous data transfer

- methods of IEEE 802.11 MAC protocol,” *Wireless Networks*, vol. 3, no. 3, 1997, pp. 217–234.
- [86] K. Medepalli and F. A. Tobagi, “Towards performance modeling of IEEE 802.11 based wireless networks: a unified framework and its applications,” in *Proc. of the 25th IEEE INFOCOM*, April 2006, pp. 1–12.
- [87] M. Chaudhry and J. Templeton, “First course in bulk queues,” Wiley, New York, U.S.A., 1983.
- [88] G. Briere and M. Chaudhry, “Computational Analysis of Single-Server Bulk-Service Queues, M/G Y/1,” *Advances in Applied Probability*, vol. 21, no. 1, 1989, pp. 207–225.
- [89] P. Bahl, R. Chandra, and J. Dunagan, “SSCH: slotted seeded channel hopping for capacity improvement in IEEE 802.11 ad-hoc wireless networks,” in *Proc. of the ACM MobiCom*, September 2004, pp. 216–230.
- [90] H. So, J. Walrand, and J. Mo, “McMAC: a parallel rendezvous multi-Channel MAC protocol,” in *Proc. of the IEEE Wireless Communications and Networking Conference (WCNC)*, March 2007, pp. 334–339.
- [91] H. So and J. Walrand, “Design of a multi-channel medium access control protocol for ad-hoc wireless networks,” Tech. Rep., UCB/EECS-2006-54, University of California at Berkeley, May 2006.
- [92] J. So and N. H. Vaidya, “Multi-channel MAC for ad hoc networks: handling multi-channel hidden terminals using a single transceiver,” in *Proc. of the ACM MobiHoc*, May 2004, pp. 222–233.

- [93] F. F. Digham, M.-S. Alouini, and M. K. Simon, "On the energy detection of unknown signals over fading channels," *IEEE Transactions on Communications*, vol. 55, no. 1, January 2007, pp. 21–24.
- [94] A. Ghasemi and E. S. Sousa, "Collaborative spectrum sensing for opportunistic access in fading environments," in *Proc. of the First IEEE International Symposium on New Frontiers in Dynamic Spectrum Access Networks (DySPAN)*, November 2005, pp. 131–136.
- [95] G. Bianchi, "Performance analysis of the IEEE 802.11 distributed coordination function," *IEEE Journal on Selected Areas in Communications*, vol. 18, no. 3, March 2000, pp. 535–547.
- [96] H. Su, X. Zhang, P. Qiu, and M. Guizani, "An enhanced IEEE 802.11 MAC algorithm for tradeoff between delay and energy-consumption," in *Proc. of the IEEE International Conference on Communications (ICC)*, vol. 9, June 2006, pp. 3935–3940.
- [97] M. Wellens, J. Riihijarvi, and P. Mhnen, "Spatial statistics and models of spectrum use," *Elsevier Computer Communications*, vol. 32, 2009, pp. 1998–2011.
- [98] D. Chen, S. Yin, Q. Zhang, M. Liu, and S. Li, "Mining spectrum usage data: a large-scale spectrum measurement study," in *Proc. of the ACM MobiCom*, September 2009, pp. 13–24.
- [99] S. W. Kim, "Adaptive rate and power DS/CDMA communications in fading channels," *IEEE Communications Letters*, vol. 3, no. 4, April 1999, pp. 85–87.
- [100] A. Belegundu, L. Berke, and S. Patnaik, "An optimization algorithm based on

- the method of feasible directions,” *Structural and Multidisciplinary Optimization*, vol. 9, no. 2, pp. 83–88, 1995.
- [101] R. Jain, D. Chiu, and W. Hawe, “A quantitative measure of fairness and discrimination for resource allocation in shared systems,” Tech. Rep., DEC Research Report TR-301, Digital Equipment Corporation, Hudson, Massachusetts, U.S.A., 1984.
- [102] W.-Y. Lee and I. F. Akyildiz, “Optimal spectrum sensing framework for cognitive radio networks,” *IEEE Transactions on Wireless Communications*, vol. 7, no. 10, October 2008, pp. 3845–3857.
- [103] P. Papadimitratos, S. Sankaranarayanan, and A. Mishra, “A bandwidth sharing approach to improve licensed spectrum utilization,” *IEEE Communications Magazine*, vol. 43, December 2005, no. 12, pp. 10–14.
- [104] Y. Chen, Q. Zhao, and A. Swami, “Joint design and separation principle for opportunistic spectrum access in the presence of sensing errors,” *IEEE Transactions on Information Theory*, vol. 54, no. 5, May 2008, pp. 2053–2071.
- [105] R. Knopp and P. A. Humblet, “Information capacity and power control in single-cell multiuser communications,” in *Proc. of the IEEE International Conference on Communications (ICC)*, vol. 1, June 1995, pp. 331–335.
- [106] P. Viswanath, D. N. C. Tse, and R. Laroia, “Opportunistic beamforming using dumb antennas,” *IEEE Transactions on Information Theory*, vol. 48, no. 6, June 2002, pp. 1277–1294.
- [107] M. Andrews, K. Kumaran, K. Ramanan, A. Stolyar, P. Whiting, and R. Vijayakumar, “Providing quality of service over a shared wireless link,” *IEEE*

Communications Magazine, vol. 39, no. 2, February 2001, pp. 150–154.

- [108] Q. Liu, S. Zhou, and G. B. Giannakis, “Queuing with adaptive modulation and coding over wireless links: cross-layer analysis and design,” *IEEE Transactions on Wireless Communications*, vol. 4, no. 3, May 2005, pp. 1142–1153.
- [109] S. Srinivasa and S. A. Jafar, “The throughput potential of cognitive radio: a theoretical perspective,” in *Proc. Fortieth Asilomar Conference on Signals, Systems and Computers (ACSSC)*, October 2006, pp. 221–225.
- [110] A. Goldsmith, “Wireless Communications,” Cambridge University Press, Cambridge, England, 2005.
- [111] Y. Ephraim and N. Merhav, “Hidden markov processes,” *IEEE Transactions on Information Theory*, vol. 48, no. 6, June 2002, pp. 1518–1569.
- [112] C. Bishop, “Neural networks for pattern recognition,” Oxford University Press, Oxford, England, 1995.
- [113] A. Kandel, M. Last, and H. Bunke, “Fuzzification and reduction of information-theoretic rule sets,” *Data Mining and Computational Intelligence (Studies in Fuzziness and Soft Computing, Volume 68)*, Physica Verlag, Heidelberg, Germany, 2001, pp. 63–93.
- [114] V. Kecman, “Learning and soft computing: support vector machines, neural networks, and fuzzy logic models,” The MIT Press, Cambridge, Massachusetts, U.S.A., 2001.

APPENDIX A

THE PROOF OF PROPOSITION 1 IN CHAPTER II

Proof. To prove the proposition, we only need to show that $|B_0(t) \cup B_1(t)| \leq |B_0(t+1) \cup B_1(t+1)|$ holds for any given time slot, indexed by t with $t = 0, 1, 2, \dots$. There are three cases. First, all the secondary users fail to send RTS/CTS packets during the negotiating phase in t -th time slot. None of them will change the channel to sense in the $(t+1)$ -th time slot. This implies that the number of sensed channels in the $(t+1)$ -th time slot is the same as that in t -th time slot, i.e., $|B_0(t) \cup B_1(t)| = |B_0(t+1) \cup B_1(t+1)|$. Second, a given secondary user successfully sends the RTS/CTS packets. There is no other secondary users which sense the same channel as this given secondary user. In this case, no secondary users will change their sensing channels in the $(t+1)$ -th time slot, implying that $|B_0(t) \cup B_1(t)| = |B_0(t+1) \cup B_1(t+1)|$ holds. Third, a given secondary user successfully transmits the RTS/CTS packets during the negotiating phase and the channel sensed by this given secondary user is sensed by at least another one or more secondary users, the other secondary users select different channels from the set of $(B_1(t) \cup B_2(t))$ for sensing in the $(t+1)$ -th time slot. Consequently, the channels in $B_2(t)$ may be selected as well, implying that $|B_2(t)| \geq |B_2(t+1)|$, and thus $|B_0(t) \cup B_1(t)| \leq |B_0(t+1) \cup B_1(t+1)|$. According to the above three cases, $|B_0(t) \cup B_1(t)| \leq |B_0(t+1) \cup B_1(t+1)|$ always holds, completing the proof. \square

APPENDIX B

THE DERIVATIONS OF THE CLOSED-FORM EXPRESSIONS FOR EQ. (5.27)
AND EQ. (5.33) UNDER THE DIFFERENT DISTRIBUTIONS

1) The Lognormal Distribution:

If the duration of the OFF period follows the lognormal distribution, then we get its cdf as

$$C_{\tau_0}(t) = \frac{1}{2} \left[1 + \operatorname{erf} \left(\frac{\log(t) - \mu}{\sqrt{2}\sigma} \right) \right] \quad (\text{B.1})$$

and its pdf as

$$A_{\tau_0}(t) = \frac{1}{t\sqrt{2\pi\sigma^2}} e^{-\frac{[\log(t)-\mu]^2}{2\sigma^2}} \quad (\text{B.2})$$

where μ and σ are the mean and standard deviation, respectively, in the form of natural logarithm, and $\operatorname{erf}(x) \triangleq (2/\sqrt{\pi}) \int_0^x e^{-t^2} dt$ is the error function. Plugging Eqs. (B.1) and (B.2) into Eq. (5.27), we obtain the followings:

$$D(\tau_t, \tau_f) = \frac{2}{1 - \operatorname{erf} \left(\frac{\log(\tau_f) - \mu}{\sqrt{2}\sigma} \right)} \left\{ \frac{\tau_t + \tau_f}{2} \left[\operatorname{erf} \left(\frac{\log(\tau_t + \tau_f) - \mu}{\sqrt{2}\sigma} \right) - \operatorname{erf} \left(\frac{\log(\tau_f) - \mu}{\sqrt{2}\sigma} \right) \right] - \frac{e^{\mu + \frac{\sigma^2}{2}}}{2} \left[\operatorname{erf} \left(\frac{\mu + \sigma^2 - \log(\tau_f)}{\sqrt{2}\sigma} \right) - \operatorname{erf} \left(\frac{\mu + \sigma^2 - \log(\tau_f + \tau_t)}{\sqrt{2}\sigma} \right) \right] \right\}. \quad (\text{B.3})$$

Likewise, for the mean squared estimation error of t_{sp} , if the duration of the ON period also follows the lognormal distribution, substituting $C_{\tau_1}(t)$ and $A_{\tau_1}(t)$, which have the same expressions as those on the righthand sides of Eqs. (B.1) and (B.2),

respectively, into Eq. (5.33), we can obtain

$$\begin{aligned}
\epsilon(t_{sp}, \tau_i) &= 2\sqrt{\frac{2}{\pi}} e^{\frac{(\mu+\sigma^2)^2}{2\sigma^2}} (t_{sp} - t'_{sp}) \left[\frac{\operatorname{erf}\left(\frac{\log(\tau_{ls}+\tau_i)-\mu-\sigma^2}{\sqrt{2}\sigma}\right) - \operatorname{erf}\left(\frac{\log(\tau_{ls})-\mu-\sigma^2}{\sqrt{2}\sigma}\right)}{\operatorname{erf}\left(\frac{\log(\tau_{ls}+\tau_i)-\mu}{\sqrt{2}\sigma}\right) - \operatorname{erf}\left(\frac{\log(\tau_{ls})-\mu}{\sqrt{2}\sigma}\right)} \right] \\
&\quad - \sqrt{\frac{2}{\pi}} e^{\frac{(\mu+\sigma^2)^2}{2\sigma^2}} \left[\frac{\operatorname{erf}\left(\frac{\log(\tau_{ls}+\tau_i)-\mu-2\sigma^2}{\sqrt{2}\sigma}\right) - \operatorname{erf}\left(\frac{\log(\tau_{ls})-\mu-2\sigma^2}{\sqrt{2}\sigma}\right)}{\operatorname{erf}\left(\frac{\log(\tau_{ls}+\tau_i)-\mu}{\sqrt{2}\sigma}\right) - \operatorname{erf}\left(\frac{\log(\tau_{ls})-\mu}{\sqrt{2}\sigma}\right)} \right] \\
&\quad + \sqrt{\frac{2}{\pi}} e^{\frac{\mu^2}{2\sigma^2}} (t_{sp} - t'_{sp})^2. \tag{B.4}
\end{aligned}$$

2) The Gamma Distribution:

If the duration of the OFF period follows the gamma distribution, then we have its cdf as

$$C_{\tau_0}(t) = 1 - \frac{\Gamma(\alpha, \frac{t}{\beta})}{\Gamma(\alpha)} \tag{B.5}$$

and we get its pdf as

$$A_{\tau_0}(t) = t^{\alpha-1} e^{-\frac{t}{\beta}} \frac{1}{\Gamma(\alpha)\beta^\alpha} \tag{B.6}$$

where α and β are the shape and scale parameters, respectively, $\Gamma(a, z) \triangleq \int_z^\infty t^{a-1} e^{-t} dt$ is the upper incomplete gamma function, and $\Gamma(a) \triangleq \int_0^\infty t^{a-1} e^{-t} dt$ is the gamma function. For the average interference duration, by plugging Eqs. (B.5) and (B.6) into Eq. (5.27) and algebraic manipulation, Eq. (5.27) can be expanded as follows:

$$\begin{aligned}
D(\tau_t, \tau_f) &= \frac{1}{\Gamma(\alpha, \frac{\tau_f}{\beta})} \left\{ (\tau_t + \tau_f) \left[\Gamma\left(\alpha, \frac{\tau_f}{\beta}\right) - \Gamma\left(\alpha, \frac{\tau_f + \tau_t}{\beta}\right) \right] \right. \\
&\quad \left. - \frac{\beta}{\Gamma(\alpha)} \left[\Gamma\left(\alpha + 1, \frac{\tau_f}{\beta}\right) - \Gamma\left(\alpha + 1, \frac{\tau_f + \tau_t}{\beta}\right) \right] \right\}. \tag{B.7}
\end{aligned}$$

Likewise, for the mean squared estimation error of t_{sp} , if the duration of the ON period also follows the gamma distribution, by substituting $C_{\tau_1}(t)$ and $A_{\tau_1}(t)$, which have the same expressions as those on the righthand sides of Eqs. (B.5) and (B.6),

respectively, into Eq. (5.33), we can obtain the followings:

$$\begin{aligned} \epsilon(t_{sp}, \tau_i) = & (t_{sp} - t'_{sp})^2 + \frac{\beta}{\Gamma(\alpha, \frac{\tau_{ls}}{\beta}) - \Gamma(\alpha, \frac{\tau_{ls} + \tau_i}{\beta})} \left\{ \left[\Gamma(2 + \alpha, \frac{\tau_{ls}}{\beta}) - \Gamma(2 + \alpha, \frac{\tau_{ls} + \tau_i}{\beta}) \right] \right. \\ & \left. + 2(t_{sp} - t'_{sp}) \left[\Gamma(1 + \alpha, \frac{\tau_{ls}}{\beta}) - \Gamma(1 + \alpha, \frac{\tau_{ls} + \tau_i}{\beta}) \right] \right\}. \end{aligned} \quad (\text{B.8})$$

3) The Pareto Distribution:

If the duration of the OFF period follows the pareto distribution, then we have its cdf as

$$C_{\tau_0}(t) = \begin{cases} 1 - \left(\frac{k}{t}\right)^\alpha, & t > k \\ 0, & \text{otherwise} \end{cases} \quad (\text{B.9})$$

and we obtain its pdf as

$$A_{\tau_0}(t) = \begin{cases} \frac{\alpha k^\alpha}{t^{\alpha+1}}, & t > k \\ 0, & \text{otherwise} \end{cases} \quad (\text{B.10})$$

where k is the minimum possible value of the random variable, and α is a positive parameter. For the average interference duration, after plugging Eqs. (B.9) and (B.10) into Eq. (5.27), we have the followings:

$$\begin{aligned} & D(\tau_t, \tau_f) \\ = & \begin{cases} (\tau_f + \tau_t) \left[1 - \frac{1}{1-\alpha} \left(\frac{\tau_f}{\tau_f + \tau_t} \right)^\alpha \right] + \frac{\alpha}{1-\alpha} \tau_f, & \tau_f > k \\ (\tau_f + \tau_t) \left[1 - \left(\frac{k}{\tau_f + \tau_t} \right)^\alpha \right] - \alpha k^\alpha \frac{(\tau_f + \tau_t)^{1-\alpha} - k^{1-\alpha}}{1-\alpha}, & \tau_f + \tau_t > k \text{ and } \tau_f < k \\ 0, & \text{otherwise.} \end{cases} \end{aligned} \quad (\text{B.11})$$

Likewise, for the mean squared estimation error of t_{sp} , if the duration of the ON period also follows the gamma distribution, by substituting $C_{\tau_1}(t)$ and $A_{\tau_1}(t)$, which have the same expressions as those on the righthand sides of Eqs. (B.9) and (B.10),

respectively, into Eq. (5.33), we obtain the followings:

$$\begin{aligned} & \epsilon(t_{sp}, \tau_i) \\ &= \begin{cases} (t_{sp} - t'_{sp})^2 (b^\alpha - a^\alpha) - \frac{2\alpha(\alpha-2)(t_{sp}-t'_{sp})(b^\alpha a - a^\alpha b)}{(\alpha^2-3\alpha+2)(b^\alpha-a^\alpha)} + \frac{\alpha(\alpha-1)(b^\alpha a^2 - a^\alpha b^2)}{(\alpha^2-3\alpha+2)(b^\alpha-a^\alpha)}, & b > k \\ 0, & \text{otherwise} \end{cases} \end{aligned} \tag{B.12}$$

where $a = \max\{\tau_{ls}, k\}$ and $b = \tau_{ls} + \tau_i$.

VITA

Hang Su was born in Wuzhou, Guangxi, China. He received the B.S. and M.S. degrees, both in electrical engineering, from Zhejiang University, Hangzhou, China, in 2002 and 2005, respectively, and received the Ph.D. degree in Computer Engineering from Texas A&M University, College Station, in 2010. He worked as a software engineer with Nokia Research Center, Hangzhou, China, in 2005. During the summer of 2009, he worked as a research intern with Mitsubishi Electric Research Laboratories (MERL), Cambridge, MA.

His research interests focus on cognitive radio networks, vehicular ad hoc networks, wireless mesh networks, cellular networks, and wireless sensor networks, with emphasis on design and analysis of physical, MAC, and routing protocols. Two of his papers on cognitive radio networks, both co-authored with his Ph.D. advisor Prof. Xi Zhang, received the Best Paper Awards at the IEEE GLOBECOM 2009 and IEEE WCNC 2010, respectively. He is serving or has served as the Web Chair for QShine 2010, Publicity Chair for IWCMC 2008, and Technical Program Committee (TPC) Members for IEEE GLOBECOM 2007, 2009, and 2010, IEEE ICC 2010 and 2011, and IEEE WCNC 2010 and 2011, respectively.

He may be reached at the Department of Electrical and Computer Engineering, Texas A&M University, College Station, TX 77843-3128. His e-mail address is su@tamu.edu.

The typist for this dissertation was the author.